Model Order Reduction Techniques for the Numerical Analysis of Linear Microwave Structures

Romanus Dyczij-Edlinger and Ortwin Farle

A. Sommer, S. Burgard, O. Floch

Y. Konkel, A. Schultschik

Laboratory for Electromagnetic Theory
Saarland University

Setting

Time-harmonic fields:

- Linear time-invariant case
- Frequency domain: $\boxed{\partial_t \leftrightarrow j\omega}$ $\quad k_0 = \frac{\omega}{c_0}$

Finite element (FE) method:

- Differential equation method
- Discretizate entire field domain

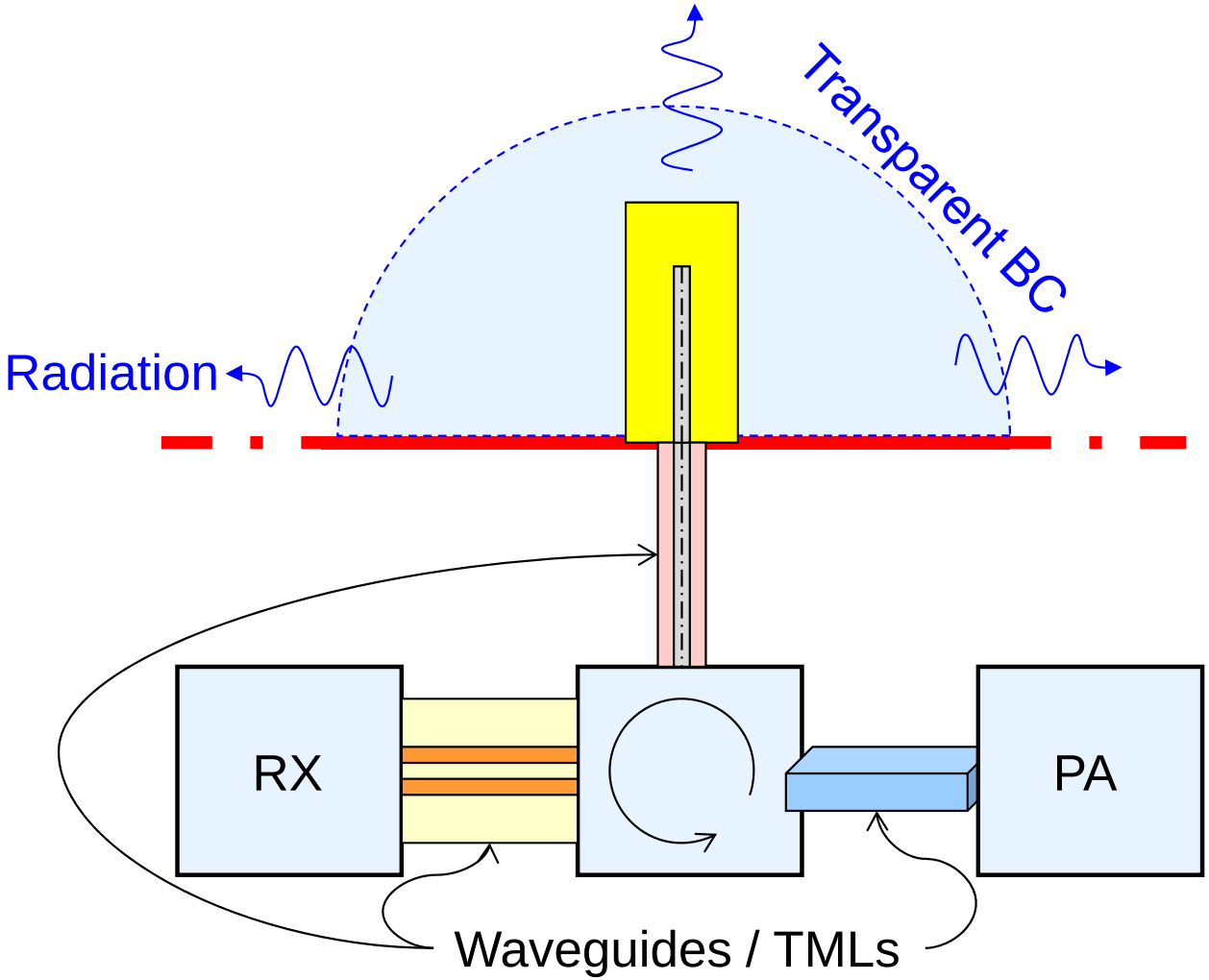

Far-field

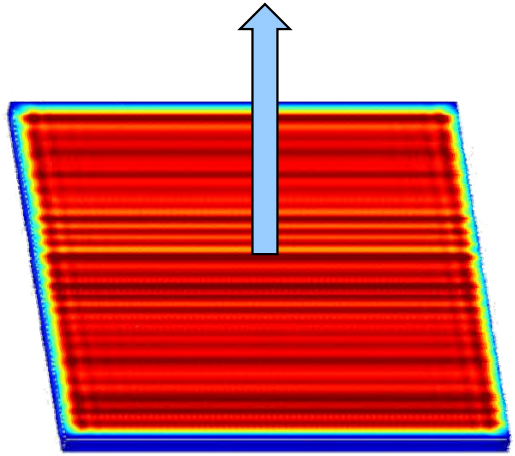

Near-field

Modeling: Generalized Circuit Concepts

Waveguides (WG):

- Cylindrical: axis $\hat{\mathbf{e}}_z$, cross-section.
- Shielded: non-radiating.
- Reciprocal.

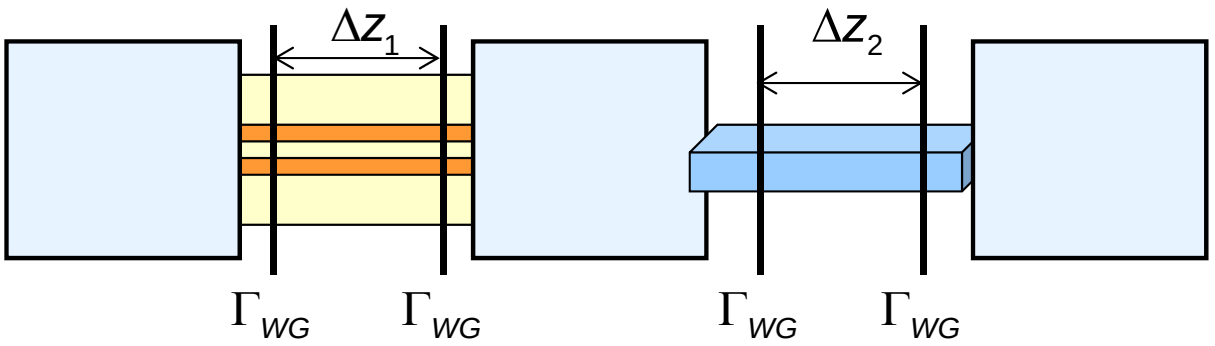

$\Rightarrow$ Discrete spectrum of modes: $\left(\gamma_n, \hat{\mathbf{e}}_n, \hat{\mathbf{h}}_n\right)(\omega)$

$\Rightarrow$ Orthogonality: $\int_{\Gamma_{WG}} \left(\hat{\mathbf{e}}_m \times \hat{\mathbf{h}}_n\right) \cdot \hat{\mathbf{e}}_z \, \mathrm{d}\Gamma = \delta_{mn}$

$\Rightarrow$ Finite number of propag. / weakly damped modes.

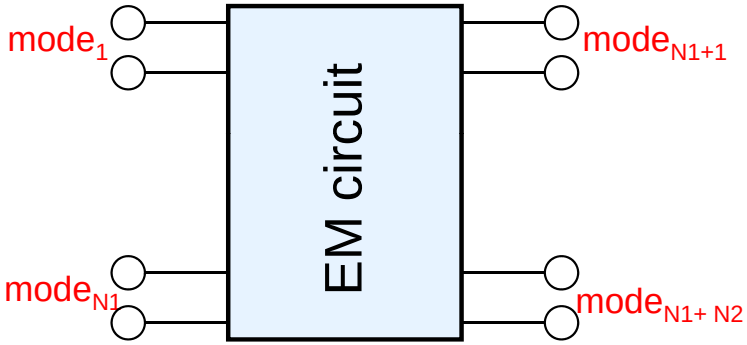

$\Rightarrow$ Modal expansion:

$$\mathbf{E}_T(z) = \sum_{n=1}^{\infty} \left(a_n e^{-\gamma_i z} + b_n e^{-\gamma_i z}\right) \hat{\mathbf{e}}_i = \sum_{n=1}^{\infty} u_n(z) \hat{\mathbf{e}}_i$$

$$\mathbf{H}_T(z) = \sum_{n=1}^{\infty} \left(a_n e^{-\gamma_i z} - b_n e^{-\gamma_i z}\right) \hat{\mathbf{h}}_i = \sum_{n=1}^{\infty} i_n(z) \hat{\mathbf{e}}_i$$

a_n, b_n …modal amplitudes

u_n, i_n …modal voltage/current

$\Rightarrow$ Away from discontinuities:

$$\mathbf{E}_T(z) \approx \sum_{n=1}^{N} \left(a_n e^{-\gamma_i z} + b_n e^{-\gamma_i z}\right) \hat{\mathbf{e}}_n$$

$$\mathbf{H}_T(z) \approx \sum_{n=1}^{N} \left(a_n e^{-\gamma_i z} - b_n e^{-\gamma_i z}\right) \hat{\mathbf{h}}_n$$

Specific Sub-problems, Motivation for MOR

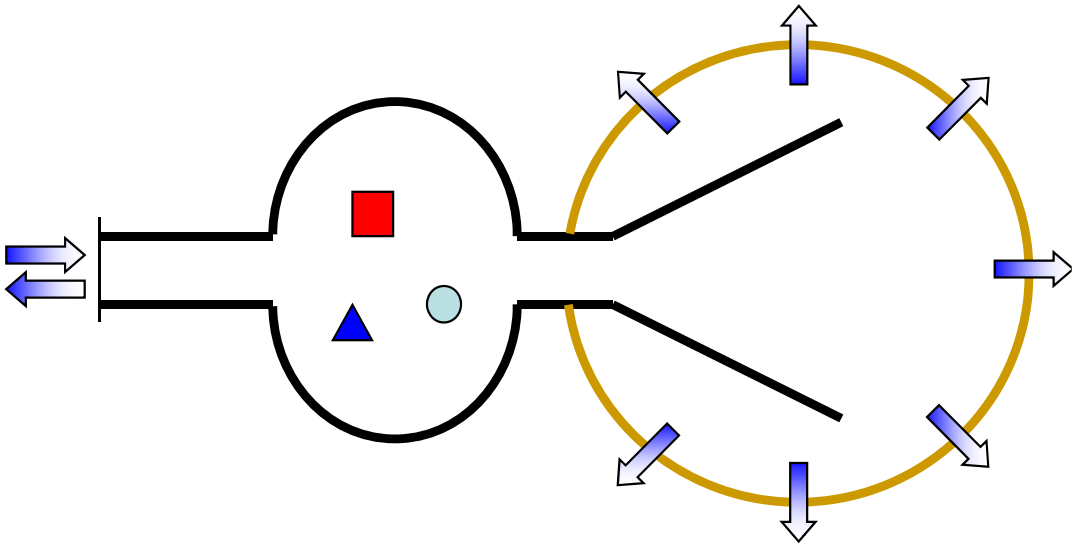

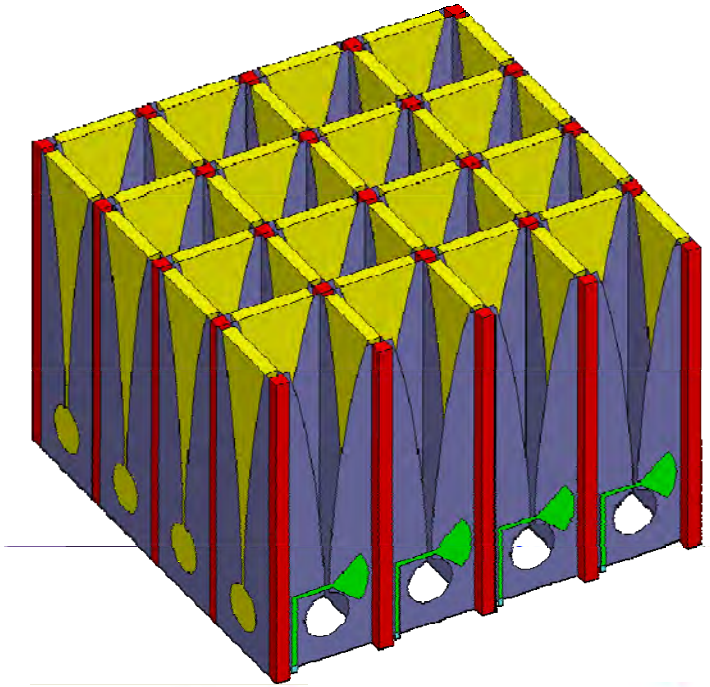

Waveguides: **modal problem**

$$\left(\mathbf{S}_0 + k_0\mathbf{S}_1 + k_0^2\mathbf{S}_2\right)\mathbf{v} = \gamma^2\mathbf{T}_0\mathbf{v}$$

Discontinuities: **driven problem**

$$\left(\mathbf{S} - k_0\mathbf{T}_{TFE} - k_0^2\mathbf{T} - \beta k_0^2\mathbf{T}_\varepsilon\right)\mathbf{x} = k_0^2\mathbf{b}$$

$$S_{ik} = \mathbf{c}^*\mathbf{x}$$

Farfields: **nearfield-to-farfield transform.**

$$\mathbf{F}(\hat{\mathbf{r}},k) = \oint_{S_0} e^{jk\hat{\mathbf{r}}\cdot\mathbf{r}'}\left[\hat{\mathbf{r}}\times\left(\mathbf{J}_S\times\hat{\mathbf{r}}\right) + \frac{1}{\eta}\mathbf{M}_S\times\hat{\mathbf{r}}\right]dS'$$

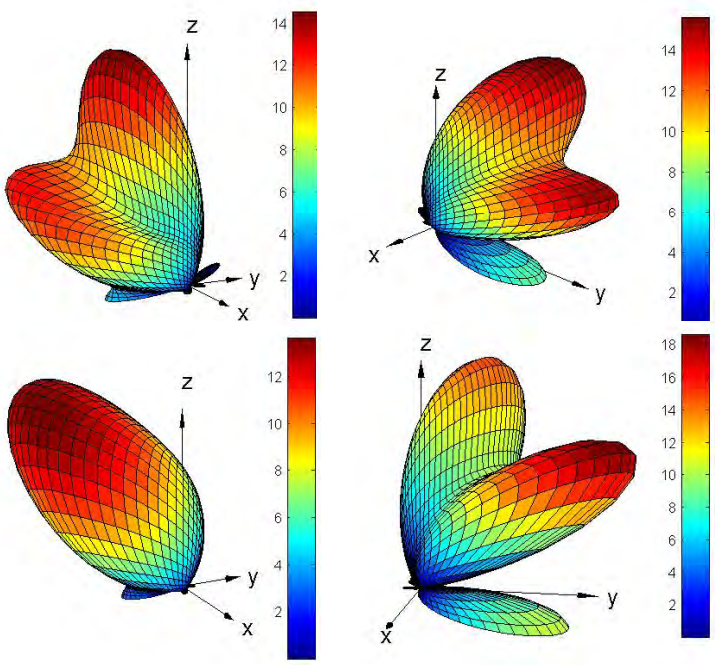

Fast Frequency Sweeps for Electromagnetic Waveguides

Goals and Limitations

- Inhomogeneous waveguides:
  - Frequency-dependent field patterns.
  - Complicated dispersion curves.
  - No analytical solutions: FEM.

- Goals:
  - Broadband analysis: DC to GHz / THz.
  - Much faster than FEM.
  - Controlled accuracy.

- Necessary steps:
  - LF stability: FE formulation.
  - Speed: multi-point MOR.
  - Adaptive point-placing strategy.

- Limitations:
  - No ohmic losses or ABCs.
  - Reciprocal materials only.

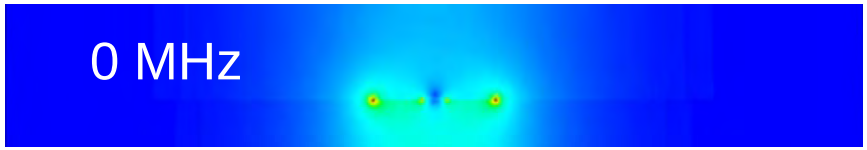

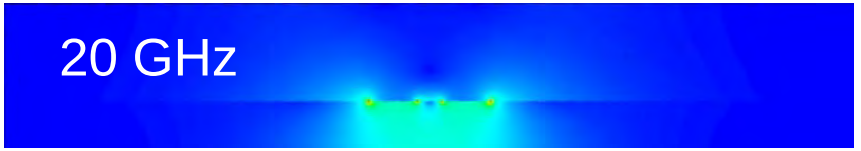

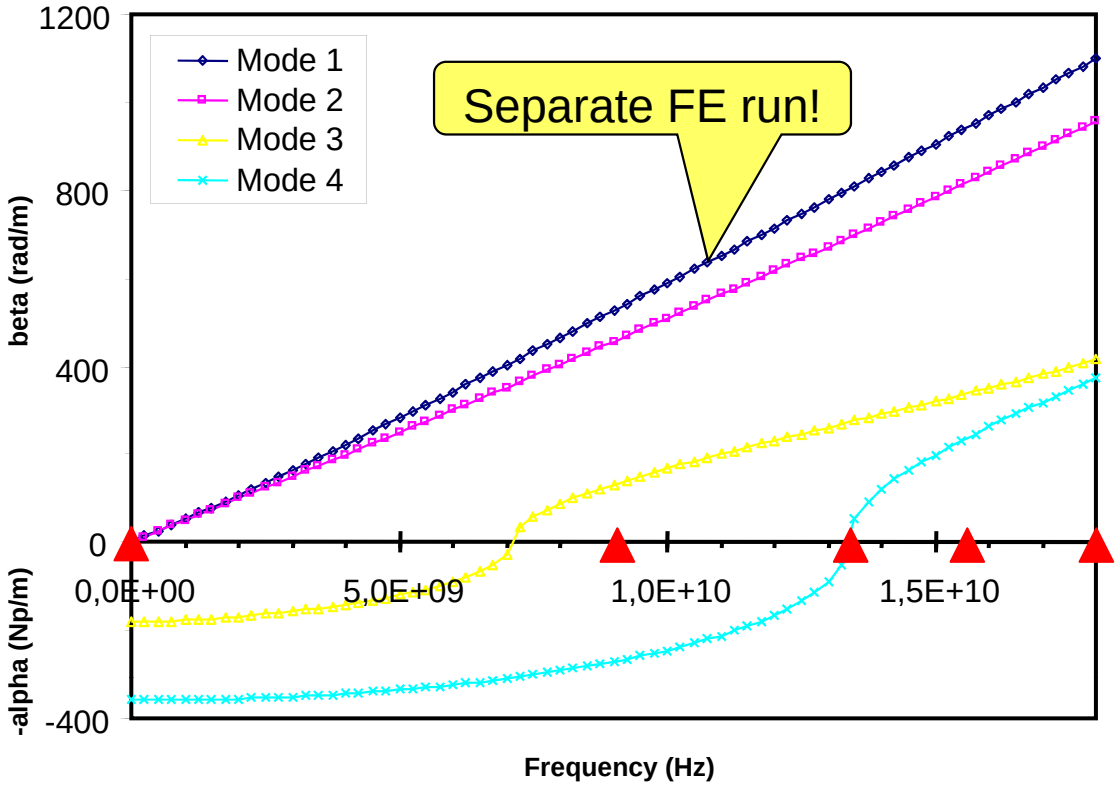

Stabilized FEM: **A**-ϕ Potential Formulation

A-ϕ Potentials: $\mathbf{B} = \nabla \times \mathbf{A}$ $\qquad \mathbf{E} = -c_0 \nabla \phi - jk_0 c_0 \mathbf{A}$

Underlying PDEs:

$$\begin{cases} \nabla \times [\nu_r] \nabla \times \mathbf{A} - k_0 [\varepsilon_r] \left(k_0 \mathbf{A} - j \nabla \phi \right) = 0 \\ \nabla \cdot [\varepsilon_r] \left(k_0 \mathbf{A} - j \nabla \phi \right) = 0 \end{cases}$$

Axial separation: $\mathbf{A} = \left(\mathbf{A}_t(x,y) + A_z(x,y) \hat{\mathbf{e}}_z \right) e^{-\gamma z}$

$\phi = V(x,y) e^{-\gamma z}$

Gauge: $\boxed{A_z \equiv 0}$

Tree elimination: $\mathbf{A}_t = \mathbf{A}_t^c(x,y) + \nabla_t \psi(x,y)$

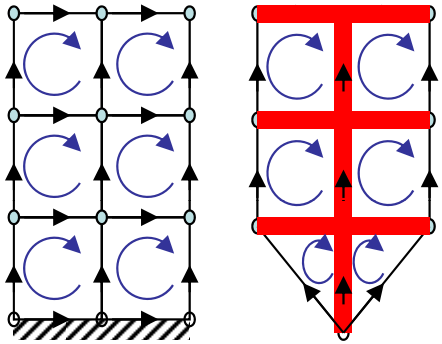

[Albanese1988]

FE discretization: $\boxed{\left(\mathbf{S}_0 + k_0 \mathbf{S}_1 + k_0^2 \mathbf{S}_2 \right) \mathbf{v} = \gamma^2 \mathbf{T}_0 \mathbf{v}}$ with $\mathbf{T}_0$ regular (SPD)

Orthogonality: $\mathbf{v}_p^T \mathbf{T}_0 \mathbf{v}_q (k_0^2) = 0$ for $p \neq q$.

Null-field solutions $\left(\vec{E} = 0, \vec{H} = 0 \right)$:

$$\left(\gamma^2 = 0, \mathbf{v}_0 = \begin{bmatrix} \vec{A}_t^c \\ \psi \\ jV \end{bmatrix} = \mathbf{N}(k_0) \psi \right) \quad \text{with } \mathbf{N}(k_0) = \begin{bmatrix} 0 \\ \mathbf{I} \\ k_0 \mathbf{I} \end{bmatrix}.$$

Numerical Example: **A**-ϕ FEM

- Krylov subspace method (Arnoldi):

  Constraint against null-fields: $\boxed{\mathbf{N}\left(k_0\right)^T \mathbf{T}_0 \mathbf{v}_i = \mathbf{0}}$.

- Shape functions : 2nd order,
- Eigenvalue problem of dimension 5991,
- 251 frequency points,
- Overall solution time 1018s $\left(16 \text{ min } 58\text{s}\right)$.

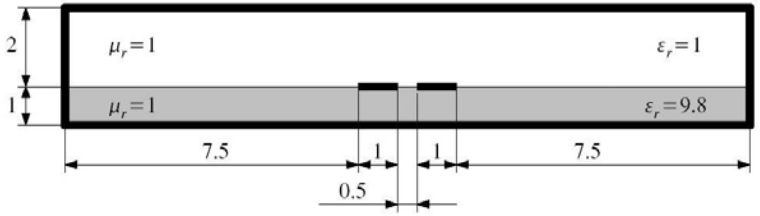

Shielded microstrip
Shielding and signal lines modeled as perfect conductors.

Propagation characteristics of 6 dominant modes

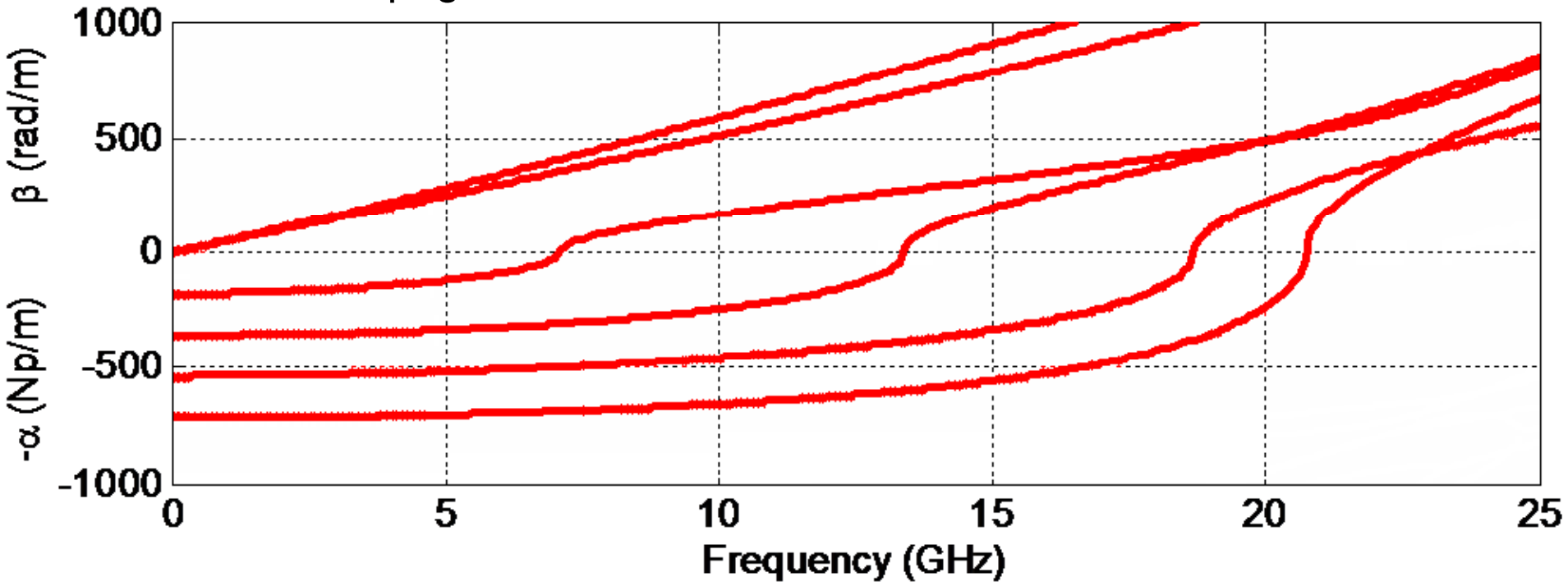

Model Order Reduction 1

- Projection approach

Approximation of eigenvalue problem in subspace of low dimension $q \ll p$.

Change of coordinates: $\mathbf{v} = \mathbf{Q}\tilde{\mathbf{v}}$ where $\mathbf{Q}$ projection matrix with dim $\mathbf{Q}=p\times q$.

Original problem: $(\mathbf{S}_0 + k_0\mathbf{S}_1 + k_0^2\mathbf{S}_2)\mathbf{v} = \gamma^2\mathbf{T}_0\mathbf{v}$ with $\dim \mathbf{v} = p$,

Galerkin projection: $(\tilde{\mathbf{S}}_0 + k_0\tilde{\mathbf{S}}_1 + k_0^2\tilde{\mathbf{S}}_2)\tilde{\mathbf{v}} = \tilde{\gamma}^2\tilde{\mathbf{T}}_0\tilde{\mathbf{v}}$ with $\dim \tilde{\mathbf{v}} = q$,

where $\tilde{\mathbf{S}}_0 = \mathbf{Q}^T\mathbf{S}_0\mathbf{Q}$, $\tilde{\mathbf{S}}_1 = \mathbf{Q}^T\mathbf{S}_1\mathbf{Q}$,

$\tilde{\mathbf{S}}_2 = \mathbf{Q}^T\mathbf{S}_2\mathbf{Q}$, $\tilde{\mathbf{T}}_0 = \mathbf{Q}^T\mathbf{T}_0\mathbf{Q}$.

- Choice of basis

Multi-point method:

m sought modes at

n expansion points.

$\mathbf{V} = \left[\mathbf{v}_1(k_1)\ldots\mathbf{v}_m(k_1);\ldots;\mathbf{v}_1(k_n)\ldots\mathbf{v}_m(k_n)\right]$

$\mathbf{V} = \mathbf{QR}$ …orthogonalization

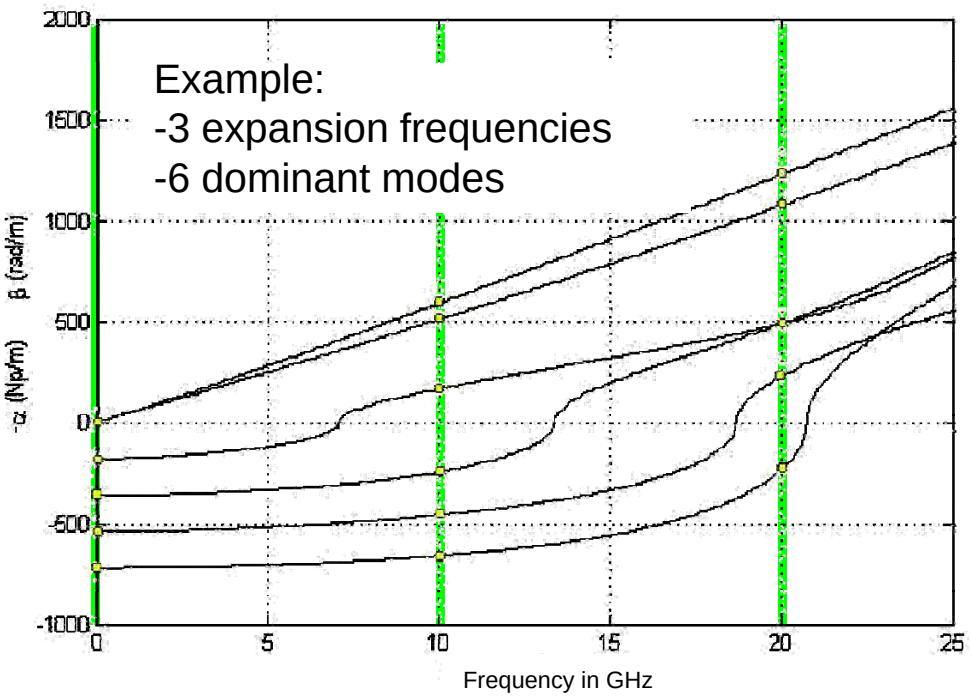

Model Order Reduction 2

- Dimension q = 18 (3 expansion points à 6 modes):
  - 6 sought modes,
  - 12 additional waveforms.

    Wanted: physical modes of higher order.

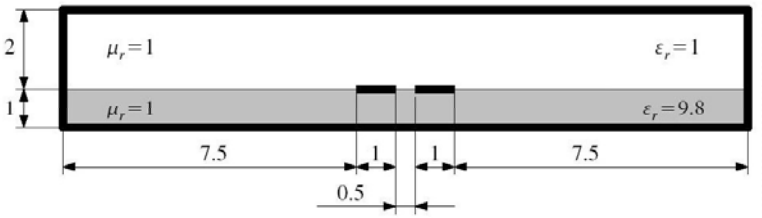

- Straight-forward application of model order reduction:
  - 6 sought modes,
  - 12 mixed waveforms: poorly approximated null-fields and higher order modes.
    - Spectral overlap with sought modes.
    - Propagable modes in static limit.

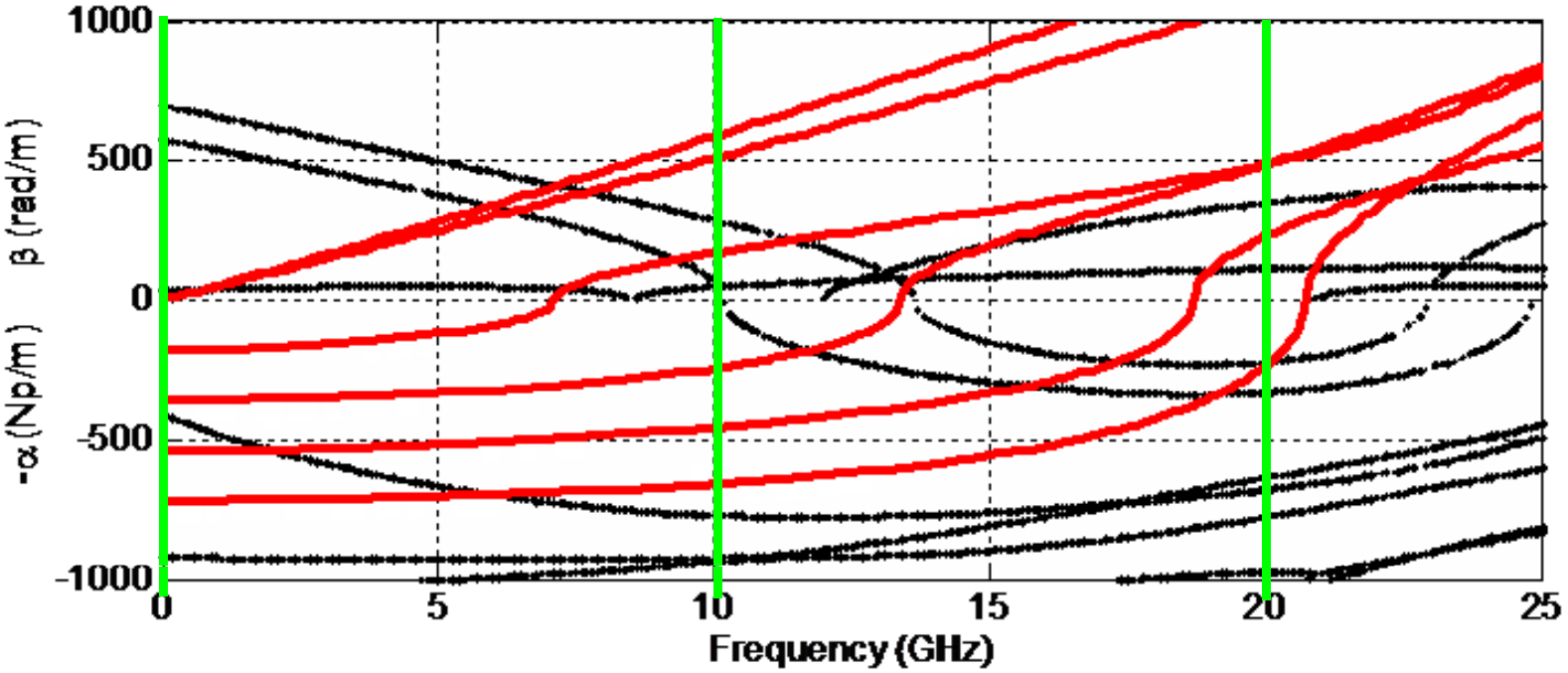

Null-Field Orthogonalization of MOR Space

- Mode orthogonality $\mathbf{N}^H\mathbf{T}\mathbf{v}_p = \mathbf{0}$:

$$\begin{bmatrix}\mathbf{0} & \mathbf{I} & k_0\mathbf{I}\end{bmatrix}\begin{bmatrix}\mathbf{T}_{AA}^{\nu\times} & \mathbf{B}_{AV}^{\nu\times} & \mathbf{0}\\ \mathbf{B}_{AV}^{\nu\times T} & \mathbf{S}_{VV}^{\nu\times} & \mathbf{0}\\ \mathbf{0} & \mathbf{0} & -\mathbf{T}_{VV}^{\varepsilon}\end{bmatrix}\begin{bmatrix}\mathbf{v}_{\vec{A}_t^c}\\ \mathbf{v}_{\psi}\\ \mathbf{v}_{jV}\end{bmatrix} = \mathbf{0}$$

$$\mathbf{v}_{\psi} = -\mathbf{S}_{VV}^{\nu\times -1}\mathbf{B}_{AV}^{\nu\times T}\mathbf{v}_{\vec{A}_t^c} - \mathbf{T}_{VV}^{\varepsilon}\mathbf{v}_{jV}$$

- Projection matrix:

$$\mathbf{Q}_0(k_0) = \begin{bmatrix}\mathbf{I} & \mathbf{0} & \mathbf{0}\\ -\mathbf{S}_{VV}^{\nu\times -1}\mathbf{B}_{AV}^{\nu\times T} & \mathbf{0} & k_0\mathbf{S}_{VV}^{\nu\times -1}\mathbf{T}_{VV}^{\varepsilon}\\ \mathbf{0} & \mathbf{0} & \mathbf{I}\end{bmatrix}\begin{bmatrix}\mathbf{Q}_{\vec{A}_t^c}\\ \mathbf{0}\\ \mathbf{Q}_{jV}\end{bmatrix}$$

- Resulting ROM:

$$\left(\hat{\mathbf{S}}_0 + k_0\hat{\mathbf{S}}_1 + k_0^2\hat{\mathbf{S}}_2 + k_0^3\hat{\mathbf{S}}_3 + k_0^4\hat{\mathbf{S}}_4\right)\hat{\mathbf{v}} = \gamma^2\left(\hat{\mathbf{T}}_0 + k_0\hat{\mathbf{T}}_1 + k_0^2\hat{\mathbf{T}}_2\right)\hat{\mathbf{v}}$$

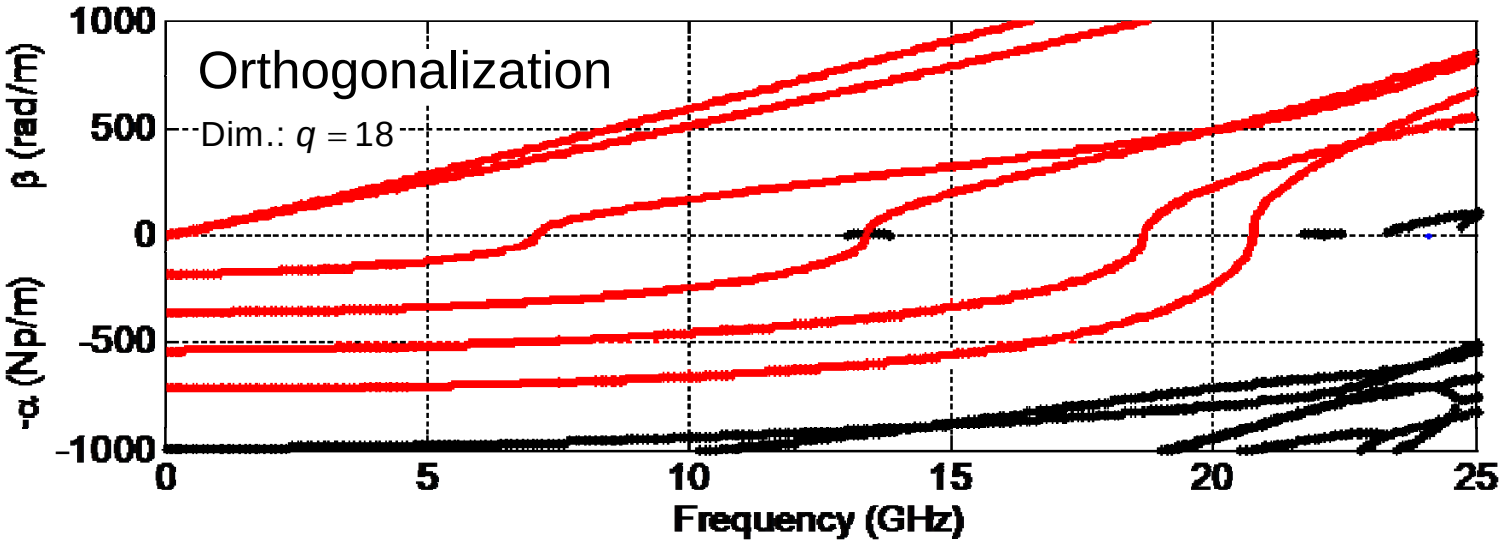

Results for Dominant Modes

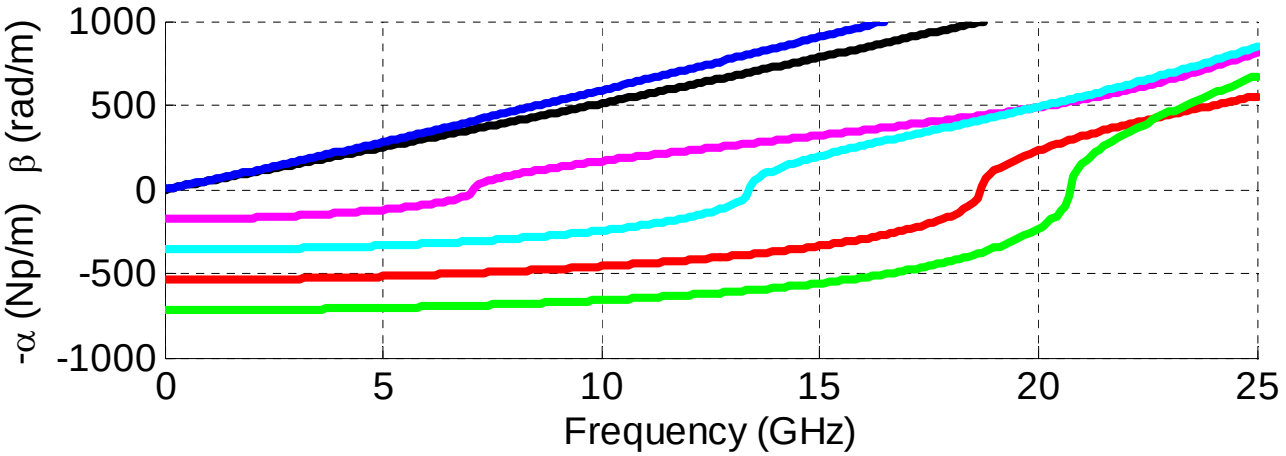

Error definition:

Eigenvalue: $e_\gamma = \left|\gamma - \tilde{\gamma}\right|$

Eigenvector: $e_v = \left\| \frac{v}{\|v\|_2} - \frac{Q_o(k)\tilde{v}}{\|Q_o(k)\tilde{v}\|_2} \right\|_2$

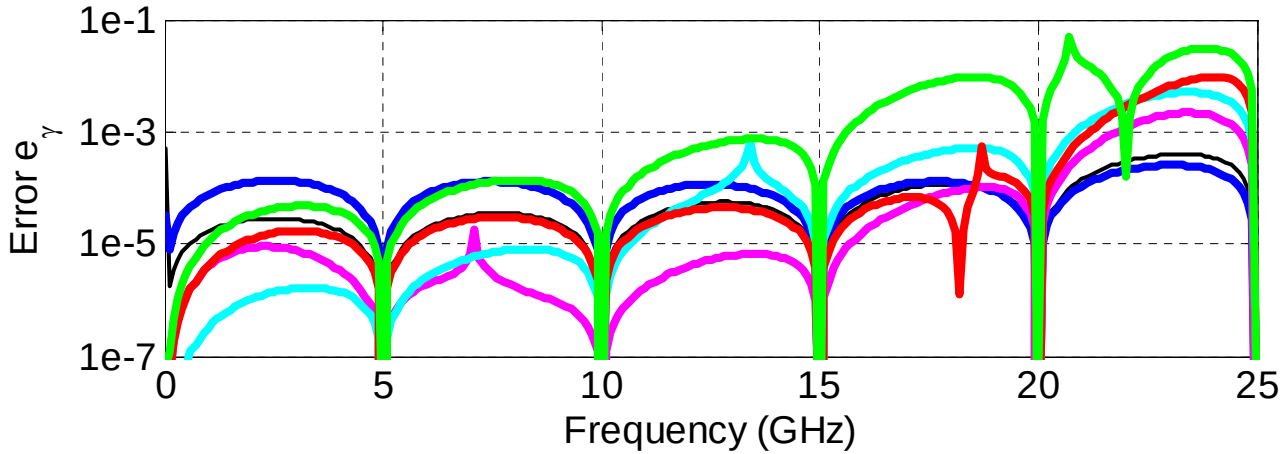

Computer runtimes:

Frequency points	251
Original problem:	1018 s
Reduced order model:	100 s
(Building 99s, Solving 0.7s)	

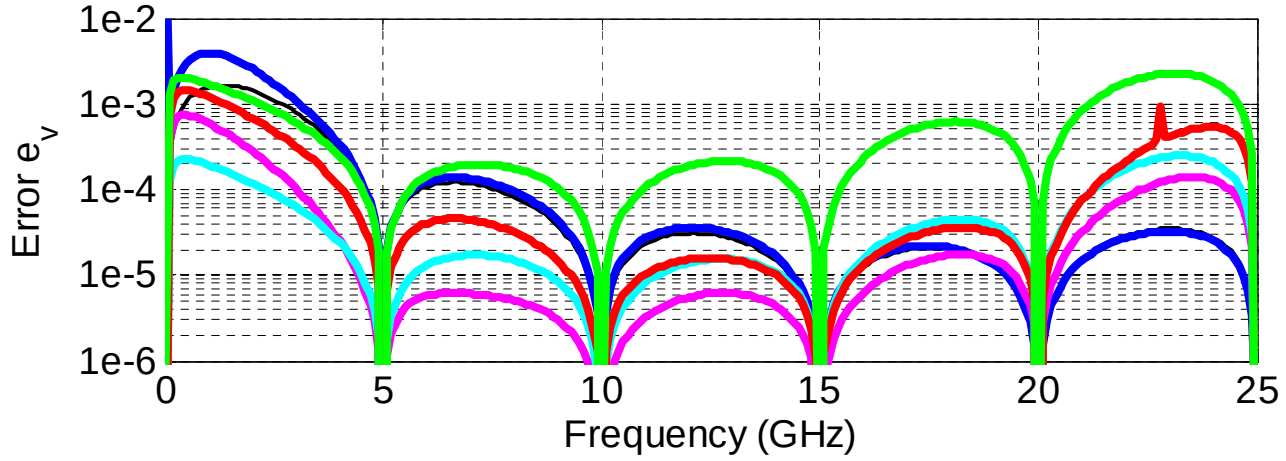

Self-Adaptive Point Placement Strategy

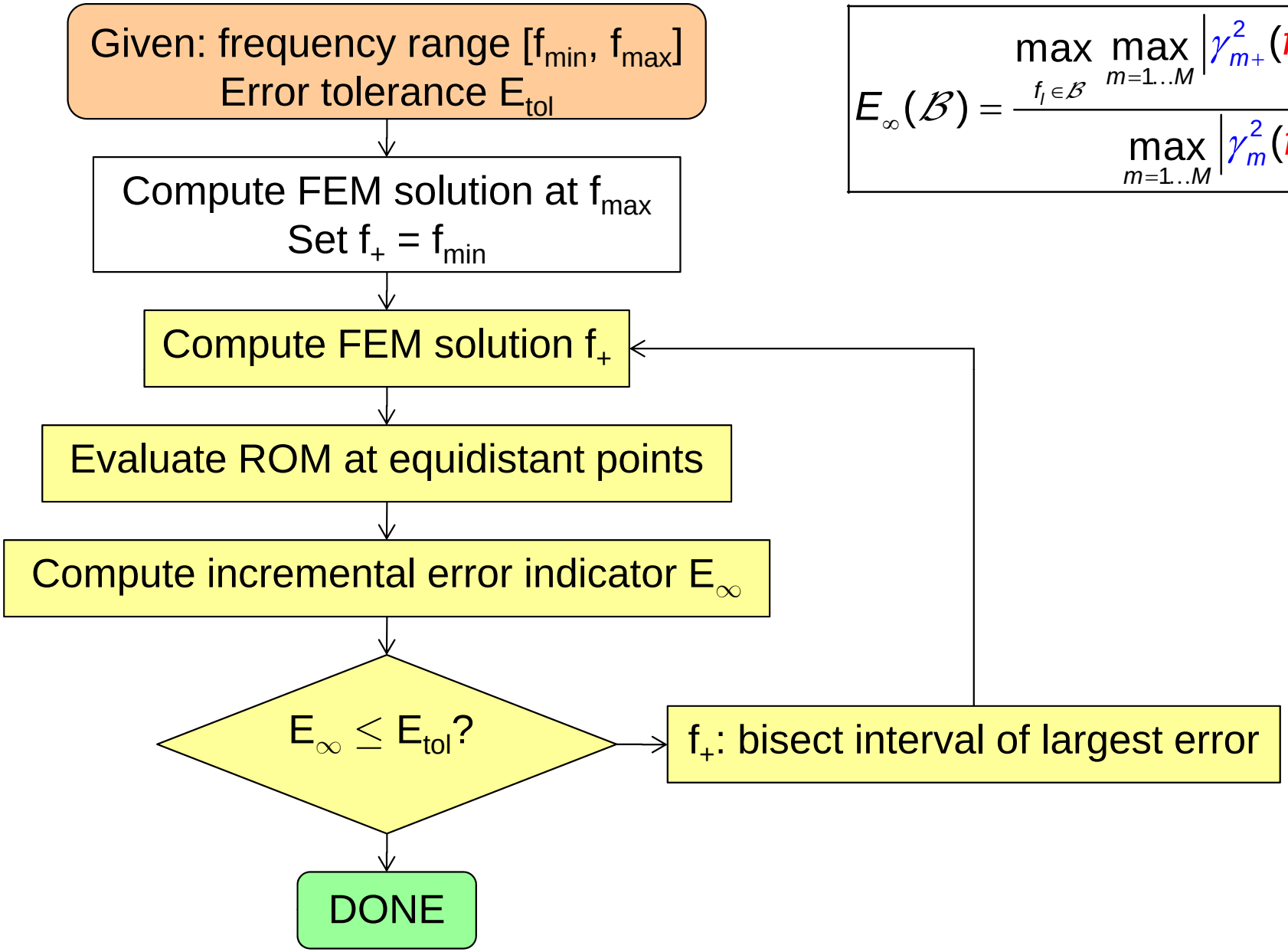

$$E_\infty(\mathcal{B}) = \frac{\max\limits_{f_l \in \mathcal{B}} \max\limits_{m=1..M} \left| \gamma_{m+}^2(f_l) - \gamma_{m-}^2(f_l) \right|}{\max\limits_{m=1..M} \left| \gamma_m^2(f_{max}) \right|}$$

Example: Dielectric Loaded Waveguide

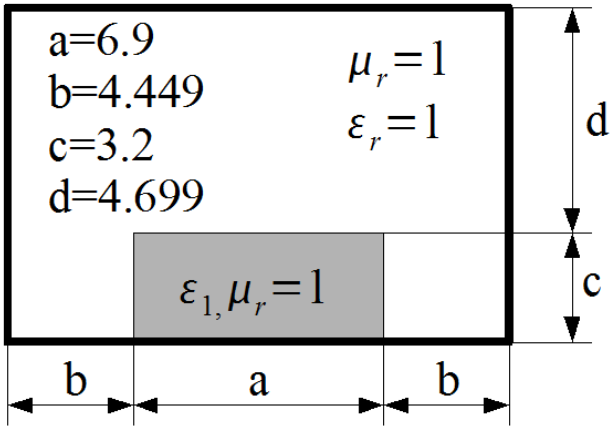

Parameters:

Substrate:	$\varepsilon_1 = 9\varepsilon_0$
Modes:	19 (23)
Evaluation points:	1001
Order of FE basis:	2
Unknowns:	12612
Error threshold E_{tol}:	10^{-6}
ROM dimension:	161

Computer runtimes:

Original FE model:	4827s
Adaptive ROM:	402s

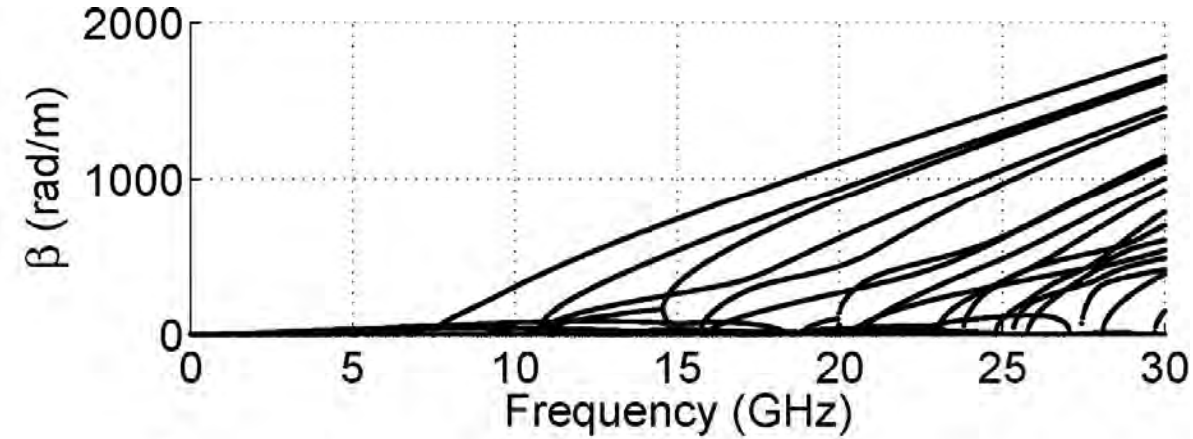

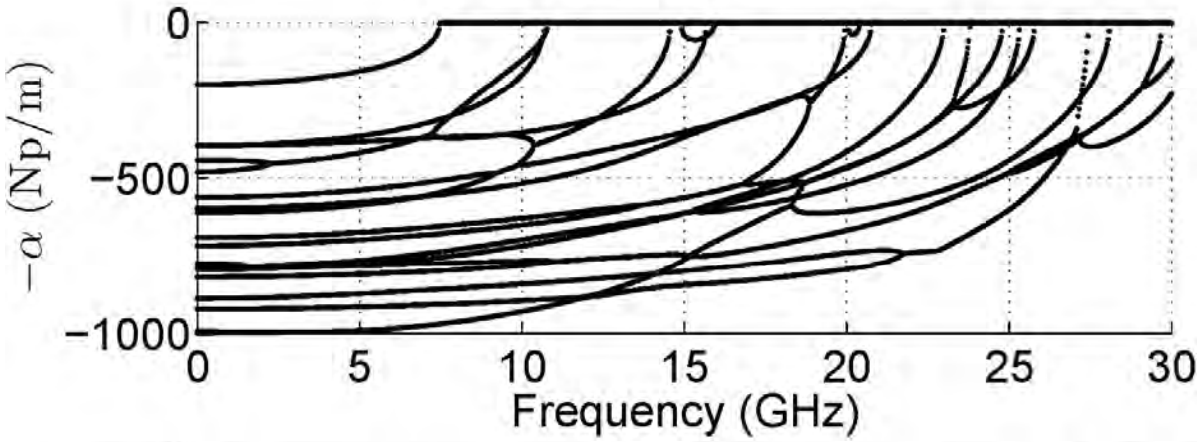

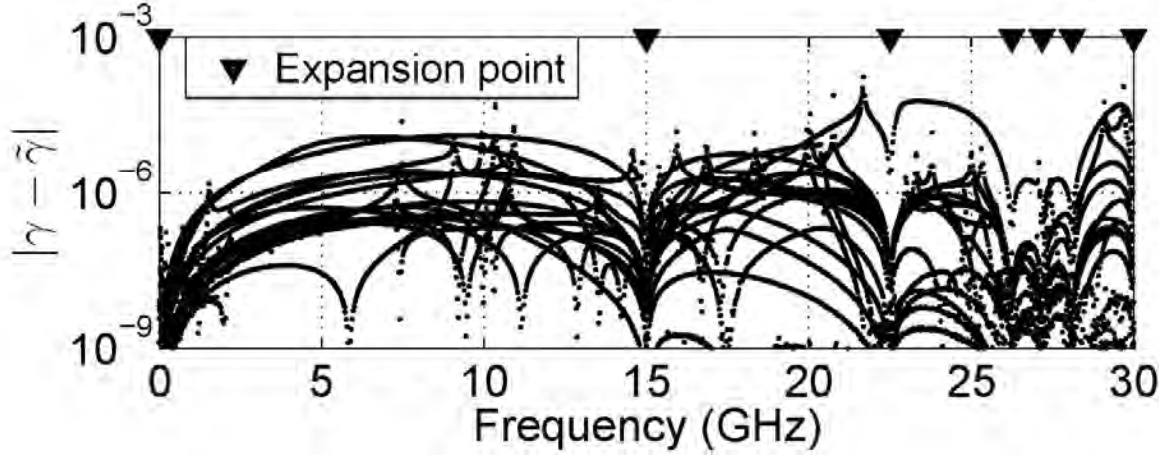

Fast Frequency Sweeps for Driven Problems

- Very large scale of FE systems
- Projection-based MOR:
  - Single-point methods: Krylov (Arnoldi, WCAWE [Slone2003])
  - Multi-point methods
- Adaptive scheme
  - Point placing as for WGs

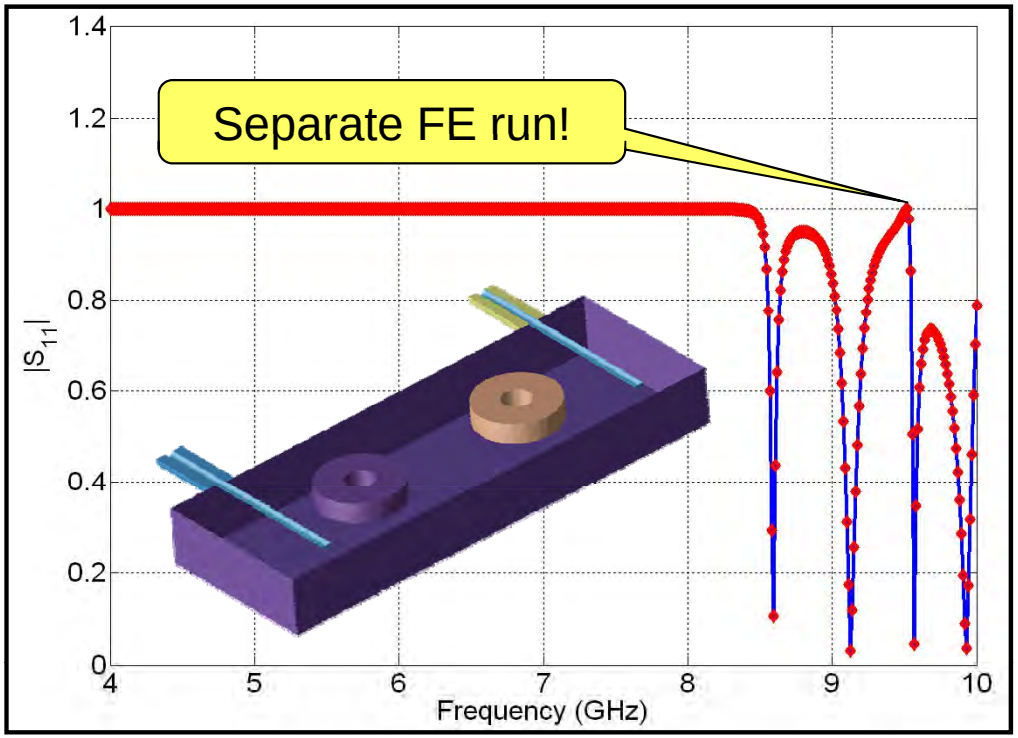

Structures Driven by Highly Dispersive WG's

Numerical Results:

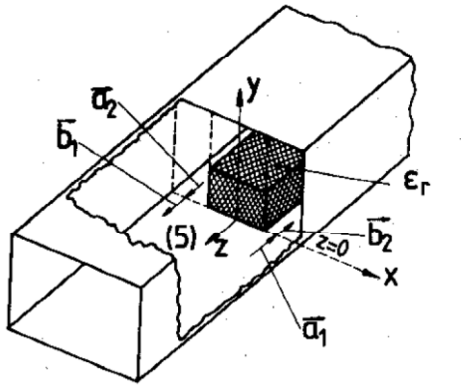

[Strube1985]

MOR for structure excited by 7 modes

MOR generation time:
(7 expansion points,)
Waveguides: 10.8s (862 dof), 11.2s (847 dof)
Structure: 119.7s (22122 dof)

MOR evaluation points: 301

MOR evaluation time:
Waveguides: 1.7s (49 dof), 2.9s (49 dof)
Structure: 5.8s (98 dof)

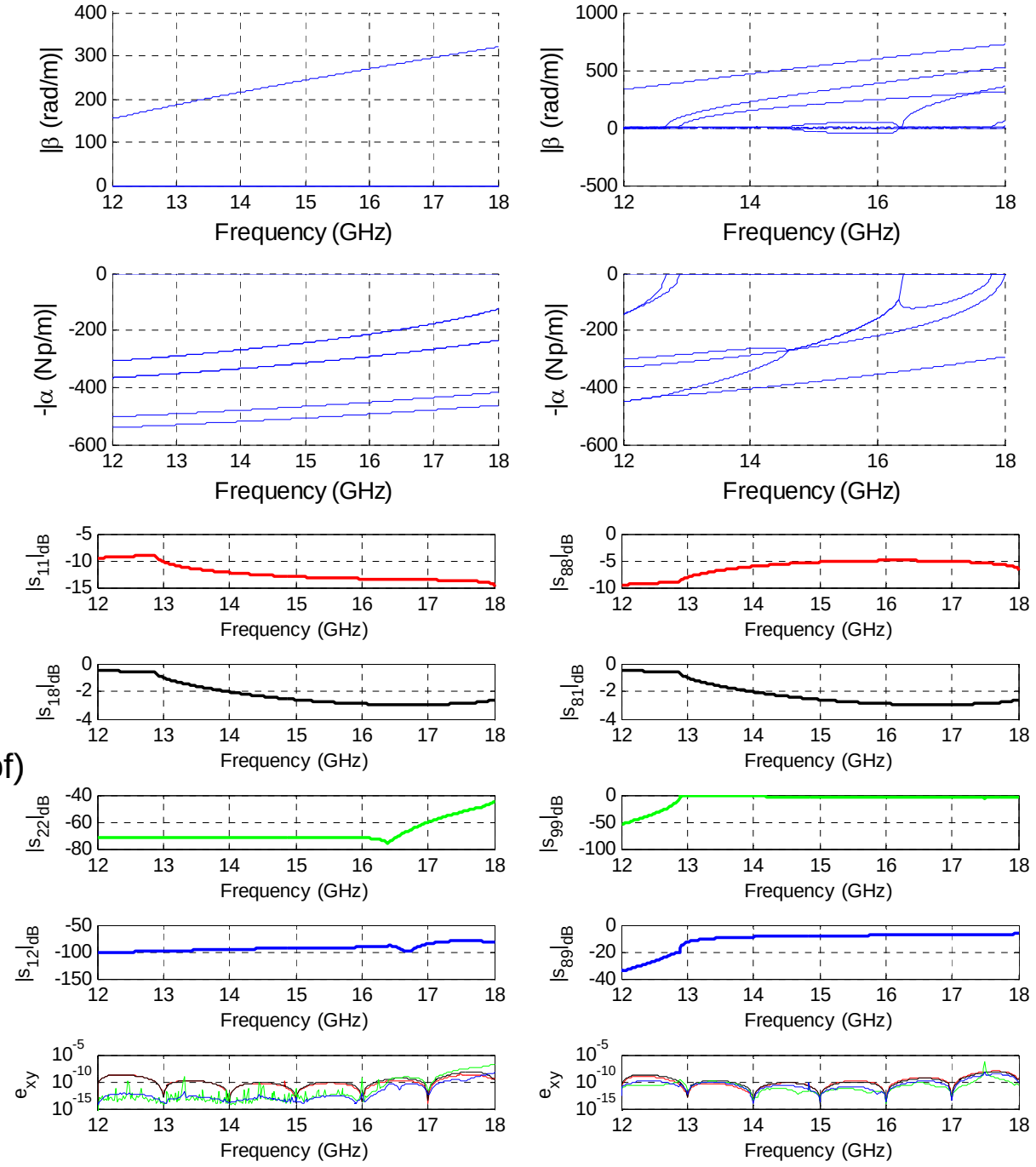

A posteriori Error Estimator for Lossless Problems

Impedance formulation: projection of linear FE system

$$\begin{cases} \left(\mathbf{S} - k_0^2\mathbf{T}\right)\mathbf{x} = jk_0\eta_0\mathbf{b}, \\ z = \mathbf{b}^T\mathbf{x}, \end{cases} \xrightarrow[\mathbf{Q}_m^T\times]{\mathbf{x}=\mathbf{Q}_m\tilde{\mathbf{x}}} \begin{cases} \mathbf{Q}_m^T(\mathbf{S} - k_0^2\mathbf{T})\mathbf{Q}_m\tilde{\mathbf{x}} = jk_0\eta_0\mathbf{Q}_m^T\mathbf{b}, \\ \tilde{z} = \mathbf{b}^T\mathbf{Q}_m\tilde{\mathbf{x}}. \end{cases}$$

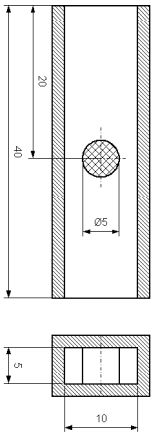

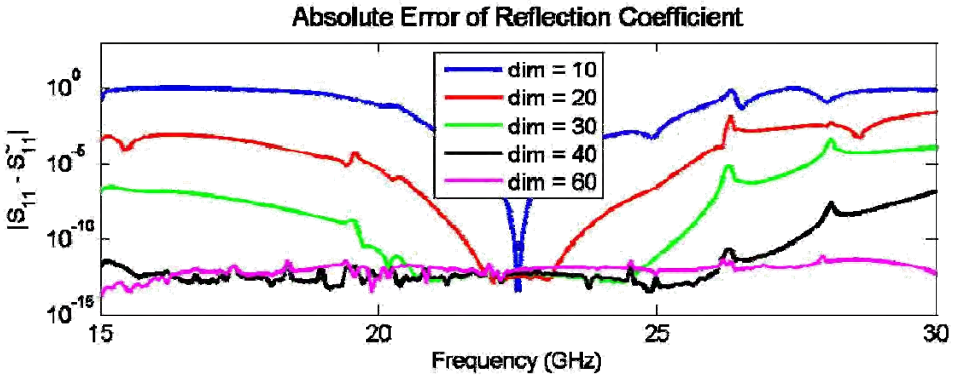

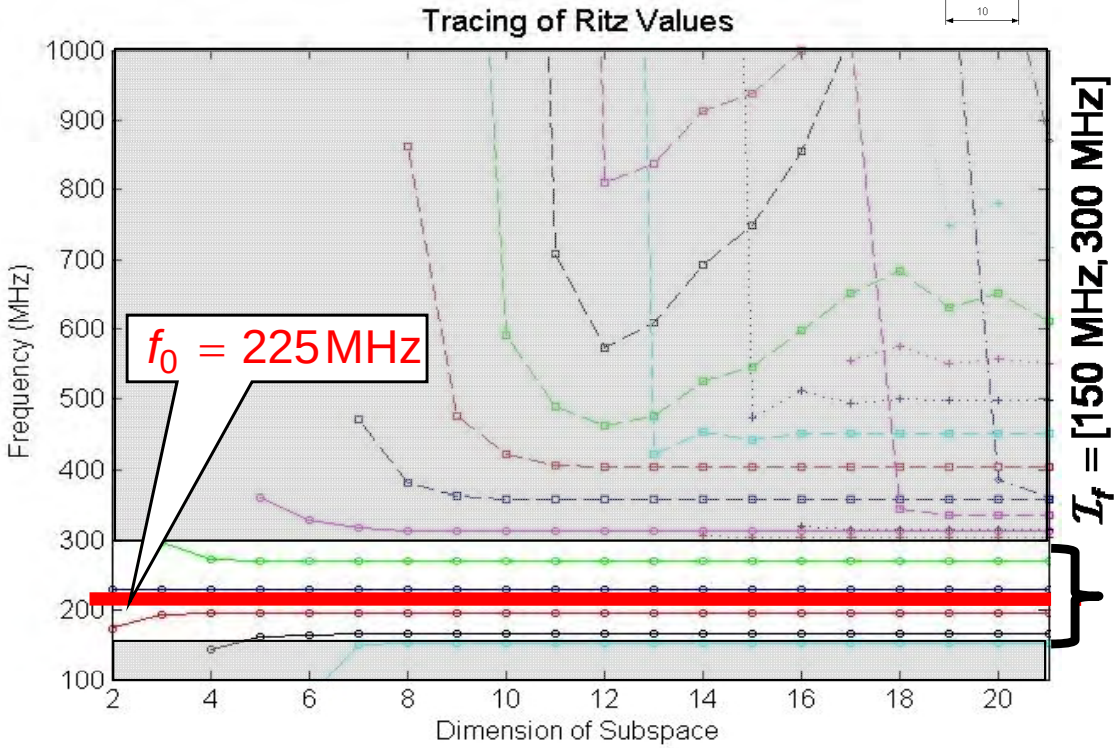

- Typical behavior of single-point ROM: quality depends strongly on model dimension.
- What is the minimal dimension that **guarantees** a given error threshold?

Error Estimator: Error Representation

Error equation

$$(\mathbf{A}_0 - \kappa \mathbf{A}_1)\mathbf{e} = \mathbf{r},$$
$$\text{with } \mathbf{e} := \mathbf{x} - \mathbf{Q}_m \tilde{\mathbf{x}}.$$

Eigenmode expansion

$$\mathbf{e}(\kappa) = \sum_{i=1}^{N} \mathbf{v}_i \frac{\mathbf{v}_i^T \mathbf{r}}{\kappa_i - \kappa}.$$

Output error

$$e_z(\kappa) = z(\kappa) - \tilde{z}(\kappa) = jk_0\eta_0 \mathbf{b}^T \mathbf{e}(\kappa),$$
$$\Rightarrow e_z(\kappa) = jk_0\eta_0 \sum_{i=1}^{N} \frac{(\mathbf{b}^T \mathbf{v}_i)(\mathbf{v}_i^T \mathbf{r})}{\kappa_i - \kappa}.$$

Partition the sum:

- S_p : Contribution from $\mathcal{I}_f$
- S_N : Contribution exterior of $\mathcal{I}_f$

$$e_z(\kappa) = jk_0\eta_0 \left(\underbrace{\sum_{i=1}^{p} \frac{(\mathbf{b}^T \mathbf{v}_i)(\mathbf{v}_i^T \mathbf{r})}{\kappa_i - \kappa}}_{=: S_p} + \underbrace{\sum_{i=p+1}^{N} \frac{(\mathbf{b}^T \mathbf{v}_i)(\mathbf{v}_i^T \mathbf{r})}{\kappa_i - \kappa}}_{=: S_N} \right).$$

Strategy: S_p: Enforce convergence of in-band Ritz values and Ritz vectors.
S_N: Estimate out-of-band contributions.

Error Estimator: Computational Details

Error in in-band Ritz values:

$$\left|\tilde{\kappa}_i - \kappa_i\right| \le \left[\tilde{\kappa}_i^2 (\tilde{\mathbf{v}}_i^T \mathbf{e}_n)(\mathbf{r}_0^T \mathbf{A}_1^{-1} \mathbf{r}_0)(\mathbf{e}_n^T \tilde{\mathbf{v}}_i)\right]^{1/2},$$

$$\mathbf{r}_0 := h_{n+1,n} \mathbf{A}_0 \left[\mathbf{I} - \mathbf{Q}\tilde{\mathbf{V}} \operatorname{diag} \frac{1}{\tilde{\kappa}_i} \tilde{\mathbf{V}}^T \mathbf{Q}^T \mathbf{A}_0\right] \mathbf{q}_{n+1}.$$

- Computation of $\mathbf{r}_0$ is based on ROM.
- Main cost: $\mathbf{A}_1^{-1}\mathbf{r}_0$ once per iteration step.

- Assumption: $\tilde{\kappa}_i$ in $\mathcal{I}_f$ fulfills $\left|\tilde{\kappa}_i - \kappa_i\right| \le \varepsilon_\kappa$,

$$\Rightarrow (\tilde{\kappa}_i, \mathbf{Q}_m \tilde{\mathbf{v}}_i) \approx (\hat{\kappa}_i, \mathbf{v}_i) \forall i \le p.$$

- Since $\mathbf{r} \perp \operatorname{ran} \mathbf{Q}_m$ we have $S_p \approx \sum_{i=1}^{p} \frac{(\mathbf{b}^T \mathbf{Q}_m \tilde{\mathbf{v}}_i)\left(\tilde{\mathbf{v}}_i^T \mathbf{Q}_m^T \mathbf{r}\right)}{\tilde{\kappa}_i - \kappa} = 0.$

Output error $e_z = jk_0\eta_0 \mathbf{b}^T (\mathbf{A}_0 - \kappa \mathbf{A}_1)^{-1} \mathbf{r} = -jk_0\eta_0 \mathbf{r}^T \mathbf{V} \operatorname{diag} \frac{1}{\kappa_i - \kappa} \mathbf{V}^T \mathbf{r}.$

Contributions of out-of-band Ritz values:

- Eigenvalues in $\mathcal{I}_f$ are converged: $\operatorname{span}\{\mathbf{v}_1, \ldots, \mathbf{v}_B\} \subset \operatorname{ran} \mathbf{Q}$,

$$\left|e_z(\kappa)\right| \le k_0\eta_0 \mathbf{r}(\kappa)^T \mathbf{V} \operatorname{diag} \frac{1}{\kappa_i - \kappa} \mathbf{V}^T \mathbf{r}(\kappa)$$

$$\le \frac{k_0\eta_0}{\min\limits_{\kappa_i \notin \mathcal{I}_f} |\kappa_i - \kappa|} \mathbf{r}(\kappa)^T \mathbf{V}\mathbf{V}^T \mathbf{r}(\kappa) \le \frac{k_0\eta_0}{\min\limits_{\kappa_i \notin \mathcal{I}_f} |\kappa_i - \kappa|} \mathbf{r}^T(\kappa) \mathbf{A}_1^{-1} \mathbf{r}(\kappa).$$

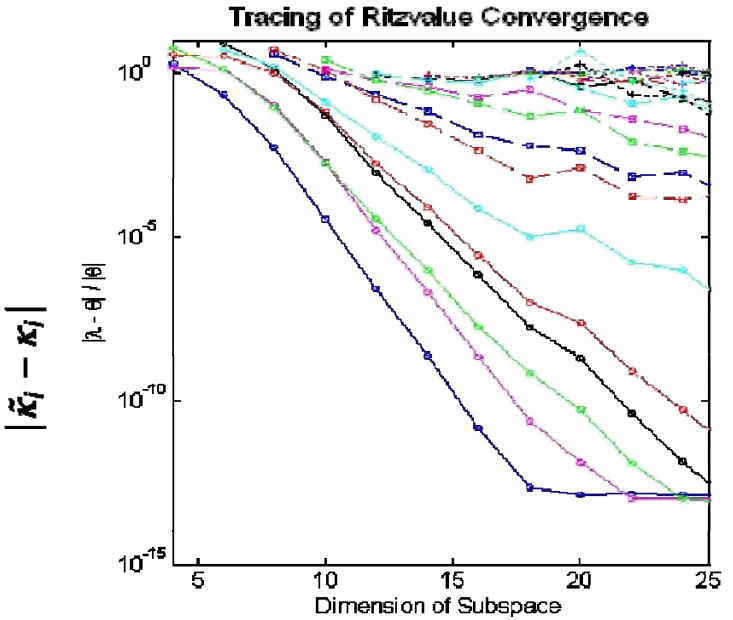

$$\left|\tilde{\kappa}_i - \kappa_i\right| \le \varepsilon_\lambda := \frac{\left\|(\mathbf{A}_0 - \tilde{\kappa}_i \mathbf{A}_1)\mathbf{Q}_m \tilde{\mathbf{v}}_i\right\|_{\mathbf{A}_1^{-1}}}{\left\|\mathbf{T}\mathbf{Q}_m \tilde{\mathbf{v}}_i\right\|_{\mathbf{A}_1^{-1}}}$$

[Bai2000, pp. 129-130]

Fast residual computation:

- Compute Ritz pairs $(\tilde{\kappa}_i, \tilde{\mathbf{v}}_i)$
- Change to Ritz basis: $\tilde{\mathbf{x}} = \tilde{\mathbf{V}}\tilde{\mathbf{w}}$,

$$\tilde{\mathbf{w}} = \operatorname{diag} \frac{1}{\tilde{\kappa}_i - \kappa} \tilde{\mathbf{V}}^T \tilde{\mathbf{b}},$$

$$\mathbf{r} = -\kappa \mathbf{r}_0 (\mathbf{e}_n^T \tilde{\mathbf{V}} \tilde{\mathbf{w}}),$$

$$\mathbf{r}(\kappa)^T \mathbf{A}_1^{-1} \mathbf{r}(\kappa) = \kappa^2 (\mathbf{e}_n^T \tilde{\mathbf{V}} \tilde{\mathbf{w}})^T \mathbf{r}_0^T \mathbf{A}_1^{-1} \mathbf{r}_0 (\mathbf{e}_n^T \tilde{\mathbf{V}} \tilde{\mathbf{w}}).$$

Example: Bandpass Filter

Error measure:

$$E_\infty(\mathbf{M}, \mathcal{I}_f) = \max_{i,j,n} \left| M_{ij}(f_n) \right|,$$

$$\mathbf{M} = \begin{cases} \mathbf{Z}^{ROM} - \mathbf{Z}^{FE} & \text{for impedance matrices,} \\ \mathbf{S}^{ROM} - \mathbf{S}^{FE} & \text{for scattering matrices.} \end{cases}$$

		Bandpass
Parameters	N	213 472
	n	12
	n_f	201
Offline time	New error est.	3 s
	State of the art	18 943 s
Online time	New error est.	1.36 s
	State of the art	1.57 s

Reference estimator: residual-based, inf-sup constant estimation by SCM method [Huynh2007], [Chen2010]

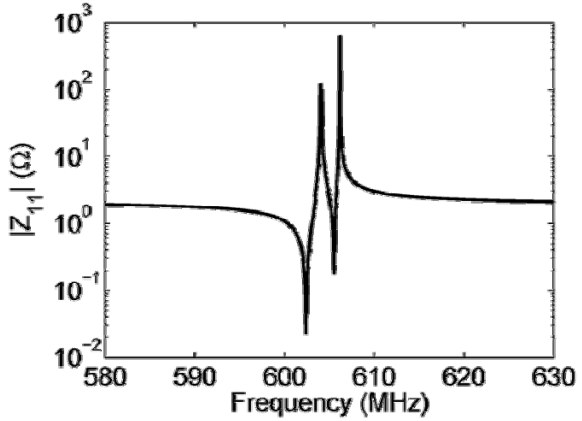

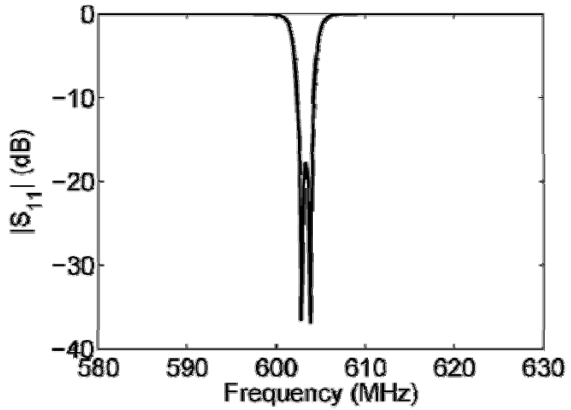

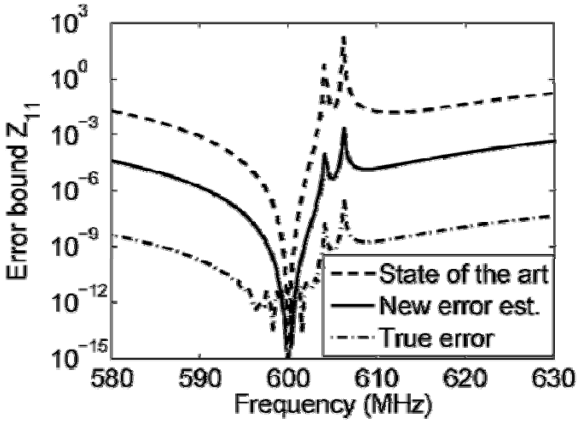

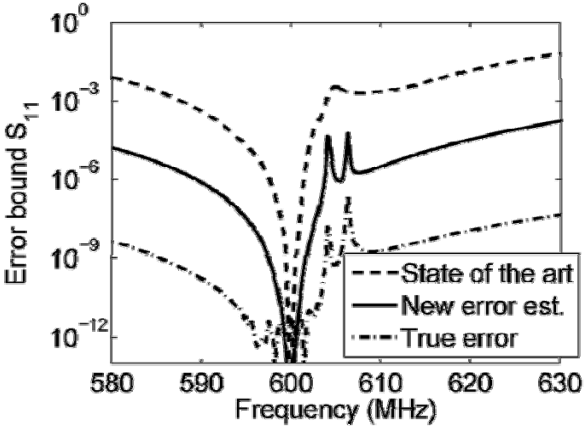

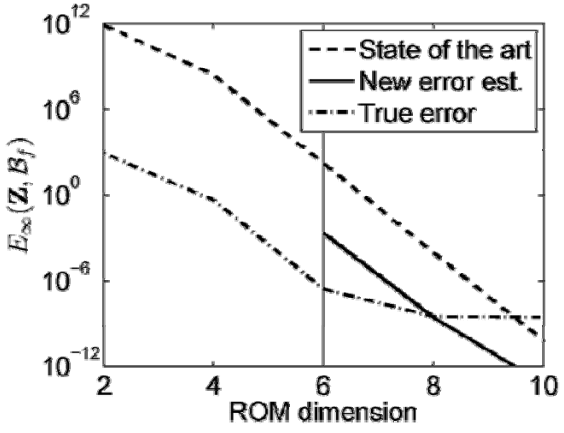

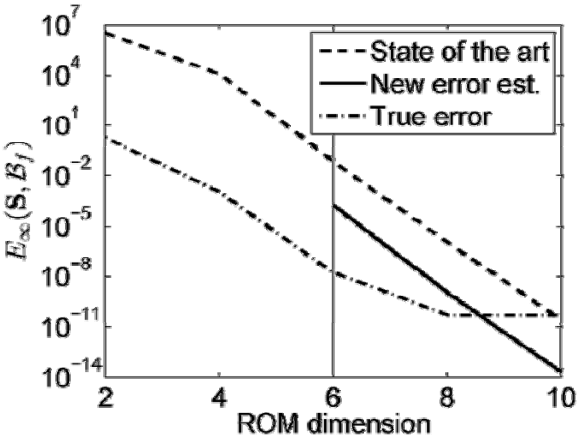

Far Field Computation

Phased Antenna Arrays

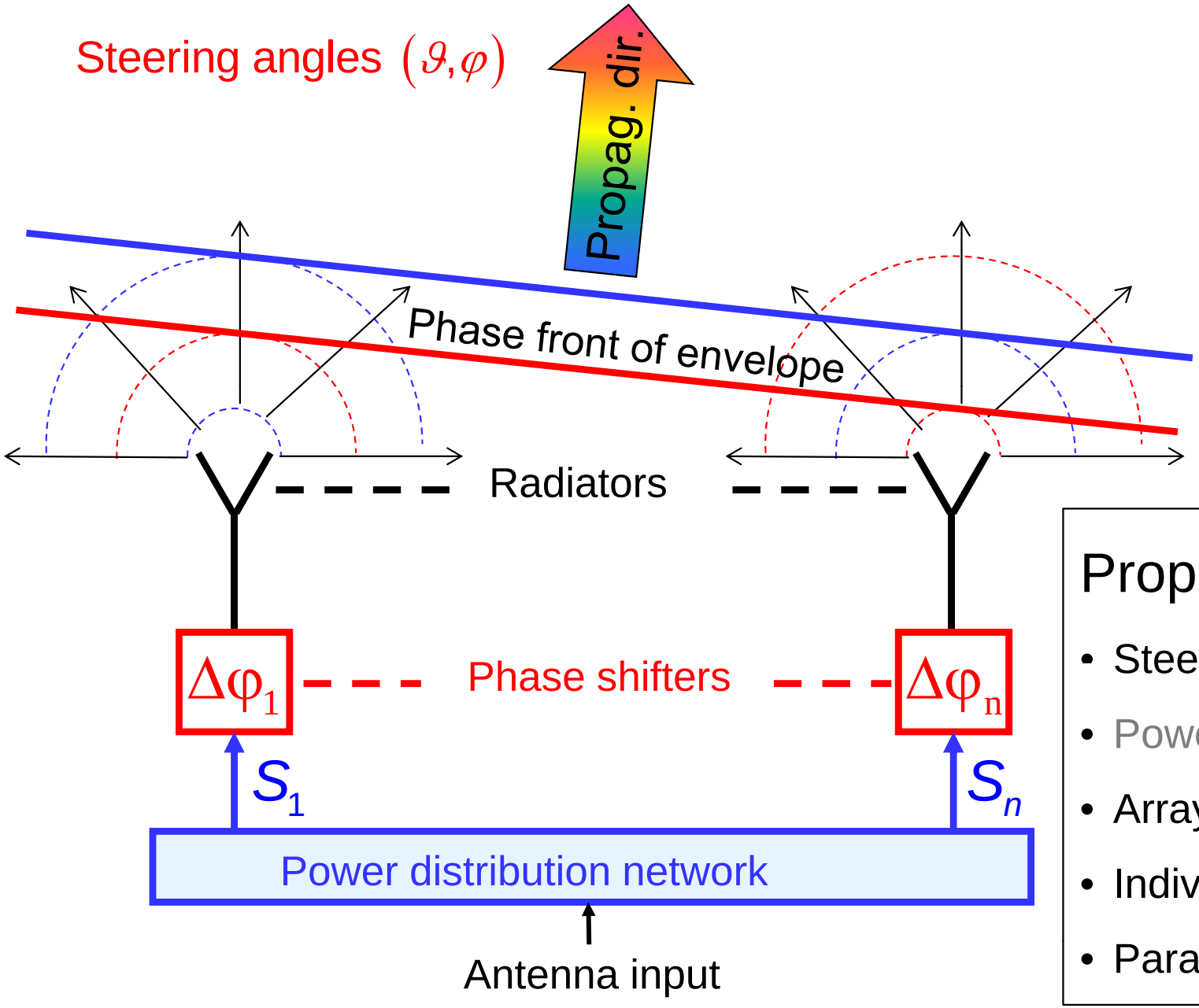

Propagation charact.

- Steering angles
- Power distribution
- Array size and structure
- Individual radiators
- Parasitic coupling

General Aspects

- **Far-Field computation of phased antenna arrays:**
  → $\mathbf{H}_F(\omega,\theta_s,\phi_s,\theta,\phi)$ and $\mathbf{E}_F(\omega,\theta_s,\phi_s,\theta,\phi)$
  → *Process depends on 5 different parameters!*

- **Numerical computation using FEM:**
  → *Time-consuming procedure even for one selected constellation of* (ω,θ_s,ϕ_s) *!*

- ***Solution:* two-step model order reduction approach:**
  → *Enables the generation of a reduced model for efficiently computing the far fields of the array!*

- ***Contributions*:**
  → Frequency slicing greedy method for direct solvers
  → Provable error bound for the directive gain
  → Sub-domain approach for fast online computations

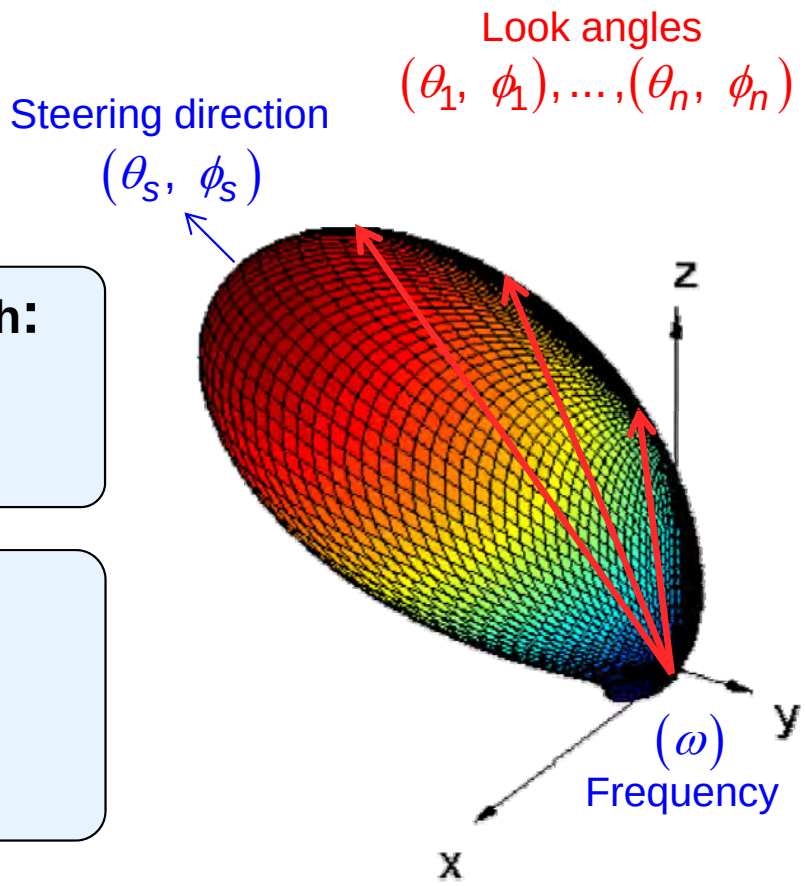

Far-Field Computation - Vector Huygens Principle

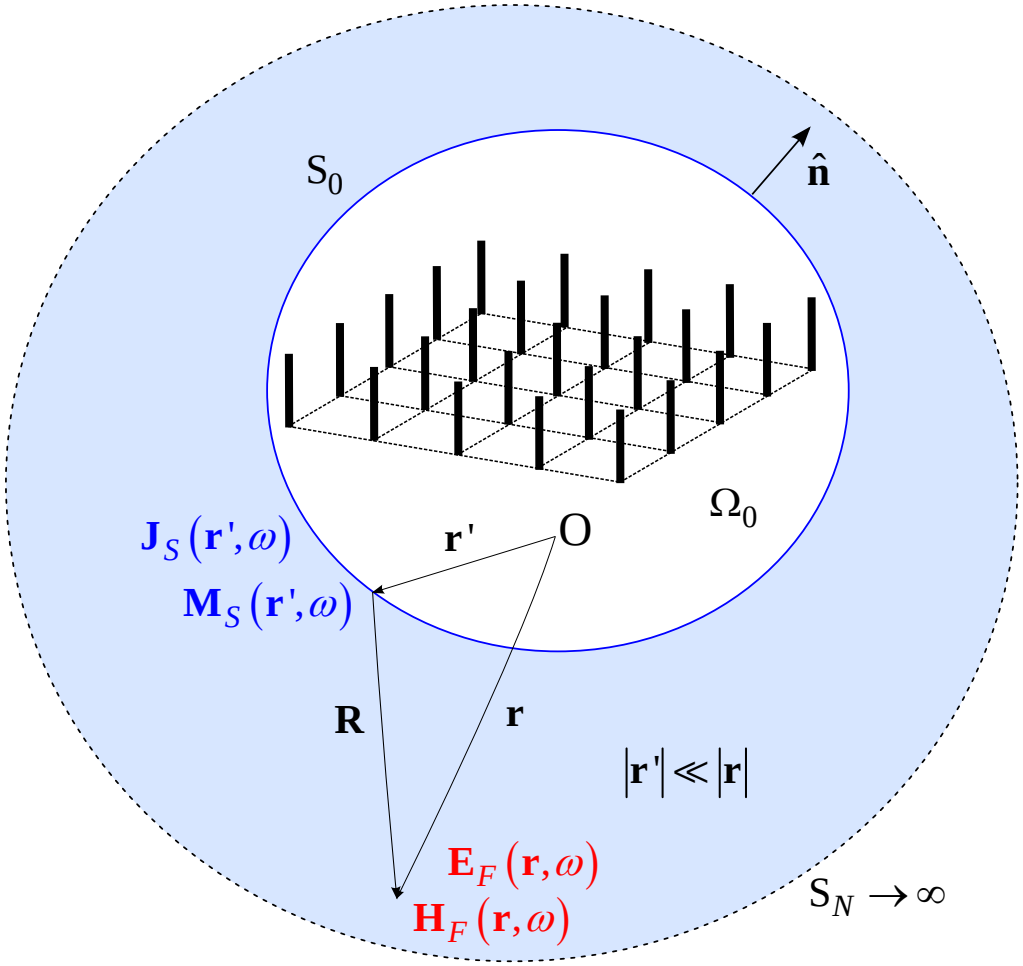

1a. Computation of the electric and magnetic near-fields in Ω_0.

$$\rightarrow \mathbf{H}(\mathbf{r}',\omega) \text{ and } \mathbf{E}(\mathbf{r}',\omega) \text{ in } \Omega_0.$$

1b. Determination of the equivalent electric and magnetic surface current densities on S_0.

$$\mathbf{J}_S(\mathbf{r}',\omega) = \hat{\mathbf{n}} \times \mathbf{H}(\mathbf{r}',\omega), \quad \mathbf{M}_S(\mathbf{r}',\omega) = -\hat{\mathbf{n}} \times \mathbf{E}(\mathbf{r}',\omega)$$

2. Computation of radiation vector, electric and magnetic far-fields, and directive gain.

$$\mathbf{F}(\hat{\mathbf{r}},\omega) = \oint_{S_0} e^{jk\hat{\mathbf{r}}\cdot\mathbf{r}'} \left[\mathbf{J}_S - \hat{\mathbf{r}}(\hat{\mathbf{r}} \cdot \mathbf{J}_S) + \frac{1}{\eta} \mathbf{M}_S \times \hat{\mathbf{r}} \right] dS'$$

$$\mathbf{E}_F(\mathbf{r}',\omega) = -j\eta k \frac{e^{-jkr}}{4\pi r} \mathbf{F}(\hat{\mathbf{r}},\omega)$$

$$\mathbf{H}_F(\mathbf{r}',\omega) = -j\eta \frac{e^{-jkr}}{4\pi r} \hat{\mathbf{r}} \times \mathbf{F}(\hat{\mathbf{r}},\omega)$$

$$D(\hat{\mathbf{r}},\omega) = 10\log_{10}\left(\frac{\eta k^2}{8\pi P_{rad}} \left(\left|F_\theta(\hat{\mathbf{r}},\omega)\right|^2 + \left|F_\phi(\hat{\mathbf{r}},\omega)\right|^2 \right) \right)$$

Numerical Near-Field Computation

1. Numerical computation of the electric and magnetic near-fields on the Huygens surface S_0.

FE discretization of a phased array of P antennas results in a system of linear equations of the form:

$$\left(\mathbf{A}_0 + \omega\mathbf{A}_1 + \omega^2\mathbf{A}_2\right)\mathbf{x}(\omega,\theta_s,\phi_s) = \omega\sum_{m=1}^{P} u_m(\omega,\theta_s,\phi_s)\mathbf{b}_m \quad \text{with} \quad \mathbf{A}_q \in \mathbb{C}^{N\times N}, \mathbf{b}_m \in \mathbb{C}^N$$

$$\mathbf{y}_{NF}(\omega,\theta_s,\phi_s) = \left(\mathbf{C}_0 + \omega^{-1}\mathbf{C}_{-1}\right)\mathbf{x}(\omega,\theta_s,\phi_s) \quad \text{with} \quad \mathbf{C}_r \in \mathbb{C}^{6H\times N}$$

FE system exhibits affine parameter dependence of the form:

$$\left(\sum_q \theta_q(\mu)\mathbf{A}_q\right)\mathbf{x}(\mu) = \sum_m \vartheta_m(\mu)\mathbf{b}_m, \quad \mathbf{y}(\mu) = \sum_r \xi_r(\mu)\mathbf{C}_r\mathbf{x}(\mu)$$

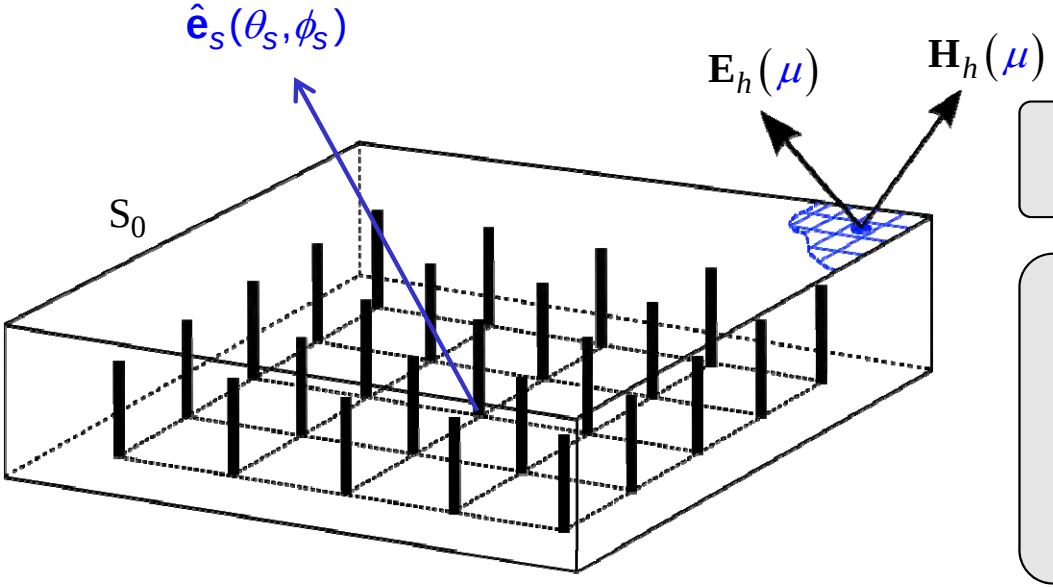

Introduction of $\mu = (\omega,\theta_s,\phi_s) \in D \subset \mathbb{R}^3$.

Problem: For each $\mu \in D$ of interest, $\mathbf{y}_{NF}(\mu)$ is obtained by solving the large-scale FE system.

→ ***Time-consuming procedure:***

Requires up to $O(N^2)$ operations!

Self-Adaptive Expansion Point Selection

Multi-point MOR method: $\text{range}\,\mathbf{V} = \text{span}\left[\mathbf{x}(\mu_1),\ldots,\mathbf{x}(\mu_n)\right]$ with $\mu_i = (\omega_i, \theta_{s,i}, \phi_{s,i}) \in D_{ex} \subset D_{train}$

Residual of the FE system: $$\mathbf{r}(\mu) = \sum_{q=0}^{2} \omega^q \mathbf{A}_q \mathbf{V}\tilde{\mathbf{x}}(\mu) - \omega \sum_{m=1}^{P} u_m(\mu)\mathbf{b}_m$$

Error indicator: $$e_r(\mu) = \frac{\|\mathbf{r}(\mu)\|_2}{\rho_0}, \quad \rho_0 = \max_{\mu \in D_{train}} \left\| \sum_{q=0}^{2} \omega^q \mathbf{A}_q \hat{\mathbf{x}}_1(\mu) - \omega \sum_{m=1}^{P} u_m(\mu)\mathbf{b}_m \right\|_2$$

Efficient evaluation:

$$\|\mathbf{r}(\mu)\|_2^2 = \mathbf{r}^H(\mu)\mathbf{r}(\mu) = \sum_{q_1=0}^{2}\sum_{q_2=0}^{2} \omega^{q_1+q_2} \tilde{\mathbf{x}}(\mu)^H \left(\mathbf{V}^H \mathbf{A}_{q_1}^H \mathbf{A}_{q_2} \mathbf{V}\right) \tilde{\mathbf{x}}(\mu)$$

$$- 2\,\text{Re}\left\{ \sum_{q=0}^{2}\sum_{m=1}^{P} \omega^{q+1} u_m(\mu) \tilde{\mathbf{x}}(\mu)^H \left(\mathbf{V}^H \mathbf{A}_q^H \mathbf{b}_m\right) \right\} + \omega^2 \sum_{m_1=1}^{P}\sum_{m_2=1}^{P} \overline{u_{m_1}(\mu)} u_{m_2}(\mu) \mathbf{b}_{m_1}^H \mathbf{b}_{m_2}$$

…independent of the dimension of the original system!

[Rubia2009]

Adaptive scheme: greedy method: next expansion point: $$\hat{\mu} = \arg\max_{\mu \in D_{train}} e_r(\mu)$$

Direct Solvers: Frequency Slicing Method [Sommer2013]

Note: FE solution $\mathbf{x}(\mu)$ has to be determined at each step of the adaptive method.

→ *Using a direct solver, an expensive factorization of* $\mathbf{A}(\hat{\omega})$ *is performed for each* $\hat{\mu} = (\hat{\omega}, \theta_s, \phi_s) \in D_{ex}$.

Computational costs: factorization … $\approx O(N^2)$ forward/back substitution … $\approx O(N^{1.4})$

Problem: New expansion point $\hat{\mu}$ does not necessarily mean that the corresponding frequency $\hat{\omega}$ is also selected for the first time by the underlying greedy algorithm!

→ *Factorizations for recurring frequency values increase computational time for generating the ROM!*

Solution: Frequency slicing greedy method for utilizing the factorization of $\mathbf{A}(\omega)$ better.

Conventional method:

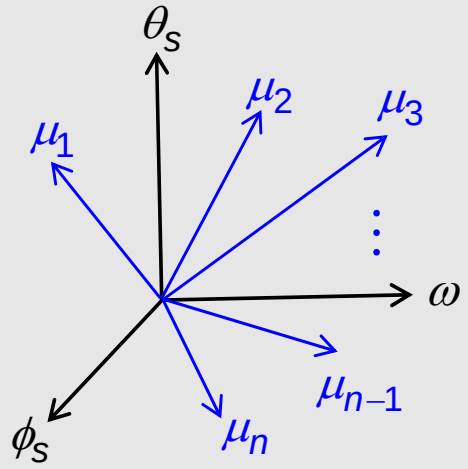

$$\rightarrow \text{range}\,\mathbf{V} = \text{span}\left[\mathbf{x}(\mu_1),\ldots,\mathbf{x}(\mu_n)\right]$$

Adapted method:

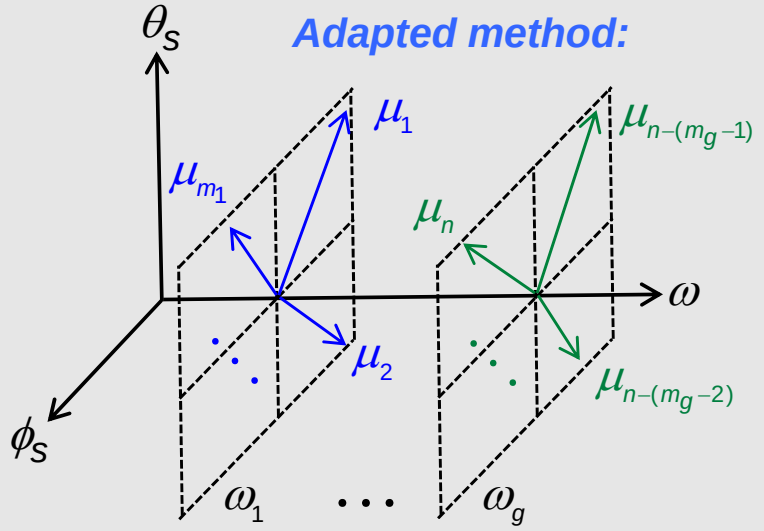

$$\rightarrow \text{range}\,\mathbf{V} = \text{span}\left[\mathbf{x}(\mu_1),\ldots,\mathbf{x}(\mu_{m_1})\,|\cdots|\,\mathbf{x}(\mu_{n-(m_g-1)}),\ldots,\mathbf{x}(\mu_n)\right]$$

Frequency slicing algorithm requires far less factorizations!

→ *Computational effort for constructing the ROM can be greatly reduced!*

Numerical Far-Field Computation

2. Numerical computation of *electric and magnetic far-fields*:

Radiation vector:

$$\mathbf{F}(\hat{\mathbf{r}}(\theta,\phi),\omega) = \hat{\mathbf{r}} \times \oint_{S_0} e^{j\omega \hat{\mathbf{r}}\cdot\mathbf{r}'/c} \mathbf{J}_s(\mathbf{r}')dS' \times \hat{\mathbf{r}} + \frac{1}{\eta} \oint_{S_0} e^{j\omega \hat{\mathbf{r}}\cdot\mathbf{r}'/c} \mathbf{M}_s(\mathbf{r}')dS' \times \hat{\mathbf{r}}$$

Introduction of the parameter vector $\gamma = (\omega,\theta,\phi) \in B \subset \mathbb{R}^3$.

Huygens sources:

$$\mathbf{J}_S(\mathbf{r}',\omega) = \hat{\mathbf{n}} \times \mathbf{H}(\mathbf{r}',\omega)$$
$$\mathbf{M}_S(\mathbf{r}',\omega) = -\hat{\mathbf{n}} \times \mathbf{E}(\mathbf{r}',\omega)$$

Consider the second integral: $\mathbf{I}(\gamma) = \oint_{S_0} e(\gamma,\mathbf{r}')\mathbf{M}_s(\mathbf{r}')dS' \approx \sum_{h=1}^{H} e(\gamma,\mathbf{r}_h')\mathbf{M}_s(\mathbf{r}_h')\Delta S_h, \quad e(\gamma,\mathbf{r}') = e^{jk\hat{\mathbf{r}}\cdot\mathbf{r}'}$

$$I_x(\gamma) = \Delta S \left[e(\gamma)\right]_{1\times H} \left[M_{s,x}\right]_{H\times 1}$$
$$= \Delta S \left[e(\gamma)\right]_{1\times H} \left([N]_{H\times H}[\mathbf{C}_0]_{H\times N}[\mathbf{x}]_{N\times 1}\right)$$
$$\approx \Delta S \left[e(\gamma)\right]_{1\times H} \left([N]_{H\times H}[\mathbf{C}_0]_{H\times N}\left[\mathbf{V}\right]_{N\times n}[\tilde{\mathbf{x}}]_{n\times 1}\right)$$

Problem: despite ROM, $O(H)$ operations are required! (*H:* number of near-field values)

Solution: affine decomposition of $\left[e(\gamma)\right]_{1\times H}$ by the *Empirical Interpolation Method* (EIM).

$$I_x(\gamma) = \Delta S \sum_{k=1}^{M} \xi_k(\gamma)\left[q_k\right]_{1\times H} \left([N]_{H\times H}[\mathbf{C}_0]_{H\times N}\left[\mathbf{V}\right]_{N\times n}[\tilde{\mathbf{x}}]_{n\times 1}\right), \qquad M \ll H$$

$$= \Delta S \sum_{k=1}^{M} \xi_k(\gamma)\left[\tilde{q}_k\right]_{1\times n}[\tilde{\mathbf{x}}]_{n\times 1}$$

→ **Only *O*(*M*) operations are required!**

[Barrault 2004] [Fares2010]

Numerical Example

- Parameter domain: $f = 2...4$ GHz
  $\theta_s = 0...\pi/3$ $\phi_s = 0...2\pi$
  $\theta = 0...\pi/2$ $\phi = 0...2\pi$
- FE dimension N: 2,553,439
- Number of near-field points H: 12800
- Dimension D_{train}^{ROM} : (30 x 568) = 17040
- ROM dimension: 300
- Dimension B_{train}^{EI} : (30 x 946) = 28380
- Number of EIM coefficients M: 350

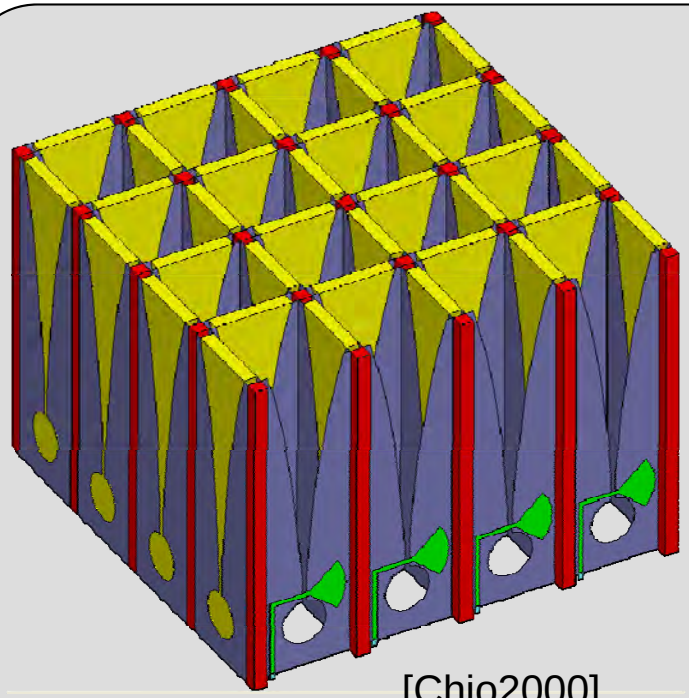

[Chio2000]

Directive gain

$f = 3.3$ GHz

$\theta_s = \pi/4,\ \phi_s = \pi/2$

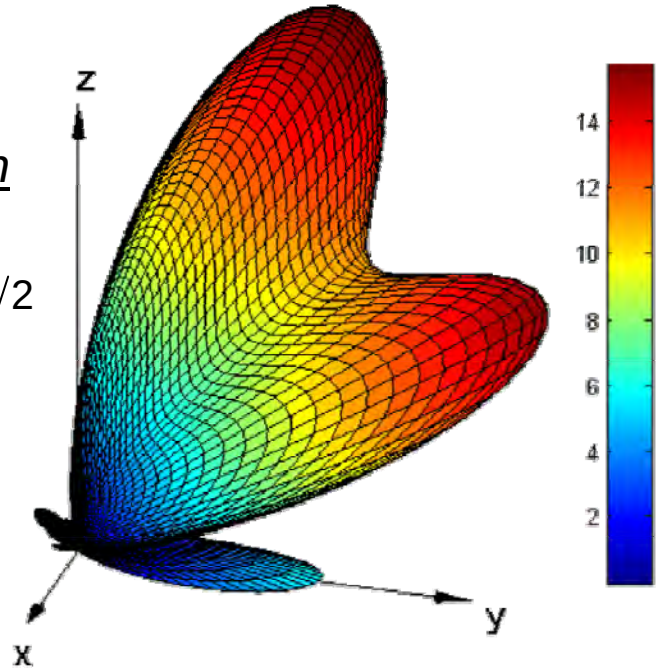

Directive gain

$f = 2.2$ GHz

$\theta_s = \pi/4,\ \phi_s = -\pi/4$

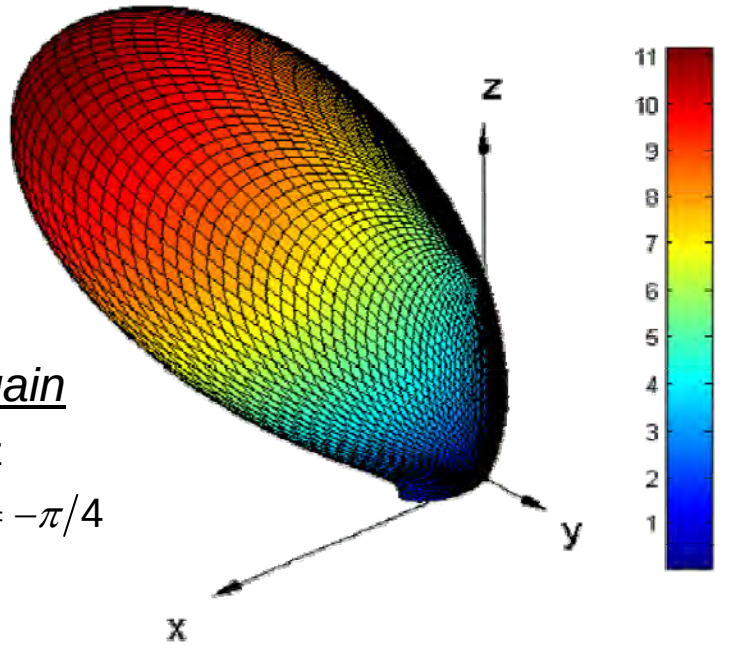

Conventional Greedy vs. Frequency Slicing Greedy

Comparison between the *Conventional Greedy Method* and the *Adapted Greedy Method*.

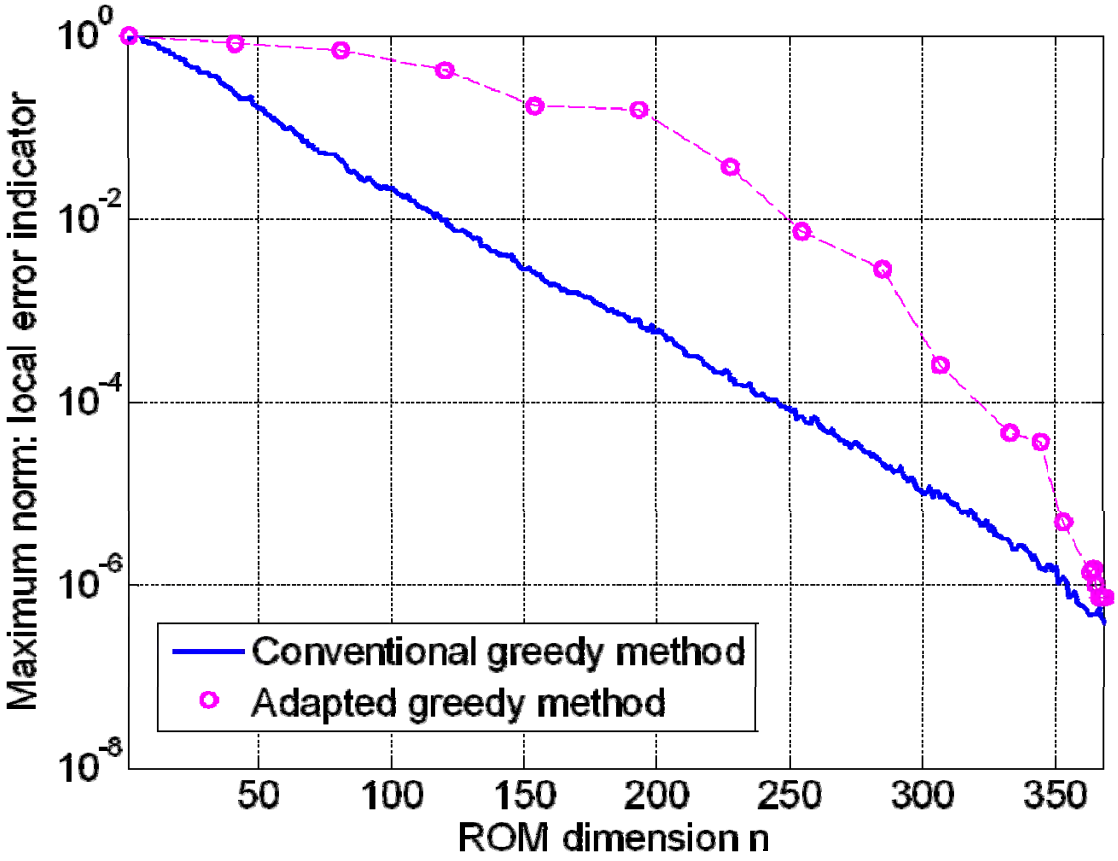

Conventional Greedy Method		
Error indicator	Computing time	ROM dimension *n*
2.62 e-3	92.16 h	153
4.61 e-5	164.98 h	265
1.27 e-6	221.32 h	346

Frequency Slicing Method		
Error indicator	Computing time	ROM dimension *n*
2.73 e-3	18.34 h	285
4.57 e-5	24.254 h	333
1.31 e-6	29.46 h	363

MATLAB code on Intel(R) Xeon(R) E5620 CPU @ 2.40GHz

→*Frequency Slicing Greedy Method reduces computing time for constructing the ROM by up to nearly one order of magnitude!*

Convergence Behavior: MOR and EIM

Convergence of *projection-based MOR*

Relative error: $e_n = \dfrac{\left\|\mathbf{x}(\mu) - \hat{\mathbf{x}}(\mu)\right\|_2}{\left\|\mathbf{x}(\mu)\right\|_2}$

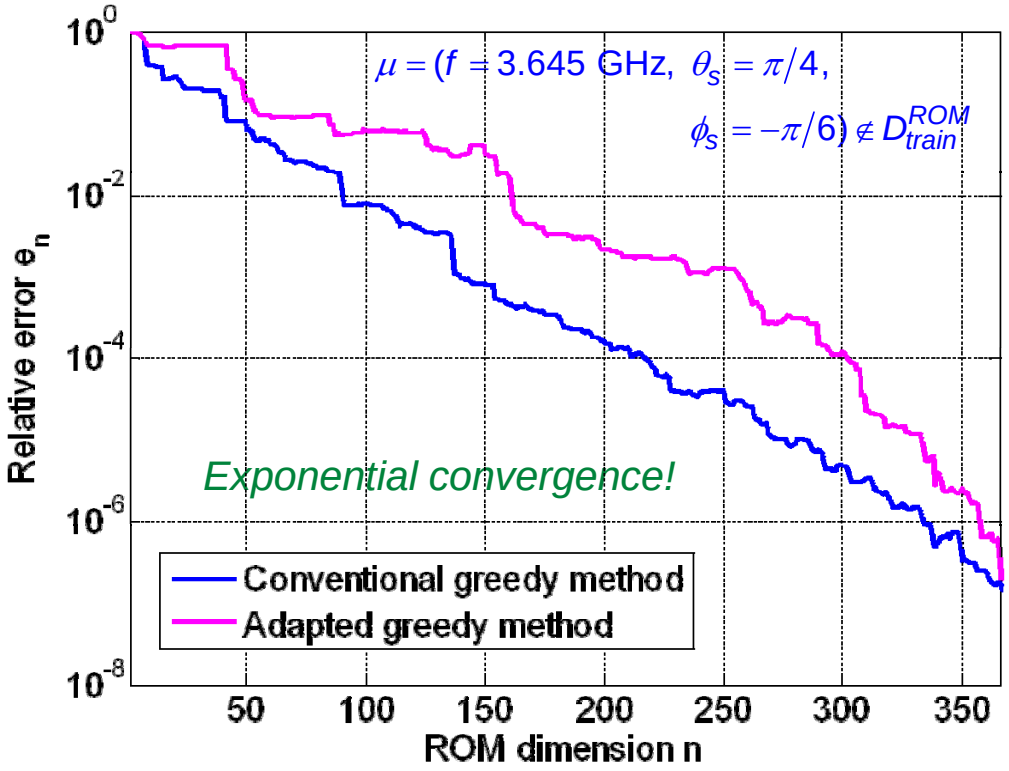

[Binev 2011] [Buffa 2012]

Convergence of *Empirical Interpolation*

Relative error: $e_m = \max_{\mathbf{r}' \in S_0^h} \left| \dfrac{f(\gamma, \mathbf{r}') - \hat{f}_m(\gamma, \mathbf{r}')}{f(\gamma, \mathbf{r}')} \right|$

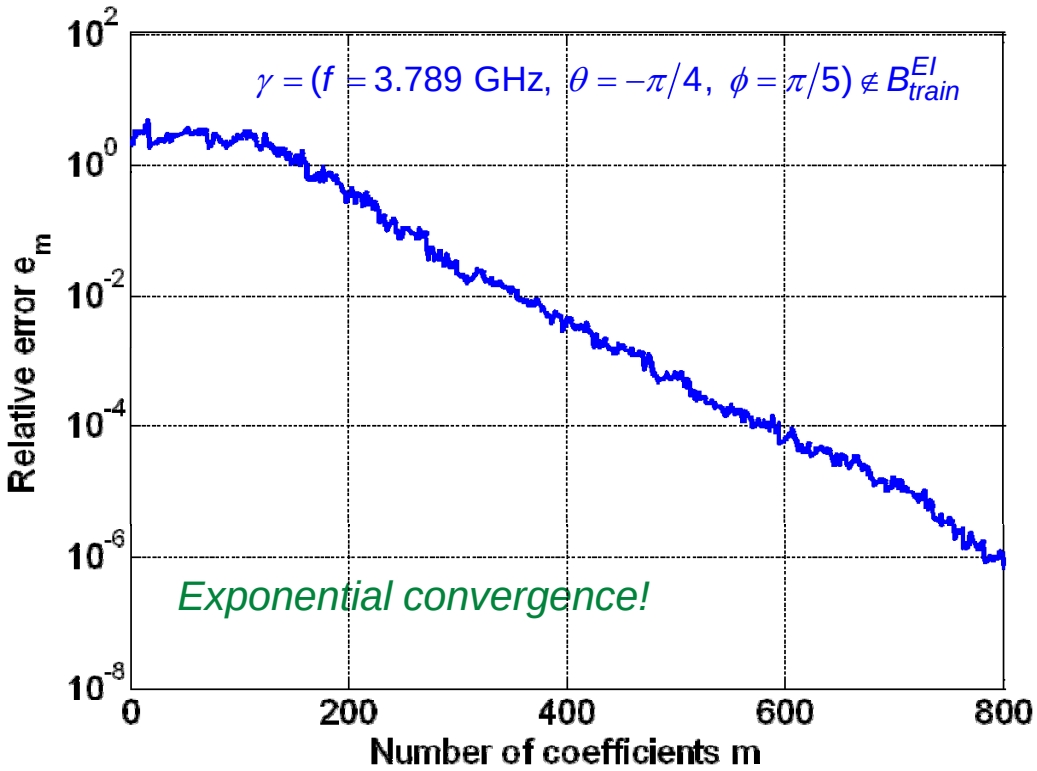

[Maday2009]

Directive Gain: Computational Data

Original model	
FE dimension N	2,553,439
Number of near-field sampling points	12,800
Time for computing solution	2167.5 s
Additional time for computing directive gain for P=4,900 look angles	24.957 s

Reduced model	$f = 2...4$ GHz, $\theta_s = 0...\pi/3$, $\phi_s = 0...2\pi$, $\theta = 0...\pi/2$, $\phi = 0...2\pi$
ROM dimension n	300
Number of EI coefficients	350
Average error of the directive gain	1 e-3
Time for generating ROM (**offline**)	20.36 h
Time for Empirical Interpolation (**offline**)	33.97 h
Time for computing solution (**online**)	0.048 s
Additional time for computing directive gain for P=4,900 look angles (**online**)	2.2794 s

MATLAB code on Intel(R) Xeon(R) E5620 CPU @ 2.40GHz

Average error of the directive gain:

$$e_D(\mu) = \frac{1}{P}\sum_{p=1}^{P}\left|\frac{D\left(\mathbf{x}(\mu), e(\gamma_p), \gamma_p\right) - \hat{D}\left(\hat{\mathbf{x}}(\mu), \hat{e}(\gamma_p), \gamma_p\right)}{D\left(\mathbf{x}(\mu), e(\gamma_p), \gamma_p\right)}\right|$$

Directive gain

$f = 2.57$ GHz

$\theta_s = \pi/5,\ \phi_s = \pi/4$

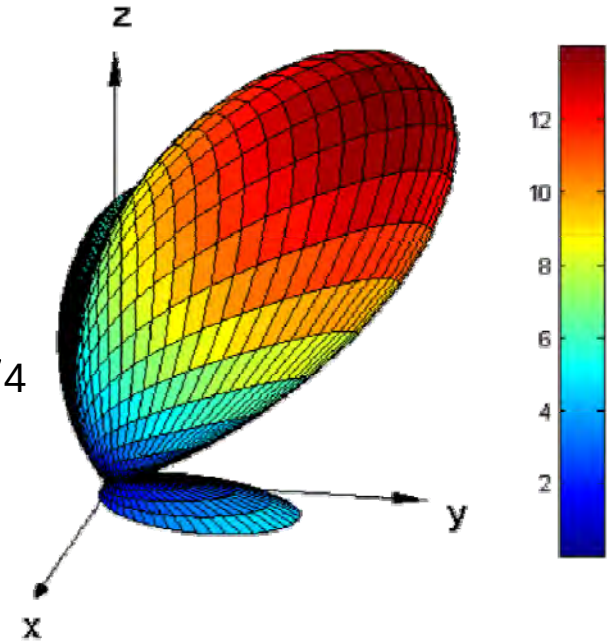

Total computing time for one single response surface:

- ***Original model:*** ***36 minutes***
- ***Reduced model:*** ***2 seconds***

→ Reduction of 3 orders of magnitude.

Efficient NF-FF Transformation Technique [Sommer2013b]

Idea: Equidistant sampling of the near-field values and partitioning of the Huygens surface S (Box) into uniform sub-faces according to:

$$S = \bigcup_{i=1}^{K_{xy}} S_{xy}^i \cup \bigcup_{i=1}^{K_{xz}} S_{xz}^i \cup \bigcup_{i=1}^{K_{yz}} S_{yz}^i .$$

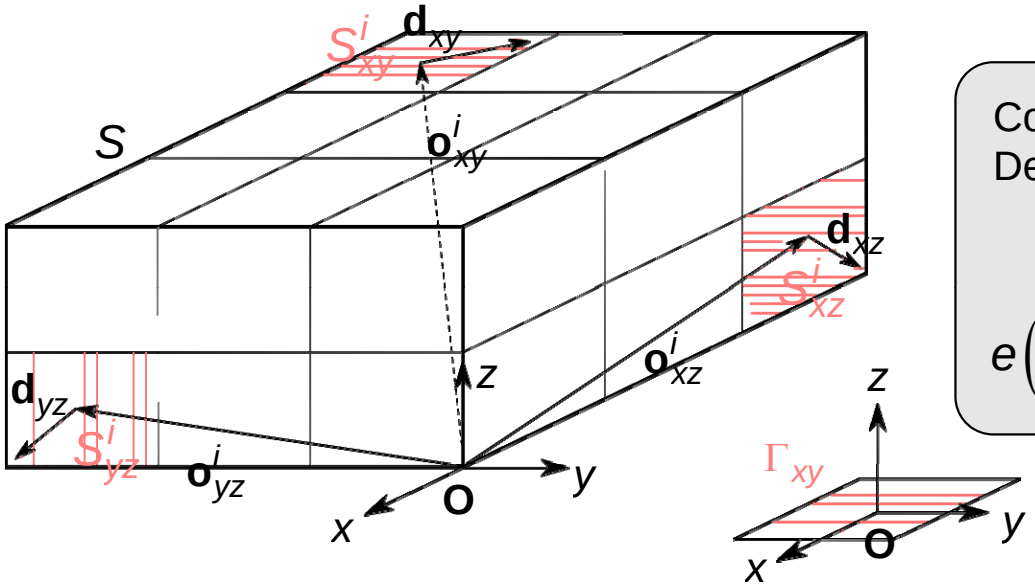

Consider sub-faces on XY plane:
Decompose the exponential function:

$$\mathbf{r}_{xy}^i = \mathbf{o}_{xy}^i + \mathbf{d}_{xy} \quad \text{with} \quad \mathbf{r}_{xy}^i, \mathbf{o}_{xy}^i \in S_{xy}^i,$$

$$e\left(\gamma, \mathbf{r}_{xy}^i\right) = e\left(\gamma, \mathbf{o}_{xy}^i\right) e\left(\gamma, \mathbf{d}_{xy}\right) \quad \text{with } \mathbf{d}_{xy} \in \Gamma_{xy}.$$

"Array factor" "Element factor"

Applying the EIM for $\left(\mathbf{d}_{xy}, \gamma\right) \in \Gamma_{xy} \times B$ leads to: (L_{xy} : number of near-field values on Γ_{xy})

$$I_{xy}^x(\gamma) = \sum_{i=1}^{K_{xy}} e\left(\gamma, \mathbf{o}_{xy}^i\right) \left[e(\gamma)\right]_{1\times L_{xy}} \left[J_{s,x}\Delta S\right]_{L_{xy}\times 1}^i \approx \sum_{i=1}^{K_{xy}} e\left(\gamma, \mathbf{o}_{xy}^i\right) \sum_{m=1}^{M_{xy}} \alpha_m(\gamma) \left[q_m\right]_{1\times L_{xy}} \left[J_{s,x}\Delta S\right]_{L_{xy}\times 1}^i .$$

→ *The EIM just needs to be performed for one single group in the XY,XZ and YZ plane!*

→ *Since the area of a single sub-face is much smaller than that of its parent surface, the EIM offline part is performed much more efficiently!*

Numerical Example

- Parameter domain: $f = 3...5$ GHz
  $\theta = 0...\pi$ $\phi = 0...\pi$
- FE dimension N: 62,565,408
- Number of near-field points H: 906,832
- Number of sub-faces K: 70
- Number of sub-domains D: 100
- Number of training points per sub-domain Q: (20 x 100) = 2,000

70×70 Vivaldi Antenna Array:

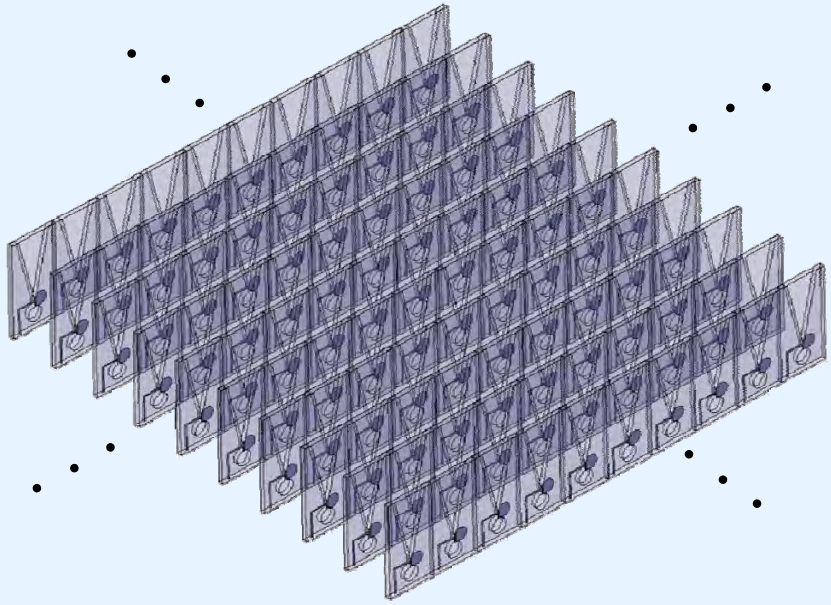

[Shin1999]

Directive gain for $f = 4$ GHz:

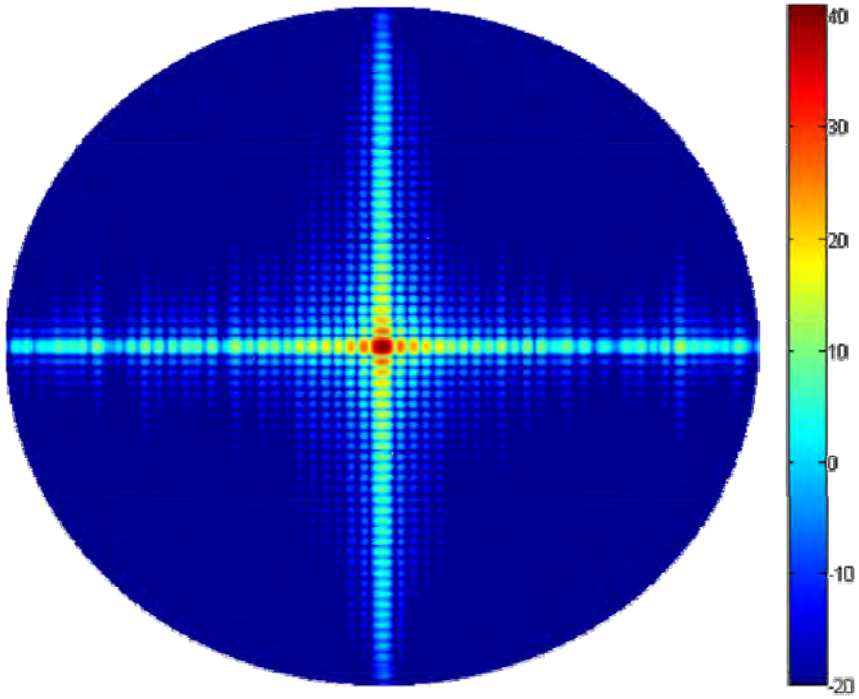

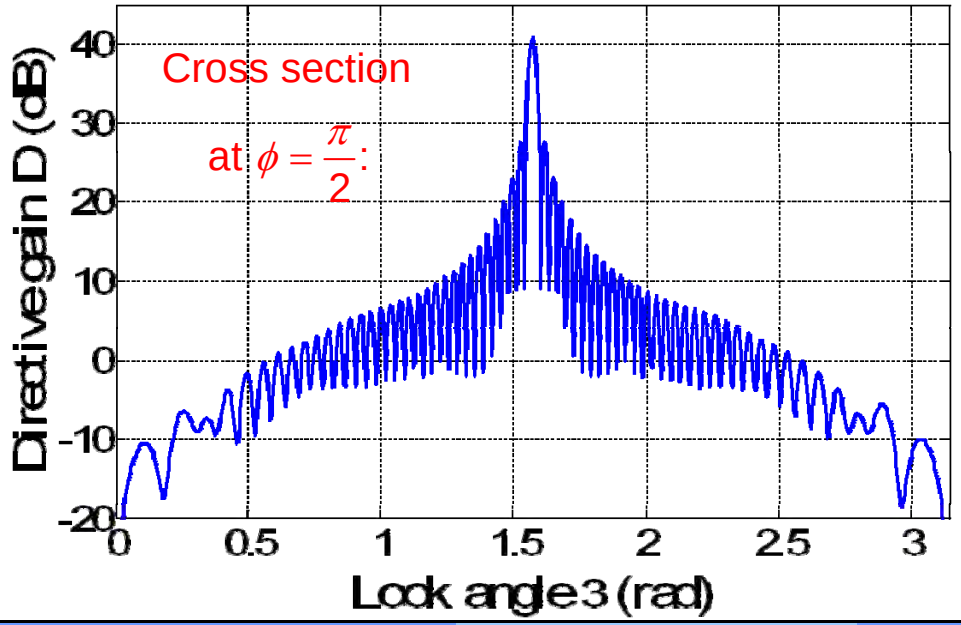

Numerical Results

Original model	
FE dimension *N*	62,565,408
Number of near-field sampling points	906,832
Number of look angles *P*	490.000
Time for solving FE system [Floch 2013]	2.851 s
Time for perfoming NF-FF transformation	4.8804 h

Efficient NF-FF Transformation Technique	$f = 3...5$ GHz, $\theta = 0...\pi$, $\phi = 0...\pi$
Number of look angles *P*	490.000
Number of sub-faces *K*	70
Number of sub-domains *D*	100
Average error of the directive gain	7.585 e-5
Offline time for EI method (8 cores)	3.325 h
Online time for NF-FF transformation	115.8 s

MATLAB code on Intel(R) Core(TM) i7-2600K CPU @ 3.40GHz

Average error of the directive gain:

$$e_D(\omega) = \frac{1}{P}\sum_{p=1}^{P}\left|\frac{D\left(\mathbf{y}_{NF}(\omega), e(\gamma_p), \gamma_p\right) - D\left(\mathbf{y}_{NF}(\omega), \hat{e}(\gamma_p), \gamma_p\right)}{D\left(\mathbf{y}_{NF}(\omega), e(\gamma_p), \gamma_p\right)}\right|$$

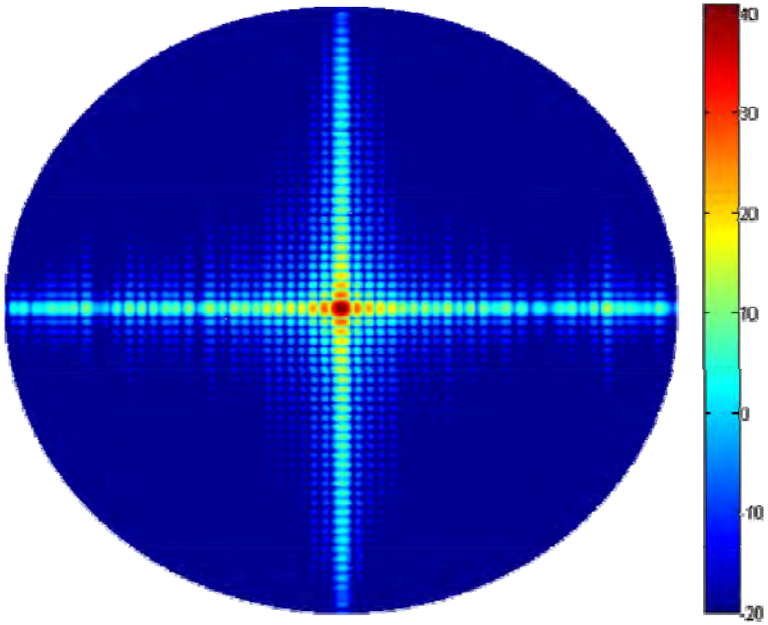

Computing time (NF-FF Transformation) for one single radiation pattern:

→ **Reduction from 4.88 h to only 116 s.**
→ **Speed-up factor of more than 150.**

Error Bounds for Directive Gain 1

Directive gain: $$D\left(\mathbf{x}(\mu),e(\gamma),\gamma\right)=10\log_{10}\left(\frac{\eta k^2}{8\pi P\left(\mathbf{x}(\mu),\omega\right)}\left\|\mathbf{F}\left(\mathbf{x}(\mu),e(\gamma),\gamma\right)\right\|_2^2\right)$$

Assumption: $$\left\|\mathbf{F}(\mu,\gamma)-\hat{\mathbf{F}}(\mu,\gamma)\right\|_2\le\varepsilon_F \quad \text{and} \quad \left|P(\mu,\gamma)-\hat{P}(\mu,\gamma)\right|\le\varepsilon_P$$ [Hesthaven2012]

Error bound for directive gain:

$$\left|D-\hat{D}\right|\le\varepsilon_D=20\max\left[\log_{10}\left(\frac{\left\|\hat{\mathbf{F}}\right\|_2+\varepsilon_F}{\left\|\hat{\mathbf{F}}\right\|_2}\right),\log_{10}\left(\frac{\left\|\hat{\mathbf{F}}\right\|_2}{\left\|\hat{\mathbf{F}}\right\|_2-\varepsilon_F}\right)\right]+10\max\left[\log_{10}\left(\frac{\hat{P}+\varepsilon_P}{\hat{P}}\right),\log_{10}\left(\frac{\hat{P}}{\hat{P}-\varepsilon_P}\right)\right]$$

Truth approximation of the radiation vector using matrix notation:

$$\mathbf{F}\left(\mathbf{x}(\mu),e(\gamma),\gamma\right)=\left[\mathbf{P}(\gamma)\right]\sum_{h=1}^{H}e(\gamma,\mathbf{r}_h')\left[\mathbf{N}(\mathbf{r}_h')\right]\mathbf{x}(\mu)=\left[\mathbf{T}(\gamma)\right]\left[\mathbf{I}_E\right]\left[\mathbf{E}(\gamma)\right]\left[\mathbf{N}\right]\mathbf{x}(\mu)$$

Error bound for radiation vector using *MOR for the primal system* and *EI for the NF-FF Operator*:

$$\begin{aligned}\left\|\mathbf{F}(\mu,\gamma)-\hat{\mathbf{F}}_p(\mu,\gamma)\right\|_2&=\left\|\left[\mathbf{T}(\gamma)\right]\left[\mathbf{I}_E\right]\left(\left[\mathbf{E}(\gamma)\right]\left[\mathbf{N}\right]\mathbf{x}(\mu)-\left[\hat{\mathbf{E}}(\gamma)\right]\left[\mathbf{N}\right]\hat{\mathbf{x}}(\mu)\right)\right\|_2\\&\le\left\|\mathbf{T}(\gamma)\right\|_2\left\|\mathbf{I}_E\right\|_2\left(\left\|\mathbf{N}\right\|_2\left\|\mathbf{x}(\mu)-\hat{\mathbf{x}}(\mu)\right\|_2+\left\|\mathbf{E}(\gamma)-\hat{\mathbf{E}}(\gamma)\right\|_2\left\|\tilde{\mathbf{N}}\tilde{\mathbf{x}}(\mu)\right\|_2\right)\\&\le\underbrace{\frac{1}{\beta_d(\omega)}\left\|\mathbf{r}(\mu)\right\|_2\left\|\mathbf{T}(\gamma)\right\|_2\left\|\mathbf{I}_E\right\|_2\left\|\mathbf{N}\right\|_2}_{\text{term 1}}+\underbrace{\left\|\mathbf{T}(\gamma)\right\|_2\max_{\mathbf{r}'\in S_0^h}\left|e(\gamma,\mathbf{r}')-e(\gamma,\mathbf{r}')\right|\left\|\tilde{\mathbf{N}}\tilde{\mathbf{x}}(\mu)\right\|_2\left\|\mathbf{I}_E\right\|_2}_{\text{term 2}}\end{aligned}$$

inf-sup constant — *error in EI*

Error Bounds for Directive Gain 2

1. Lower bound for discrete inf-sup constant:

Problem: Determination of $\beta_d(\omega)$ corresponds to the computation of the smallest singular value $\sigma_{\min}(\mathbf{A}(\omega))$.

→ *Time-consuming eigenvalue problem*!

Solution: ***Successive Constrained Method*** **(*SCM*)** enables efficient *online computation of a lower bound* $\beta_{LB}(\omega)$ *by solving a linear program (LP).*

[Huynh 2007] [Chen2010]

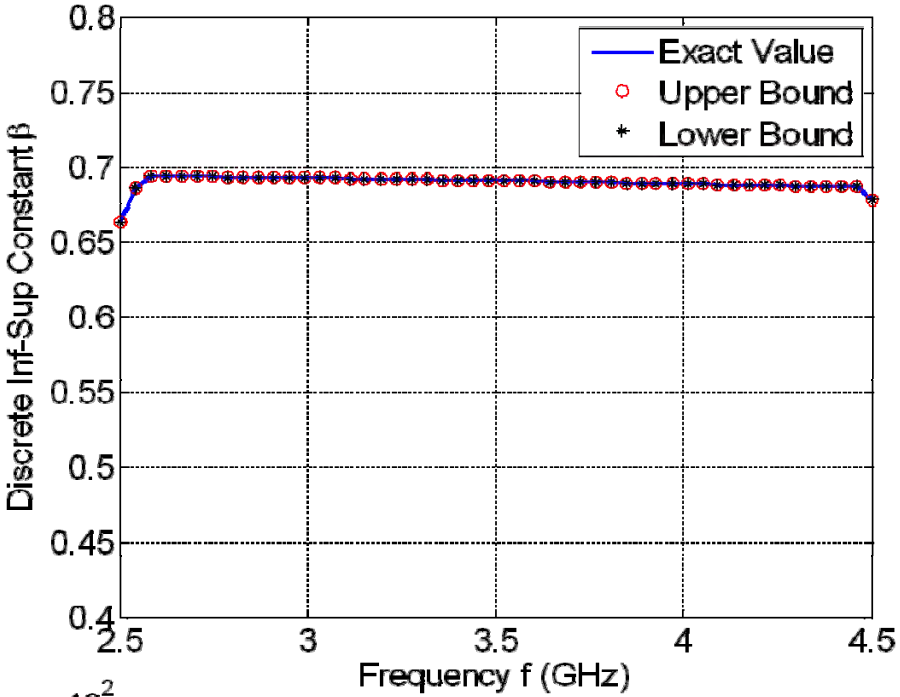

2. Error bound for the Empirical Interpolation Method:

Rigorous error bound for the EIM …

$$\max_{\mathbf{r}' \in S_0^h} \left| e(\gamma, \mathbf{r}') - e(\gamma, \mathbf{r}') \right| \leq \delta_{m,p}, \quad \forall \gamma \in B, \mathbf{r}' \in S_0^h$$

…can be computed ***offline****!!*

Bound depends on:

- *The parametric derivatives of the function.*
- *The EIM interpolant of these derivatives.*

(m: number of EIM coefficients, p: order of derivative)

[Eftang2010]

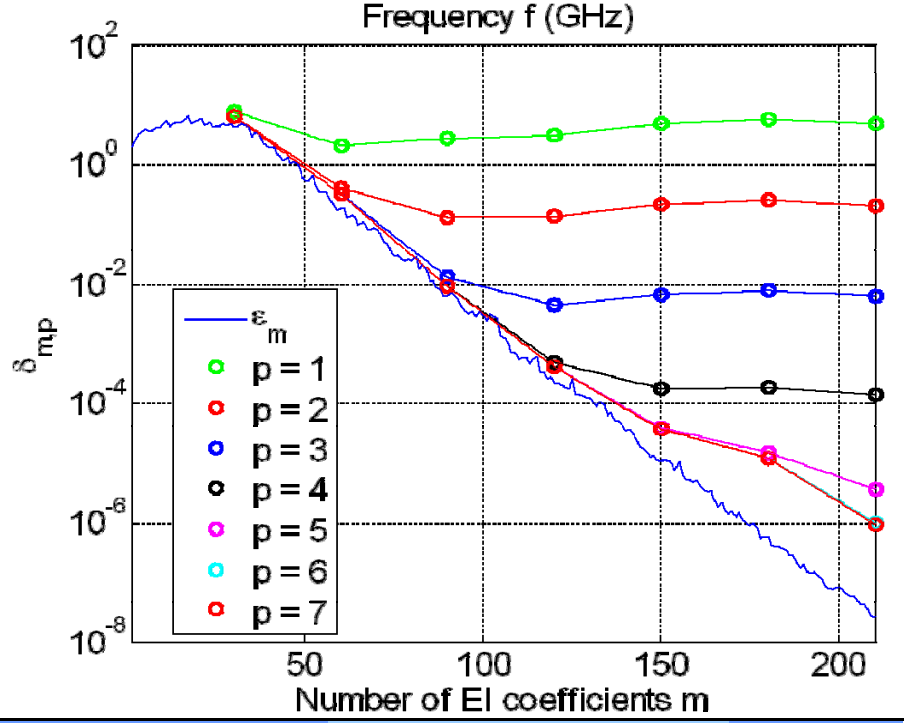

Error Bounds for Directive Gain 3

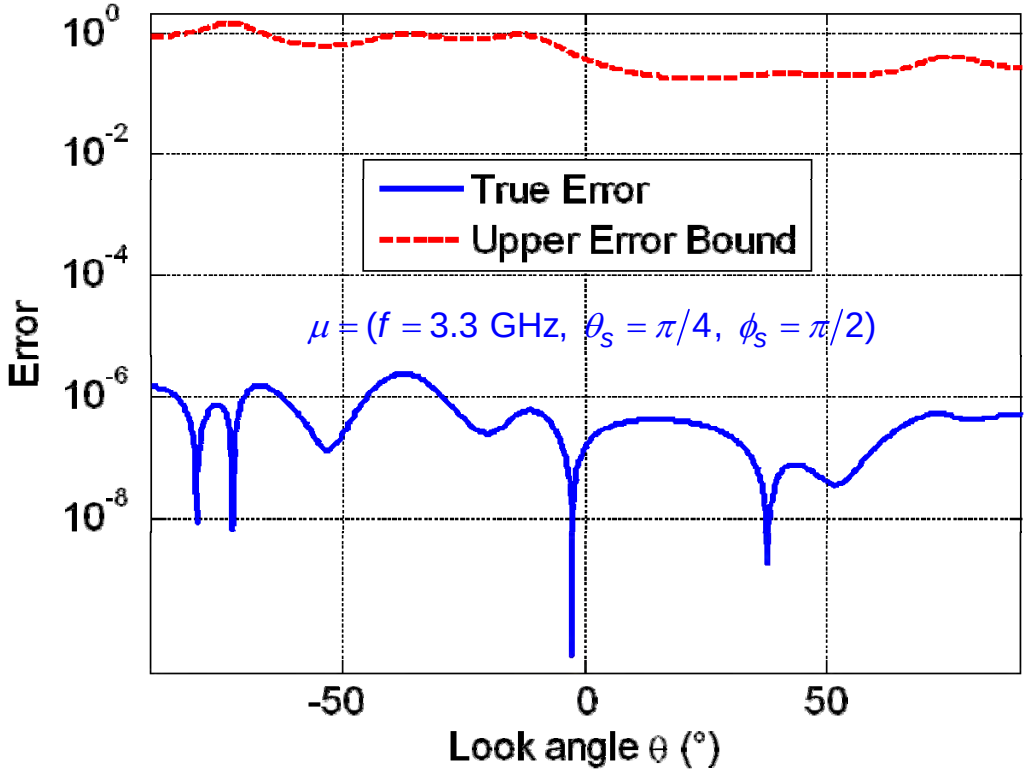

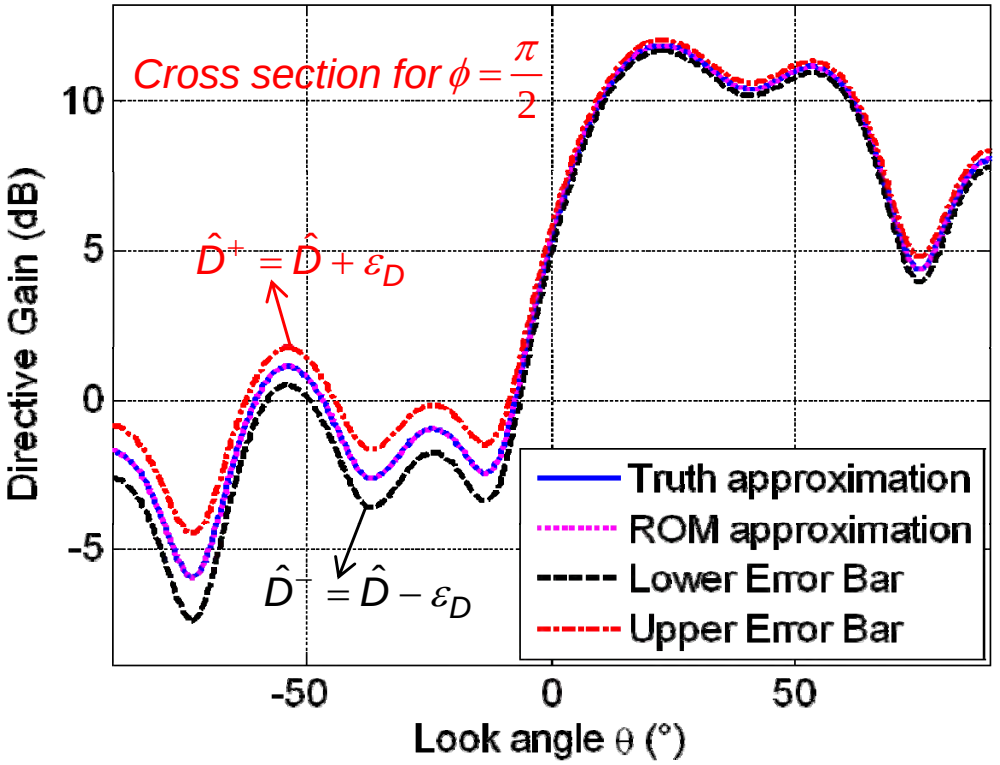

Problem: Error bound is poor because, in the conventional formula, *term 1* is not accurate enough.

Solution: Use projection-based MOR for the *dual system* to compute a dual corrected output!

Error bound for the radiation vector using *MOR and EI* for the *primal and dual system* (θ component)*:*

$$\left\| F^{\theta}(\mu,\gamma) - \hat{F}^{\theta}_{pd}(\mu,\gamma) \right\|_2 \le \frac{1}{\beta_{LB}(\omega)} \left\| \mathbf{r}_p(\mu) \right\|_2 \left\| \mathbf{r}^{\theta}_d(\mu) \right\|_2 + \left\| \mathbf{T}^{\theta}(\gamma) \right\|_2 \left[\left\| \tilde{\mathbf{N}}\tilde{\mathbf{x}}(\mu) \right\|_2 + \frac{1}{\beta_{LB}(\omega)} \left\| \mathbf{N} \right\|_2 \left\| \mathbf{r}_p(\mu) \right\|_2 \right] \left\| \mathbf{I}_E \right\|_2 \delta_{m,p}$$

(ϕ component can be computed analogously.)

Error Bounds - Numerical Results 1

Original Model	
FE dimension N	877,198
Number of near-field sampling points	12,800
Time for computing solution of the primal system	40.61 s
Additional time for computing directive gain for P=1000 look angles	2.31 s

Reduced Model $f = 2.5...4.5$ GHz, $\theta_s = 0...\pi/3$, $\phi_s = 0, \pi/2$, $\theta = 0...\pi/2$, $\phi = 0, \pi/2$	
ROM dimension n (primal/dual)	120/130
Number of EI coefficients	210
Time for generating primal and dual ROM (**offline**)	11.91 h
Time for Empirical Interpolation (**offline**)	1.101 h
SCM (**offline**)	11.55 h
Bound EIM (**offline**)	4.163 h
Time for computing solution of the reduced primal system (**online**)	0.0210 s
Total time for computing directive gain and error bounds for P=1000 look angles (**online**)	0.715 s

MATLAB Code on Intel(R) Core(TM) i7-2600K CPU @ 3.40GHz

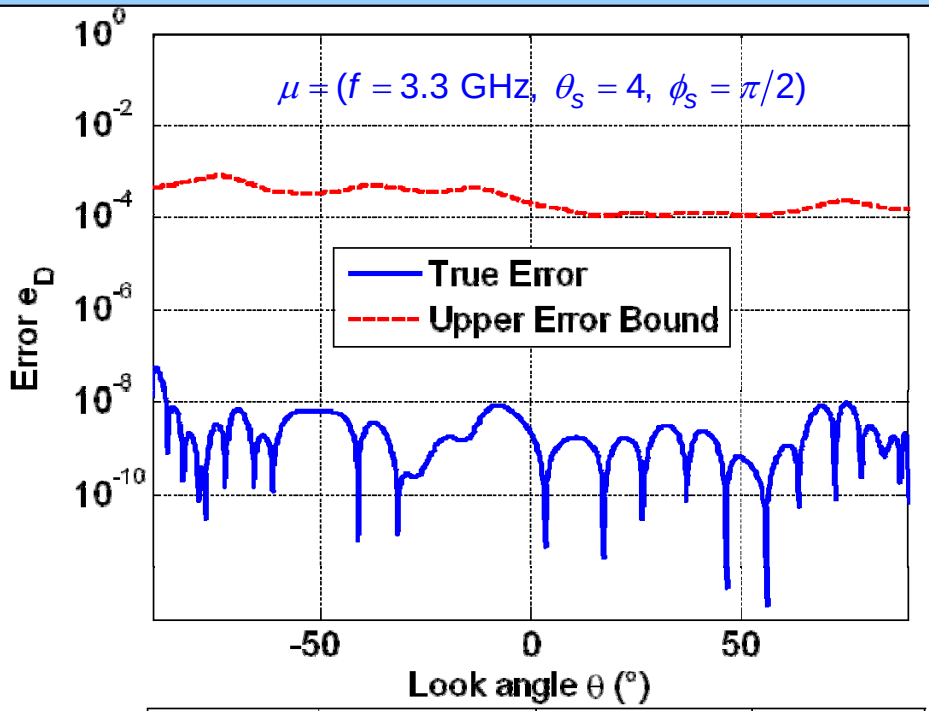

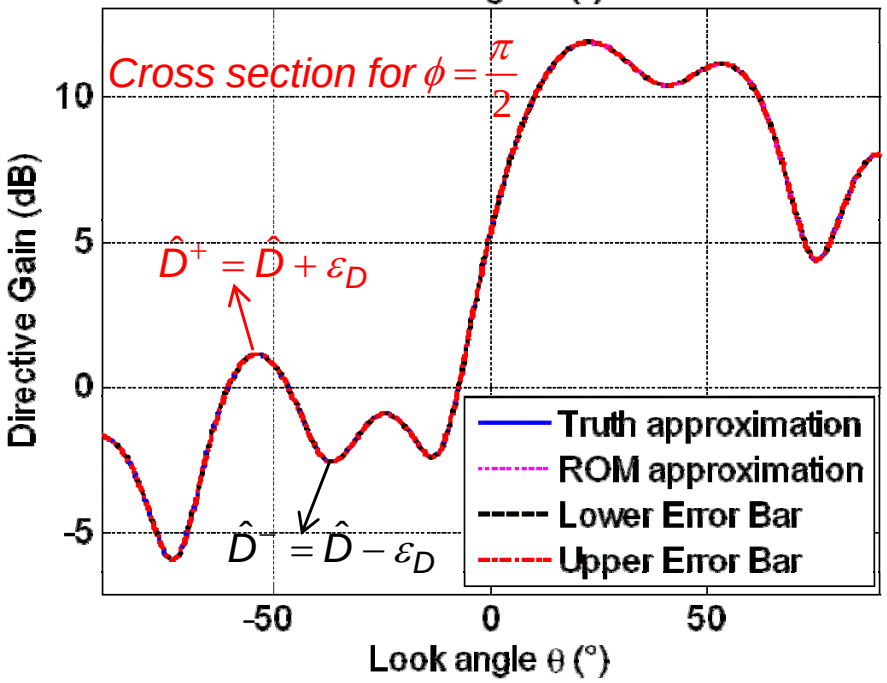

Parametric Order Reduction for Non-affine Parameters

Motivation

Example: Bandpassfilter

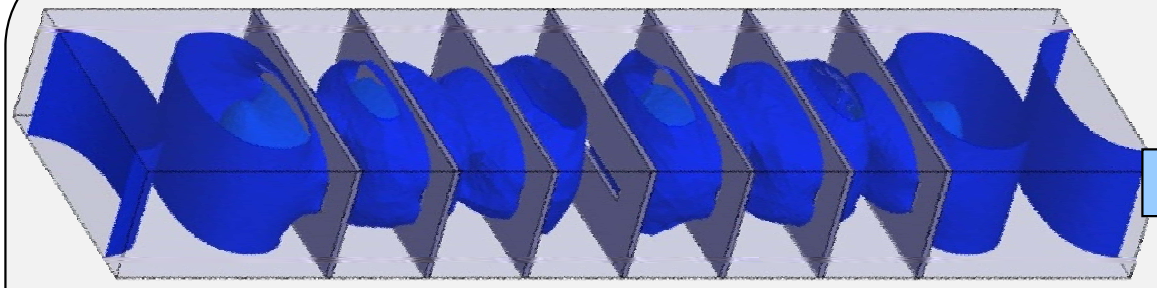

- 12 independent geometrical parameters.
- Three spacing parameters.
- Frequency.

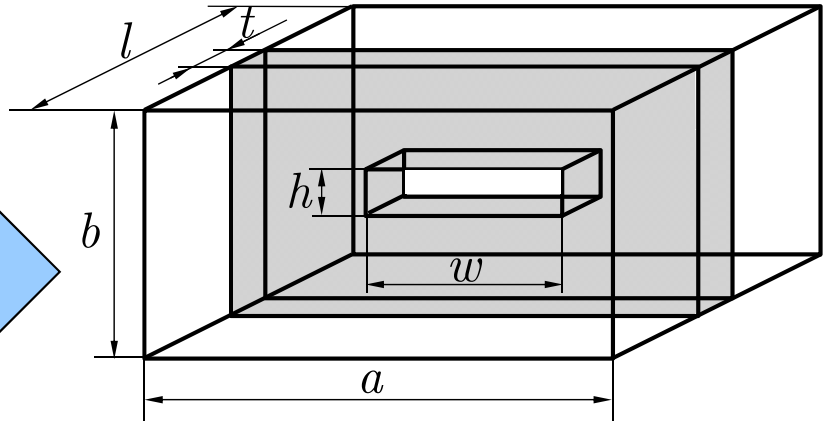

- Three geometrical parameters.
- Length parameter.
- Frequency.
- Multiple modes.

Goals

- Efficient FE analysis for parametric models.
- Large parameter variations.
- Multiple parameters including geometry.

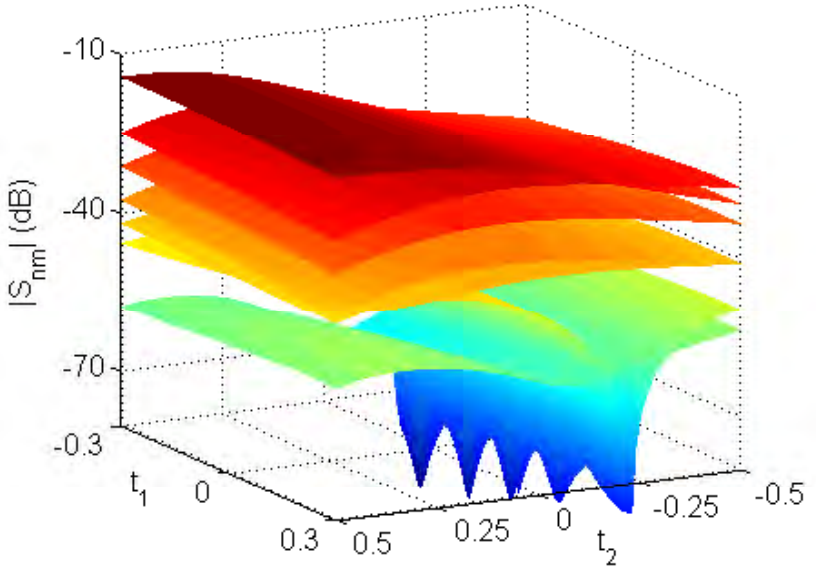

Geometry Parameterization

- Geometric parameters $\mathbf{t}$ enter system matrices during spatial discretization (Jacobian).
- Affine parameterization
  - Can be extracted explicitly for simple shape modifications ([Pomplun2010]).
  - Is hard to extract explicitly for complicated shape modifications.
- Instead: Consider geometric parameters to be of non-affine type.

Parameter classification:

1. Affine parameters: Material, frequency
   ⇒ Standard projection-based MOR applicable.
2. Non-affine parameters: Geometry
   ⇒ How to handle efficiently?

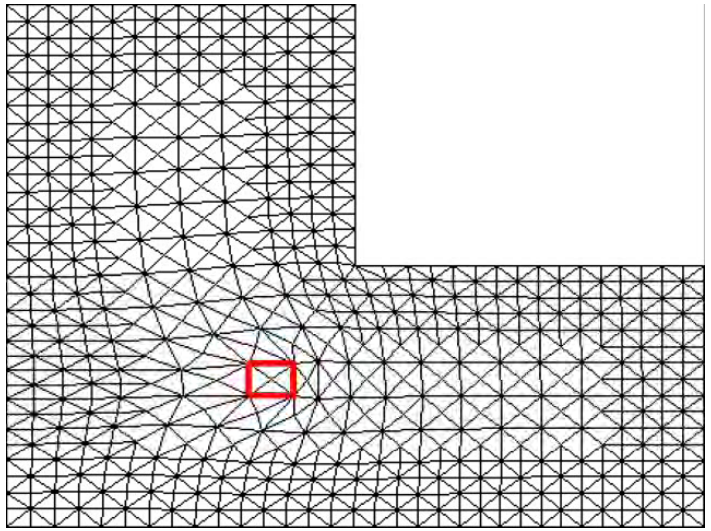

Proposed procedure:

- Introduce geometry-parameter dependent mesh $\mathcal{M}(\mathbf{t})$
  - Topology preserving mesh morphing algorithms
- Interpolation/approximation techniques

⇓

- Geometrically parameterized system matrices $\mathbf{A}_q(\mathbf{t})$.
- Geometrically parameterized projection matrices $\mathbf{V}(\mathbf{t})$.

⇒ Fully parameterized reduced model

$$\tilde{\Sigma}(s,\mathbf{p},\mathbf{t})$$

Workflow

1. Instantiate mesh at grid $\mathcal{G}$ in geometry parameter space.

2. Instantiate full-scale models.

3. Construct projection matrices by considering affine parameters solely.

   ⇨ Dimension is independent of number of geometry parameters.

4. Generate parametric ROM by decoupled interpolation of system-matrices and projection spaces.

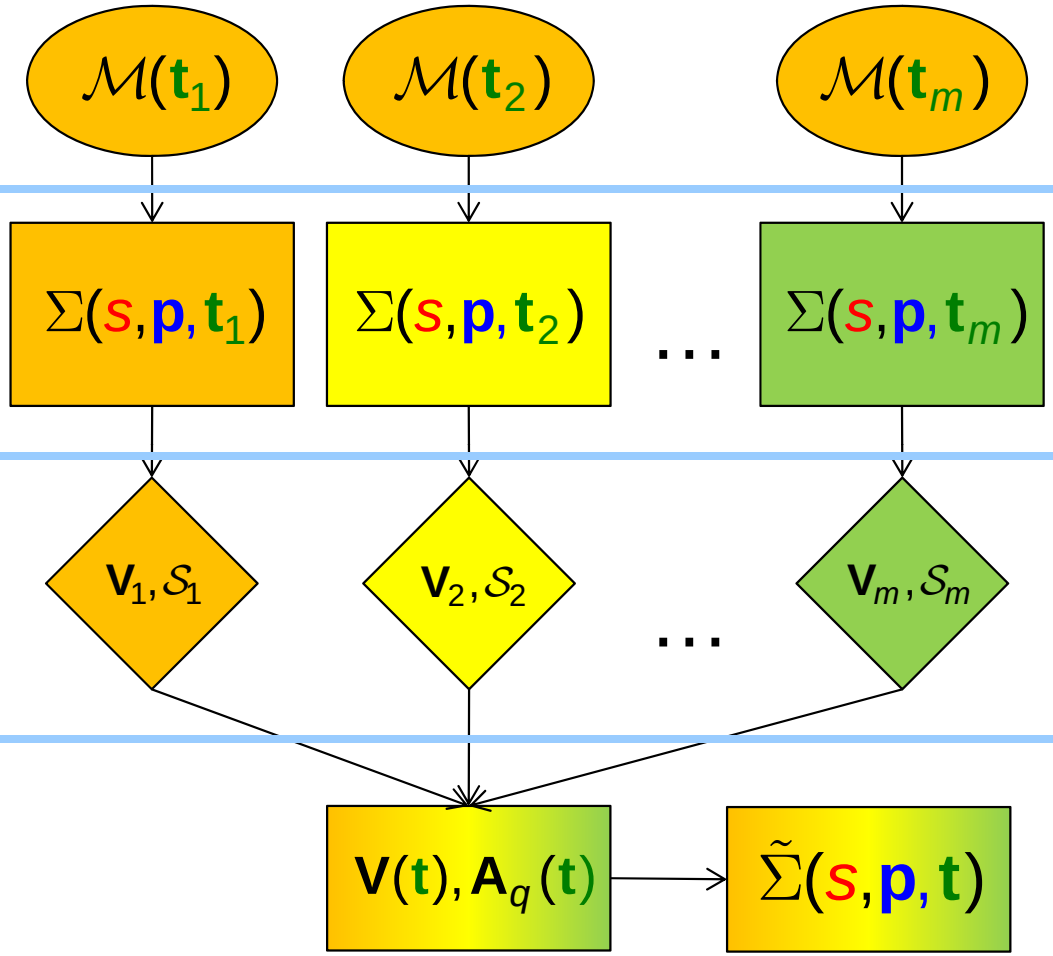

⇨ Use appropriate interpolation setting for each case.

- (High polynomial order) for system-matrices interpolation.
- Low order for projector interpolation.

Interpolation of System Matrices

Fully parameterized reduced model

$$\left.\begin{aligned} \mathbf{V}^T(\mathbf{t})\left(\sum_q \theta_q(s,\mathbf{p})\mathbf{A}_q(\mathbf{t})\right)\mathbf{V}(\mathbf{t})\mathbf{x}(s,\mathbf{p},\mathbf{t}) &= \mathbf{V}^T(\mathbf{t})\left(\sum_r \vartheta_r(s,\mathbf{p})\mathbf{B}_r\right)\mathbf{u}(s) \\ \mathbf{y}(s,\mathbf{p},\mathbf{t}) &= \left(\sum_r \vartheta_r(s,\mathbf{p})\mathbf{B}_r^T\right)\mathbf{V}(\mathbf{t})\mathbf{x}(s,\mathbf{p},\mathbf{t}) \end{aligned}\right\} \tilde{\Sigma}(s,\mathbf{p},\mathbf{t})$$

Interpolation of full-scale system matrices

$$\mathbf{A}_q(\mathbf{t}) = \sum_\beta \Gamma_\beta(\mathbf{t})\mathbf{A}_{q,\beta}, \quad \text{multi-index } \beta = [\beta_1,\cdots,\beta_P]$$

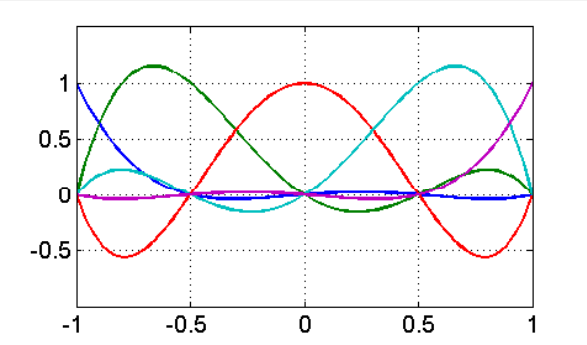

- Various interpolation/approximation schemes possible
- Here: Polynomial interpolation

$$\Gamma_\beta(\mathbf{t}) = l_{\beta_1} \otimes \ldots \otimes l_{\beta_P}(\mathbf{t}), \qquad \text{Lagrange polynomials } l_i(t) = \prod_{j=0, j\neq i}^{n} \frac{t-t_j}{t_i-t_j}$$

$$\Gamma_\beta(\mathbf{t}_\alpha) = \prod_{p=1}^{P} \delta_{\beta_p\alpha_p} \qquad \forall \mathbf{t}_\alpha \in \mathcal{G}$$

$$\Rightarrow \mathbf{A}_{q,\beta} = \mathbf{A}_q(\mathbf{t}_\beta)$$

Calculation of $\mathbf{A}_{q,\beta}$ is free of computational costs

Parameter-Dependent Projection Matrices I

How to find a valid representation for $\mathbf{V}(\mathbf{t})$?

- Direct interpolation of the bases $\mathbf{V}_i$, $\mathbf{t}_i \in \mathcal{G}$ will fail.

Transfer-matrix of $\tilde{\Sigma}(s,\mathbf{p},\mathbf{t})$

$$\mathbf{H}(s,\mathbf{p},\mathbf{t}) = \left(\sum_r \vartheta_r(s,\mathbf{p})\mathbf{B}_r^T\right)\mathbf{V}(\mathbf{t})\left[\mathbf{V}^T(\mathbf{t})\left(\sum_q \theta_q(s,\mathbf{p})\mathbf{A}_q(\mathbf{t})\right)\mathbf{V}(\mathbf{t})\right]^{-1}\mathbf{V}^T(\mathbf{t})\left(\sum_r \vartheta_r(s,\mathbf{p})\mathbf{B}_r\right)$$

- Is invariant under change of basis $\mathbf{V}(\mathbf{t}) \mapsto \mathbf{V}(\mathbf{t})\mathbf{G}$, $\mathbf{G} \in \mathrm{GL}$.
- Depends on subspace $\mathcal{S}(\mathbf{t}) = \mathrm{span}\{\mathbf{V}(\mathbf{t})\}$.

Principal idea:

- Do not base description of $\mathbf{V}(\mathbf{t})$ on bases $\mathbf{V}_i$ directly.
- Interpolate orthogonal projections onto the associated subspaces $\mathcal{S}_i$.

$$\mathbf{V}(\mathbf{t}) = \Xi(\mathbf{t})(\mathbf{V}_c), \quad \Xi(\mathbf{t}) = \sum_q \Gamma_q(\mathbf{t})\,\gamma \circ \xi_{\mathbf{V}_q}$$

$\xi_{\mathbf{V}_q}$: Orthogonal projection onto $\mathcal{S}_q$

γ : Scaling operator

$\Gamma(\mathbf{t})$: Interpolation function

$\mathbf{V}_c$: Initial basis, $\mathbf{V}_c \in \mathrm{GL}$

Parameter-Dependent Projection Matrices II

Simple example

- One-dimensional parameter space

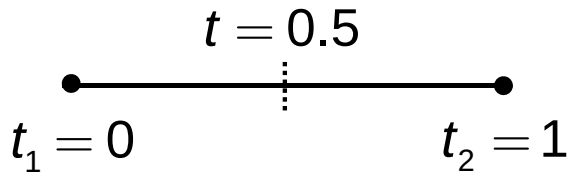

- Projection matrices and Subspaces

$$\mathbf{V}_1, \mathbf{V}_2 \in \mathbb{R}^{2\times 1}$$

$$\mathcal{S}_1 = \mathcal{S}(t_1) = \text{span}\{\mathbf{V}_1\}$$

$$\mathcal{S}_2 = \mathcal{S}(t_2) = \text{span}\{\mathbf{V}_2\}$$

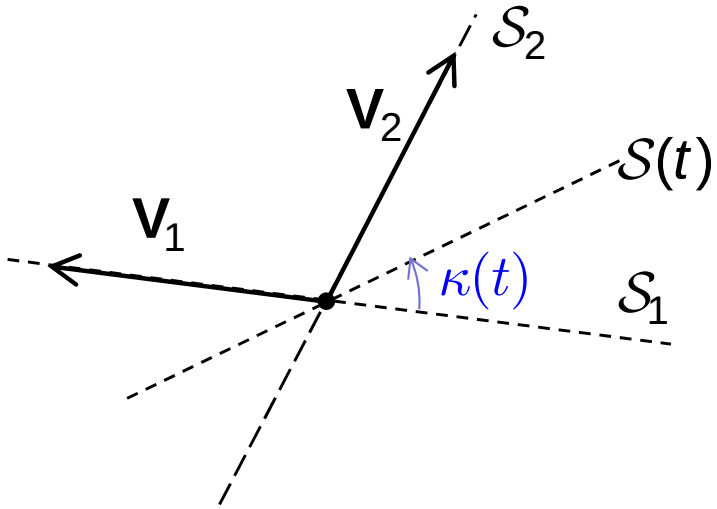

$$\mathbf{V}(\mathbf{t}) = \Xi(\mathbf{t})(\mathbf{V}_c), \quad \Xi(\mathbf{t}) = \sum_q \Gamma_q(\mathbf{t})\, \gamma \circ \xi_{\mathbf{V}_q}$$

- Linear interpolation functions

$$\Gamma_1(t) = (1-t), \Gamma_2(t) = t$$

- Initial basis

$$\mathbf{V}_c = \mathbf{V}_2$$

$$\mathbf{V}(t) = 0.5\,\gamma \circ \xi_{\mathbf{V}_1}(\mathbf{V}_2) + 0.5\,\gamma \circ \xi_{\mathbf{V}_2}(\mathbf{V}_2)$$

$$= 0.5\,\gamma \circ \xi_{\mathbf{V}_1}(\mathbf{V}_2) + 0.5\mathbf{V}_2$$

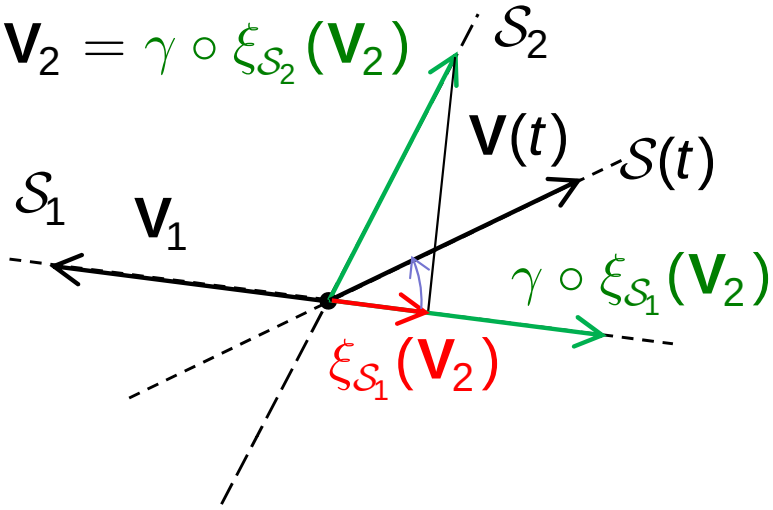

Parameter Dependent Projection Matrices III

Choice of initial basis $\mathbf{V}_c$
– $\mathbf{V}_c \in \{\mathbf{V}_1, \ldots, \mathbf{V}_m\}$

Choice of interpolation function

$$\Gamma_\beta(\mathbf{t}_\alpha) = \prod_{p=1}^{P} \delta_{\beta_p \alpha_p} \qquad \forall \mathbf{t}_\alpha \in \mathcal{G}$$

⇒ Subspace $\mathcal{S}(\mathbf{t})$ is interpolating at grid $\mathcal{G}$

Parametric reduced model $\tilde{\Sigma}(s, \mathbf{p}, \mathbf{t})$

$$[\Xi(\mathbf{t})(\mathbf{V}_c)]^T \left(\sum_q \theta_q(s,\mathbf{p}) \left(\sum_\beta \Gamma_\beta(\mathbf{t}) \mathbf{A}_{q,\beta} \right) \right) [\Xi(\mathbf{t})(\mathbf{V}_c)]\mathbf{x} = [\Xi(\mathbf{t})(\mathbf{V}_c)]^T \left(\sum_r \vartheta_r(s,\mathbf{p}) \mathbf{B}_r \right) \mathbf{u}$$

$$\mathbf{y} = \left(\sum_r \vartheta_r(s,\mathbf{p}) \mathbf{B}_r^T \right) [\Xi(\mathbf{t})(\mathbf{V}_c)]\mathbf{x}$$

Can be stated as superposition of the matrices $\mathbf{D}_{q,c}\mathbf{V}_c^T\mathbf{V}_q\mathbf{V}_q^T\mathbf{A}_{p,\beta}\mathbf{V}_r\mathbf{V}_r^T\mathbf{V}_c\mathbf{D}_{r,c}$,

$\mathbf{D}_{q,c}\mathbf{V}_c^T\mathbf{V}_q\mathbf{V}_q^T B_s$ Reduced-scale!

Benefits:

- Single-point (e.g. [Slone2003]) and multi-point (e.g. [Schultschick2009]) MOR algorithms can be used.
- No modifications of FE kernel are required.
- Various interpolation/approximation schemes are applicable.

Self-adaptive Hierarchical Tensor Grid [Burgard2014]

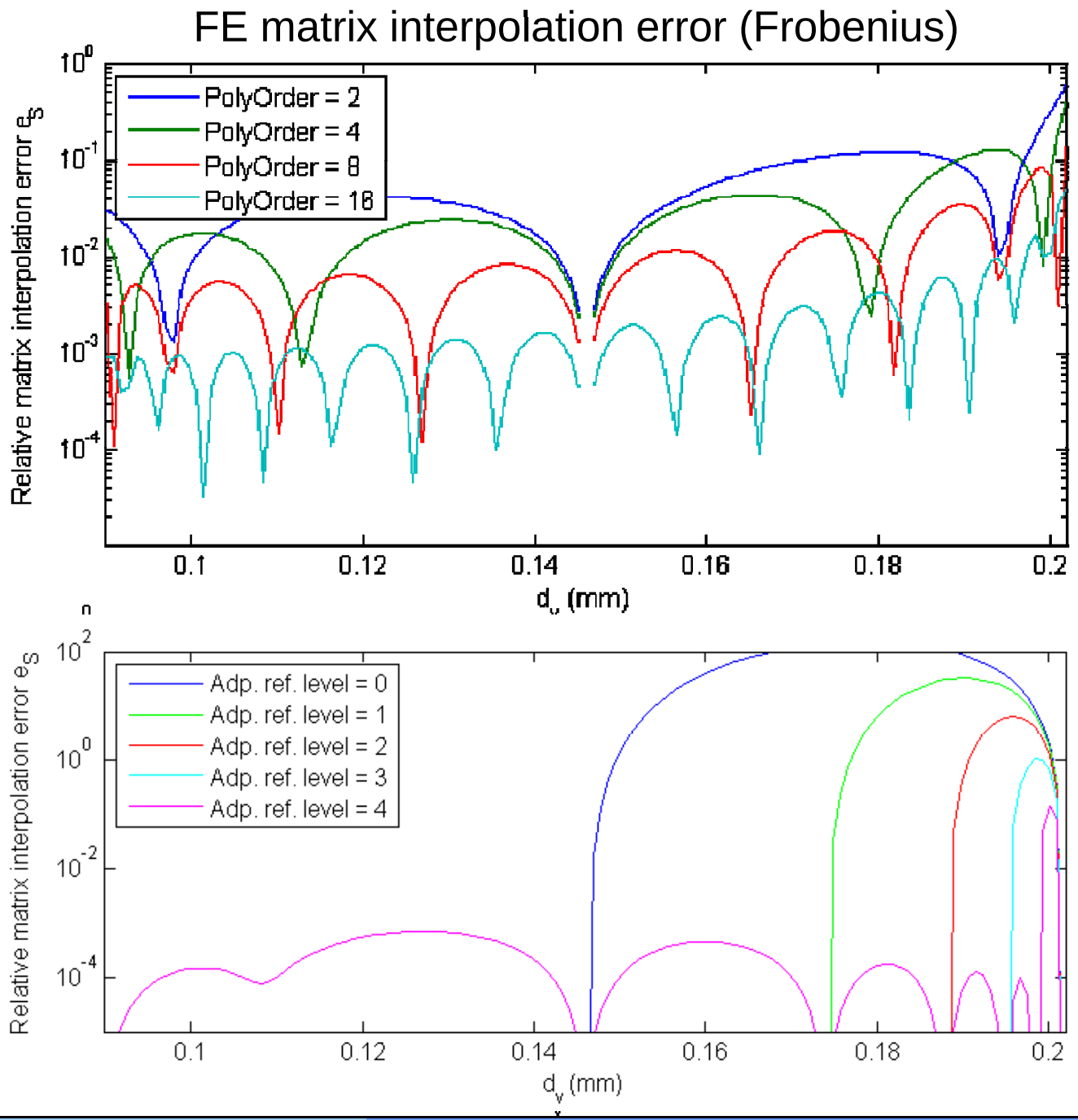

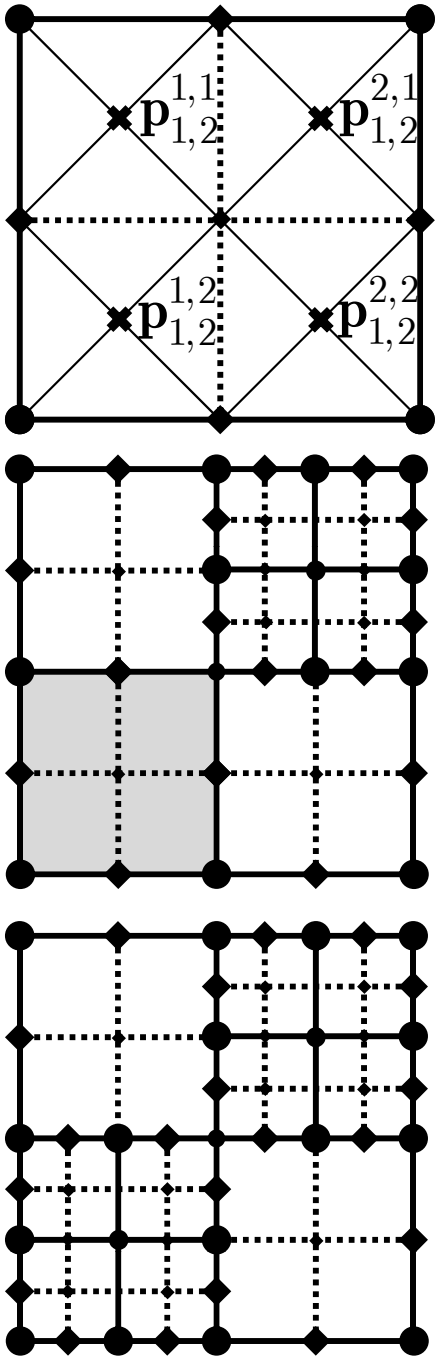

Vivaldi Antenna Element I - Modeling

Stripline-fed Vivaldi notch-antenna element
([Shin1999])

- 3D model:

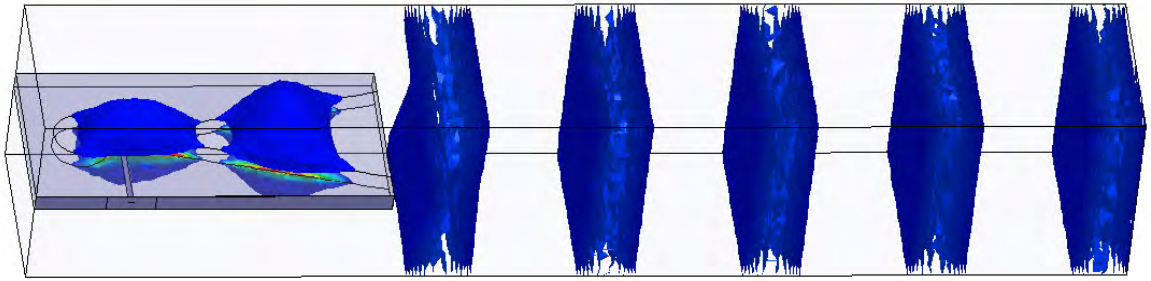

- Sketch of functional layers:

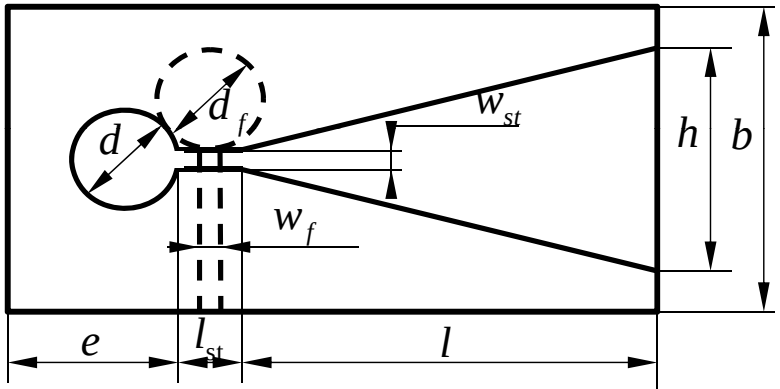

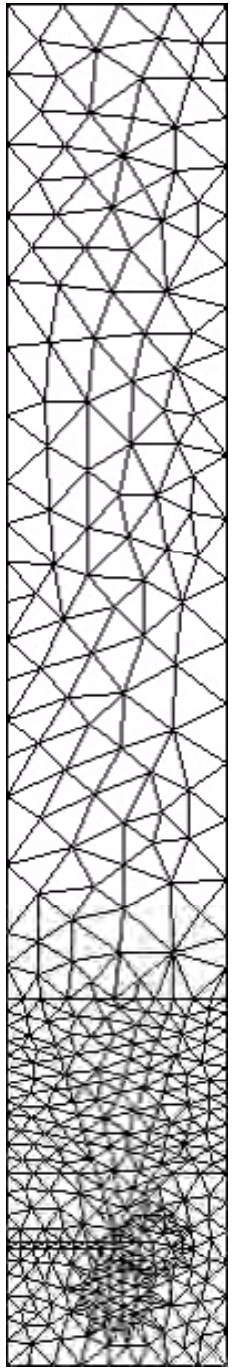

Parametric modeling

- Geometry parameter: taper length l .
- MOR: moment-matching single-point method.
- Polynomial interpolation with Lagrange basis for parameter dependent system matrices.
- Hat functions for parameter-dependent projection matrices .
- Equidistant grid $\mathcal{G}$.

$$f \in [0.8, 5.3]\,\text{GHz}$$

$$l \in [3.5, 6.5]\,\text{cm}$$

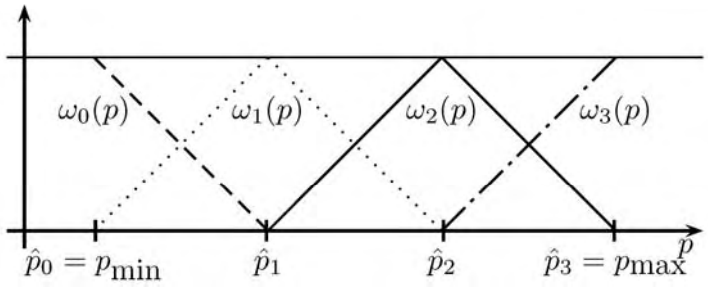

Vivaldi Antenna Element II - Convergence

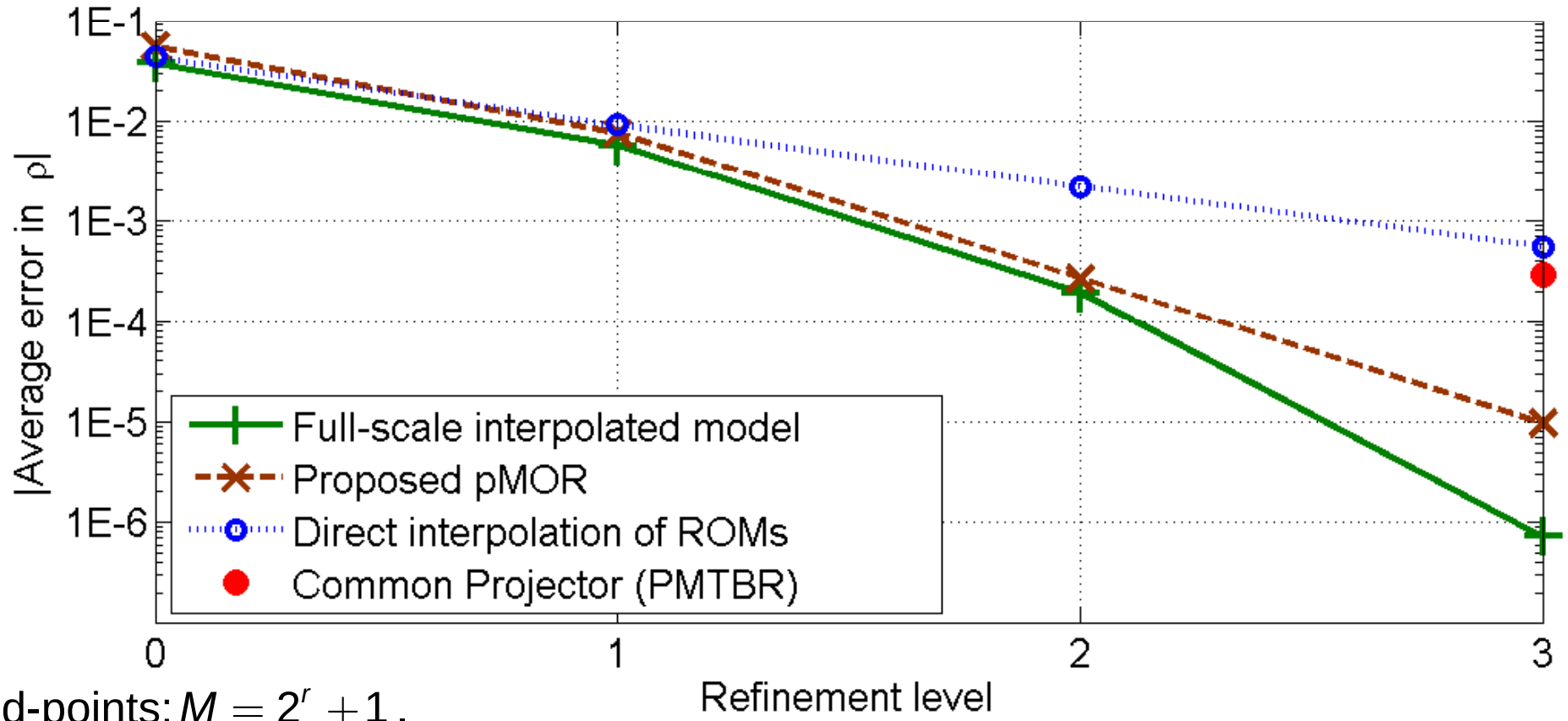

Grid-points: $M = 2^r + 1$.

Model dimensions: $n = 30$.

Single thread performance using MATLAB code and PARDISO on Intel Xeon E5620	**Full-scale FE-Model**	**Parametric reduced model**
DoF	1 045 577	30
Generation time	-	3000 s
Solution time	384 s	0.52 ms
Average error in ρ	-	4.2E-4

Vivaldi Antenna Element III – Response Surfaces

Antenna reactance

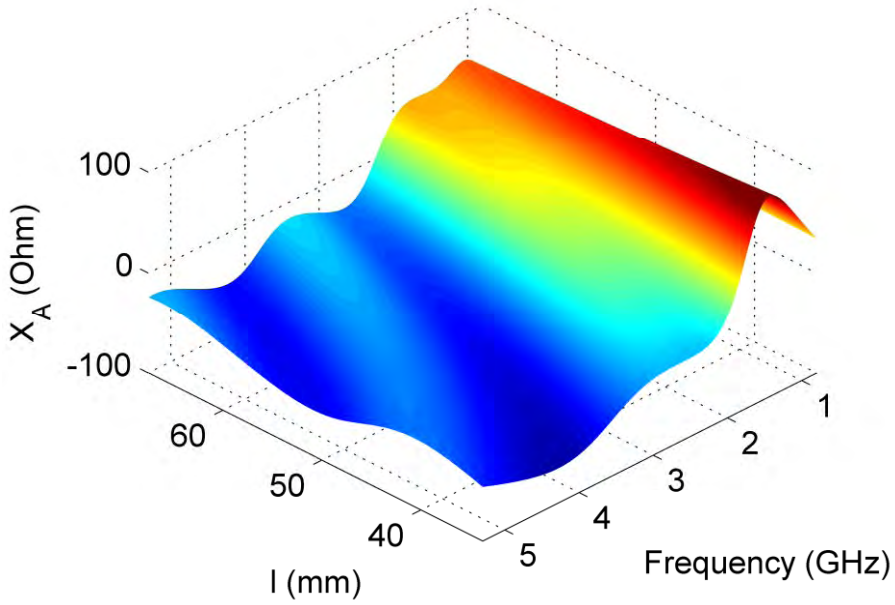

Full FE*: 447 days
pModel: 53 sec.

Antenna resistance

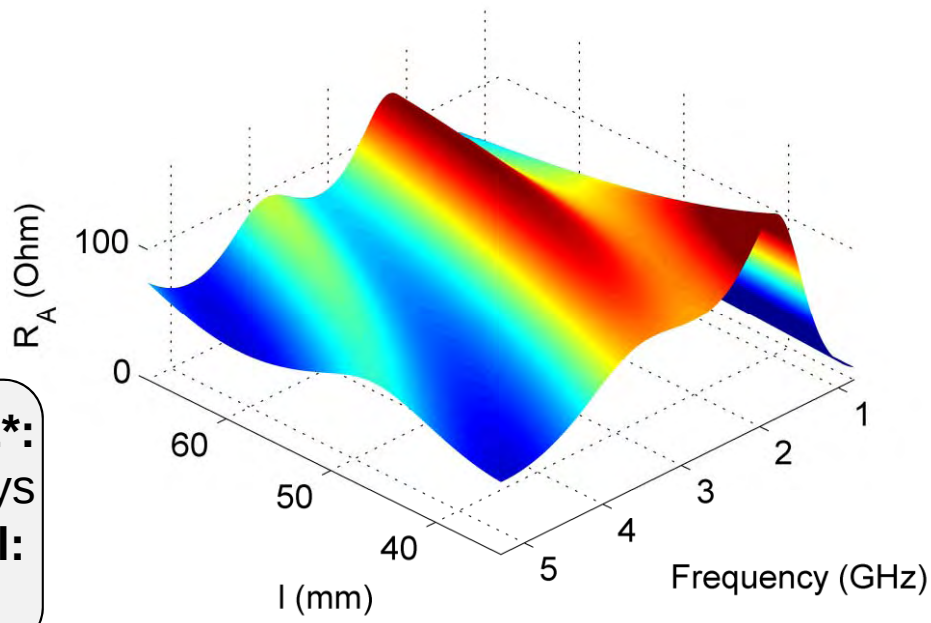

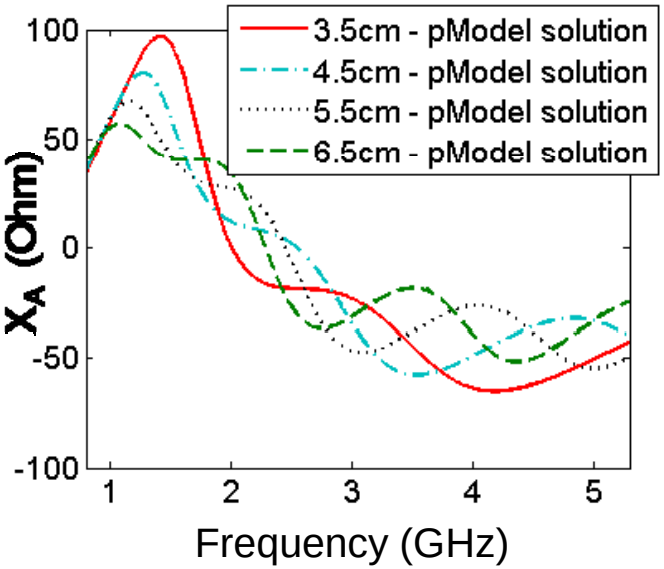

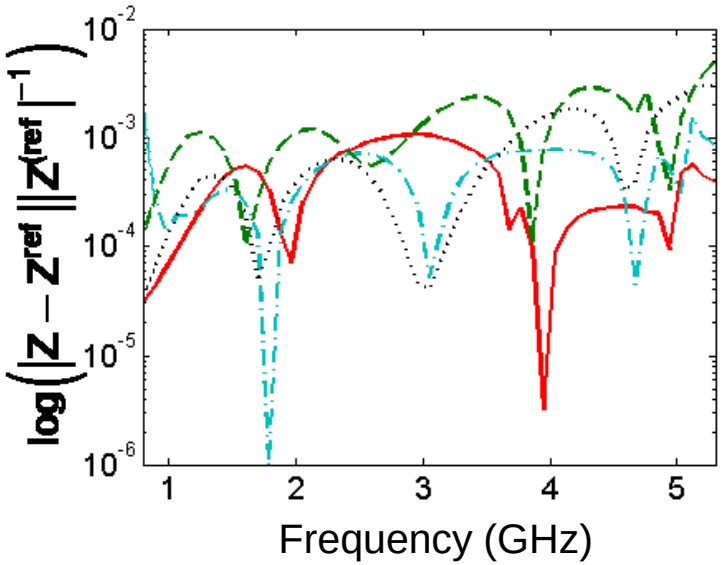

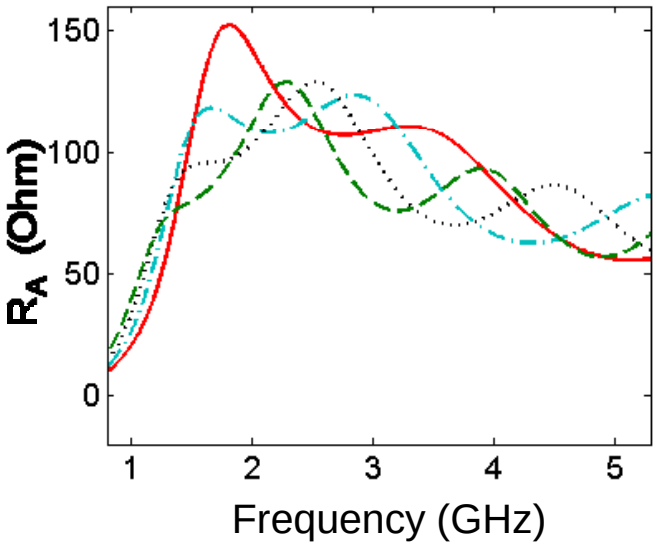

* extrapolated

Bandpass Filter I - Modeling

X-band bandpass filter

[Bornemann1990]

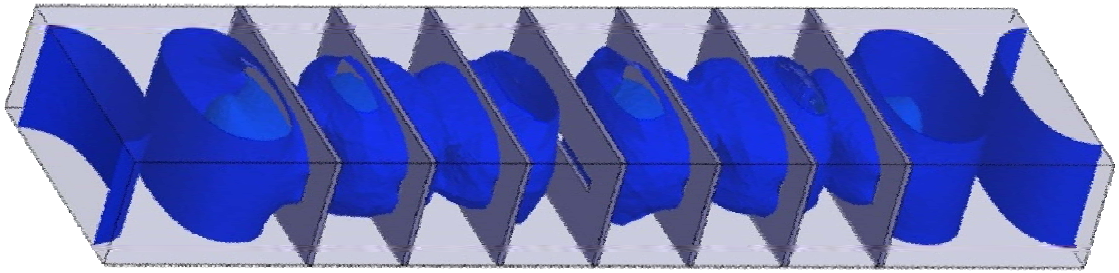

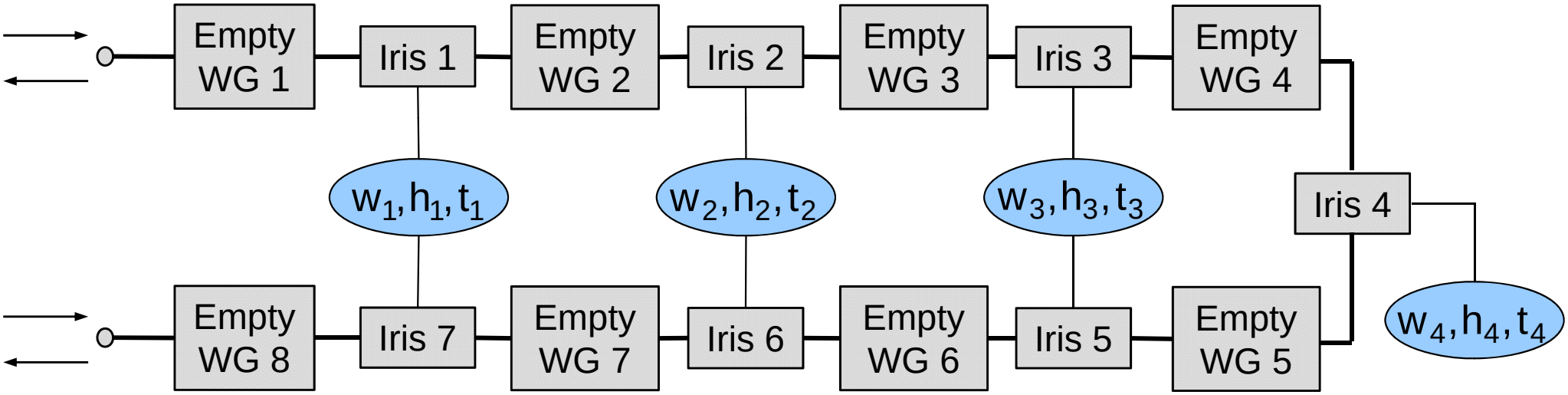

Iris segment parameterization

- Three iris parameters *h,w,t.*
- Seven excitations per port needed.
- All irides described by same parametric Model.

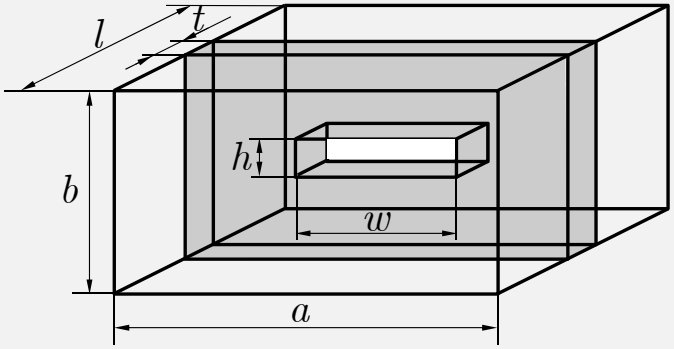

$$w = (1 + p_1) w_0$$
$$h = (1 + p_2) h_0$$
$$t = (1 + p_3) t_0$$

Bandpass Filter II - Results

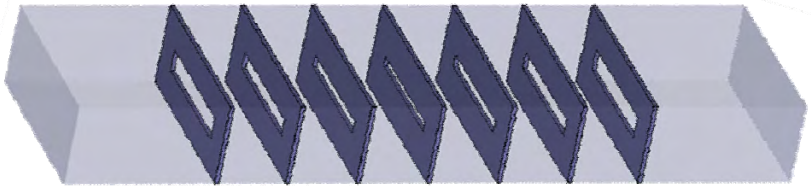

Original model	
FE-Dimension *N*	124 370
Solution time	23.614 s
Reduced-order model	
ROM dimension *n*	98
Solution time (online)	0.002 s

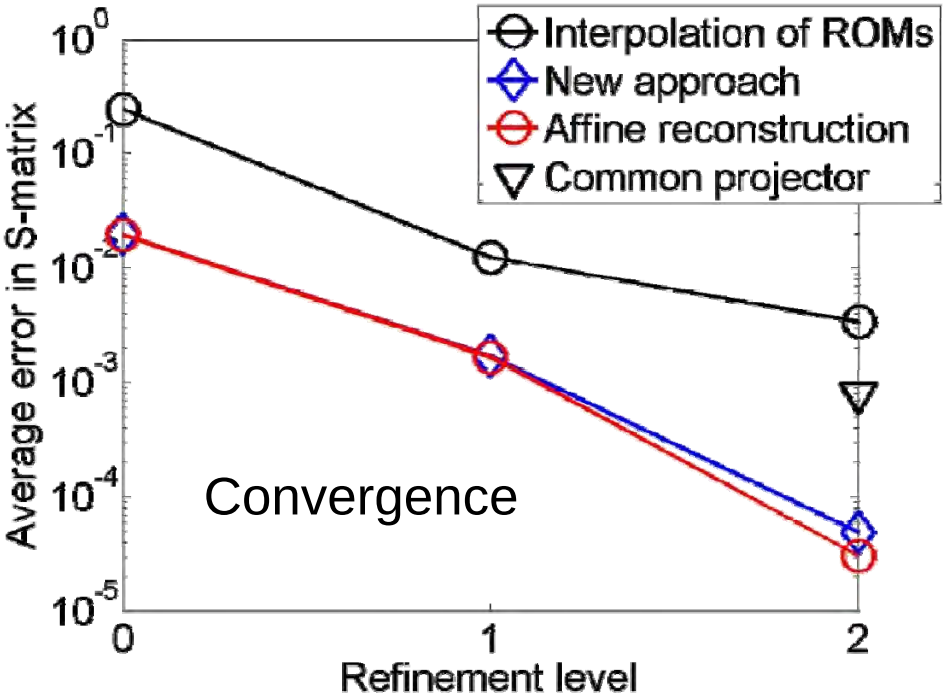

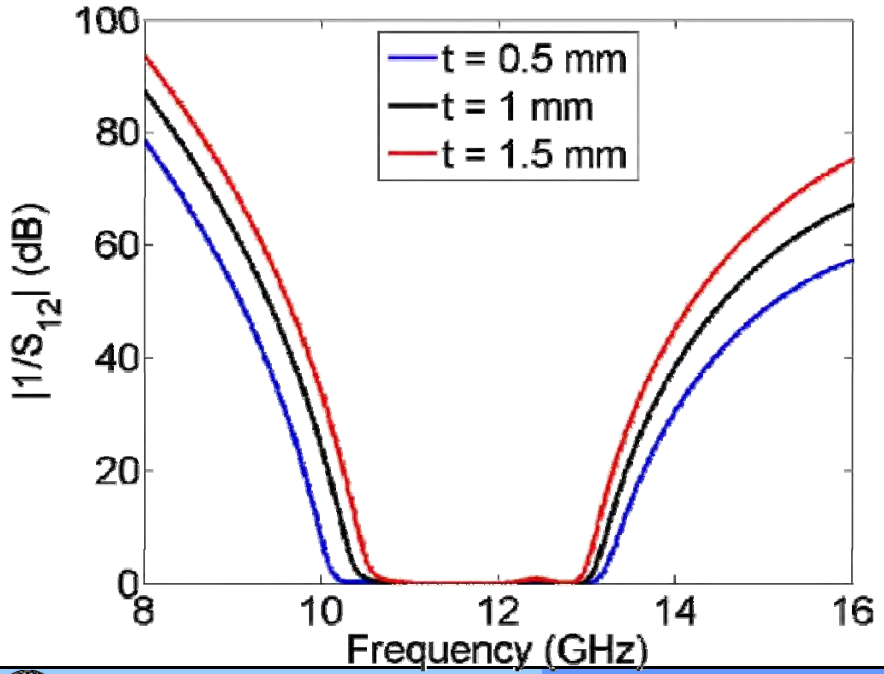

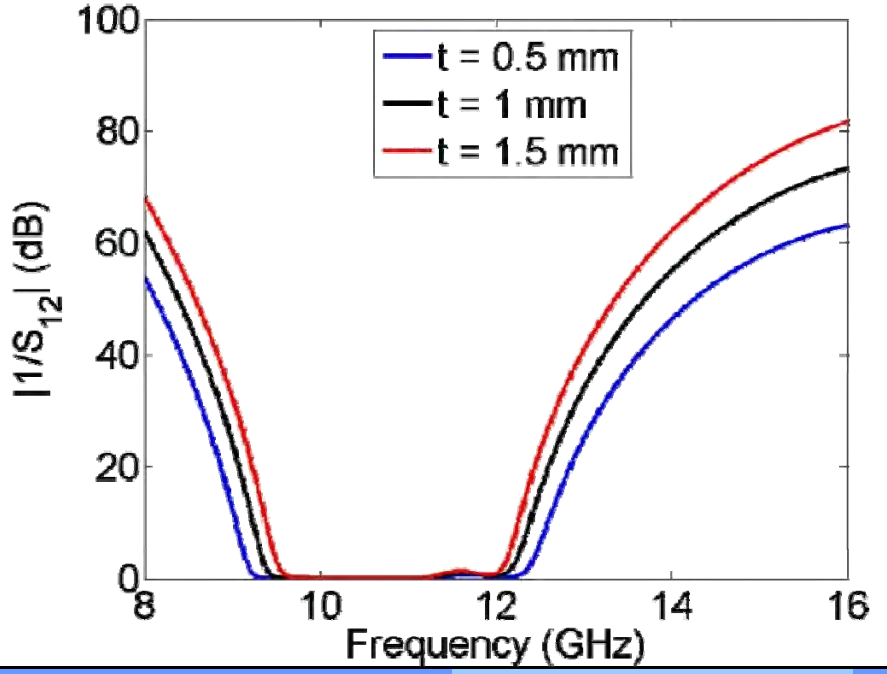

Optimization: 11 Geometric Parameters, Frequency

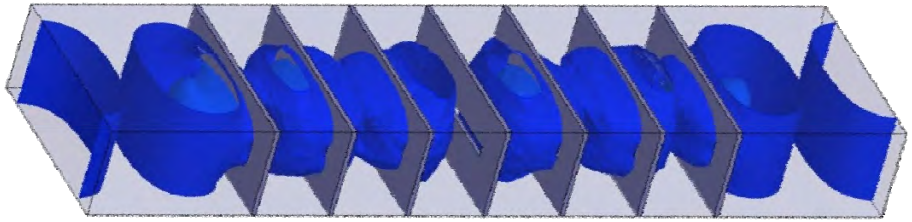

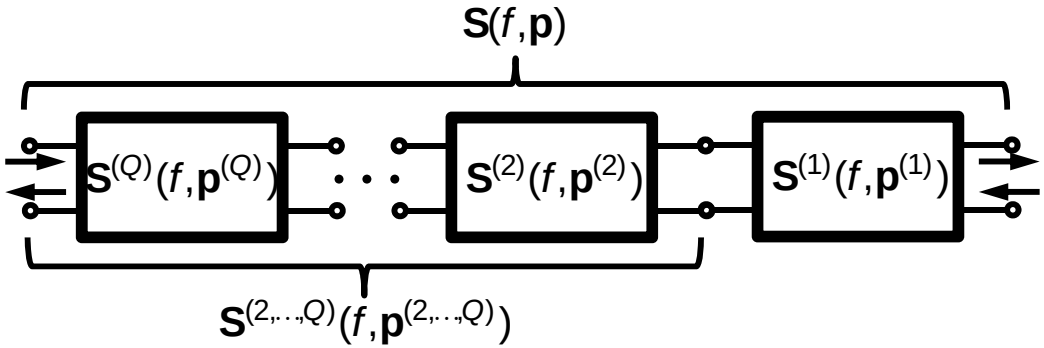

Cost function

$$c(\mathbf{p}) = \frac{1}{201}\sum_{n=1}^{201}\left(\left|S_{1,2}^{\mathrm{ref}}(f_n, f_0, f_c)\right| - \left|S_{1,2}(f_n, \mathbf{p})\right|\right)^2$$

$\left|S_{1,2}^{\mathrm{ref}}(f_n, f_0, f_c)\right|$ ...nominal amplitude response (Butterworth),

$f_c = 11.5$ GHz ...center frequency,

$f_0 = 12.55$ GHz ...upper half-power frequency,

$f_n \in [8,16]$ GHz ...equidistant frequency samples.

- Supports 5 dominant modes per port
- Error in the order of 10E-3 … 10E-2

	PROM	FE model
Model dimension	70	124,370
Model generation (s)	8839.72	-
Model evaluation (s)	9.47e-4	23.61
Cost function eval. (s)	1.58	18,983

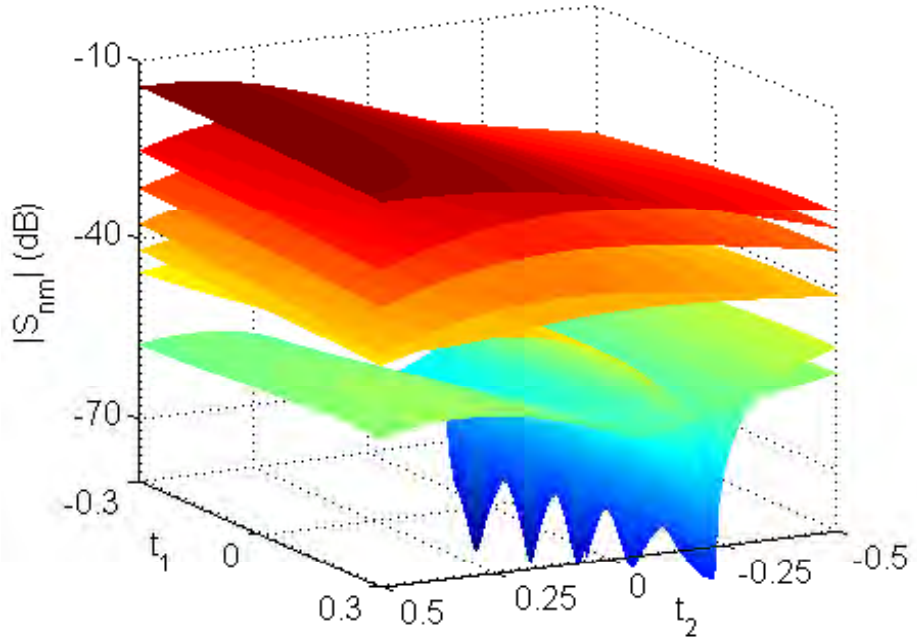

Optimized Filter PROM: Solutions and Error

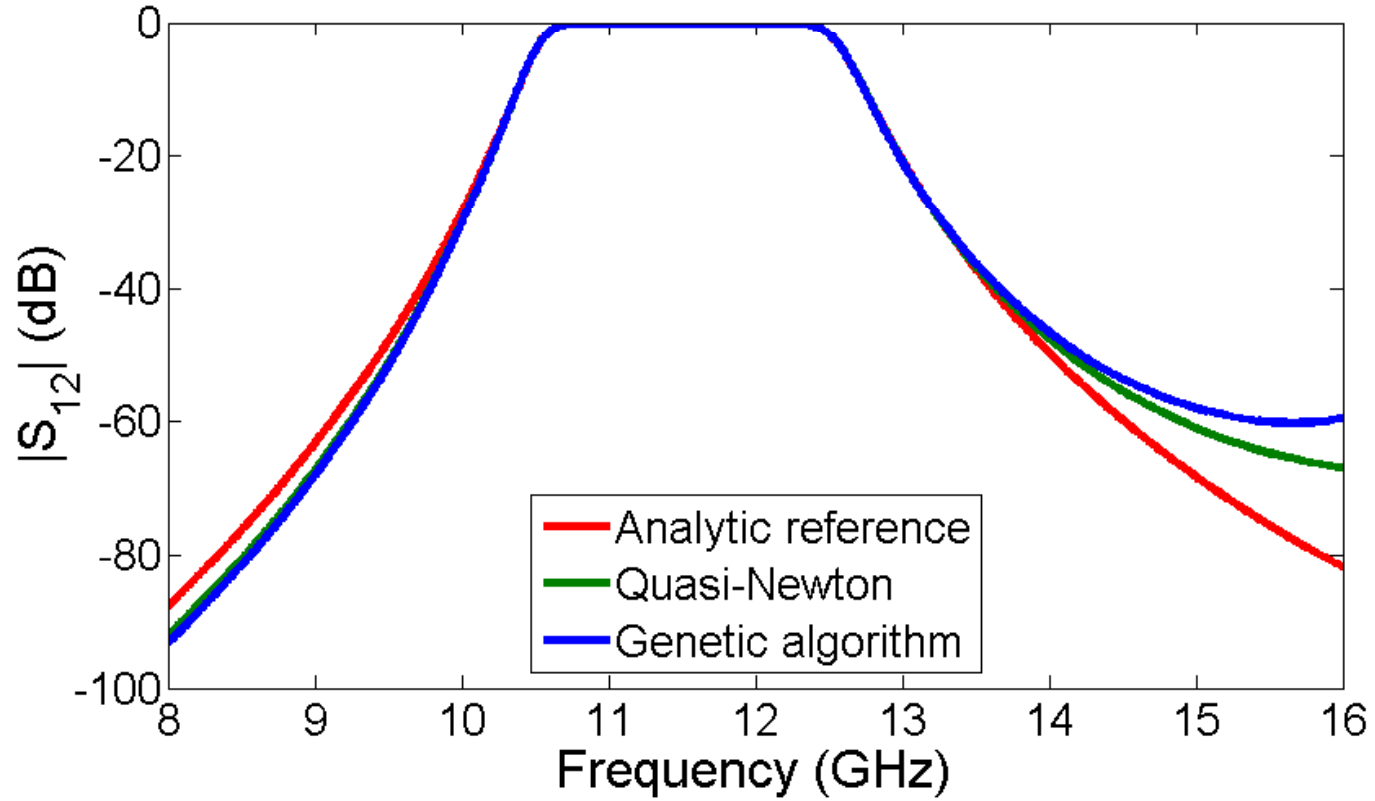

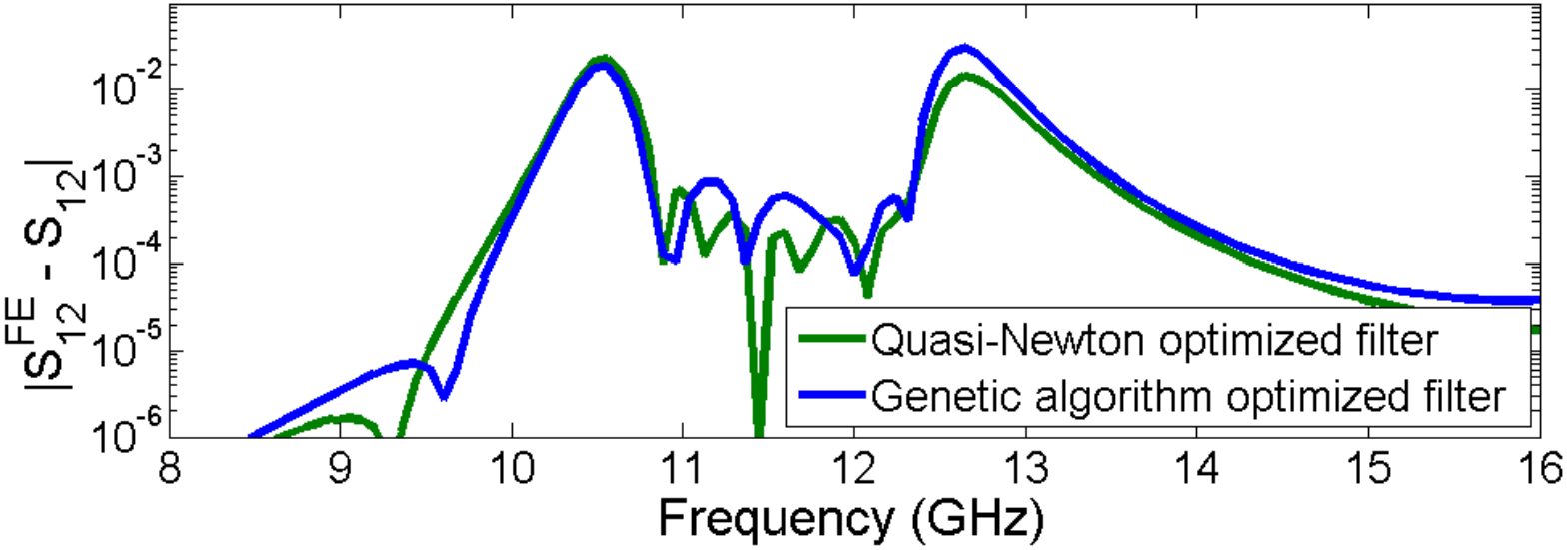

Optimization Performance

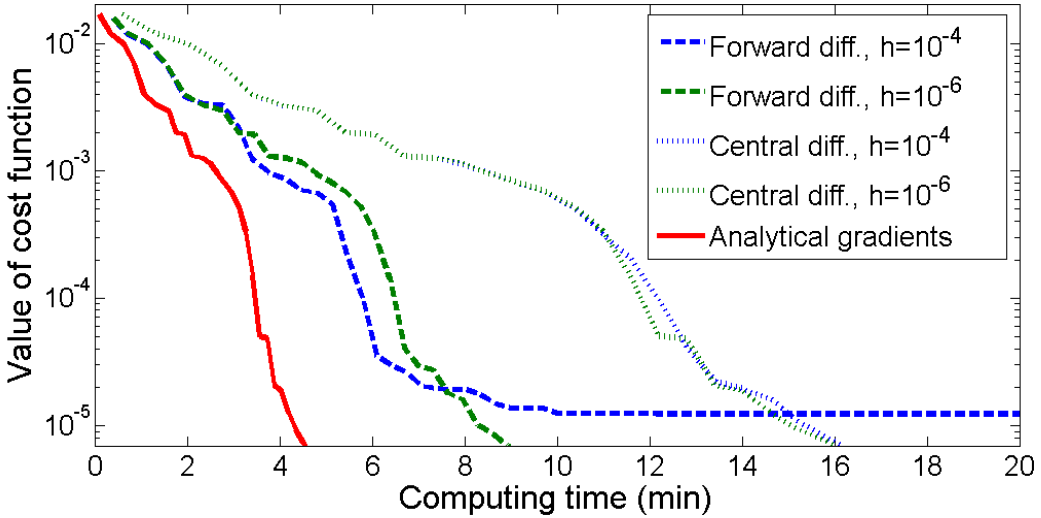

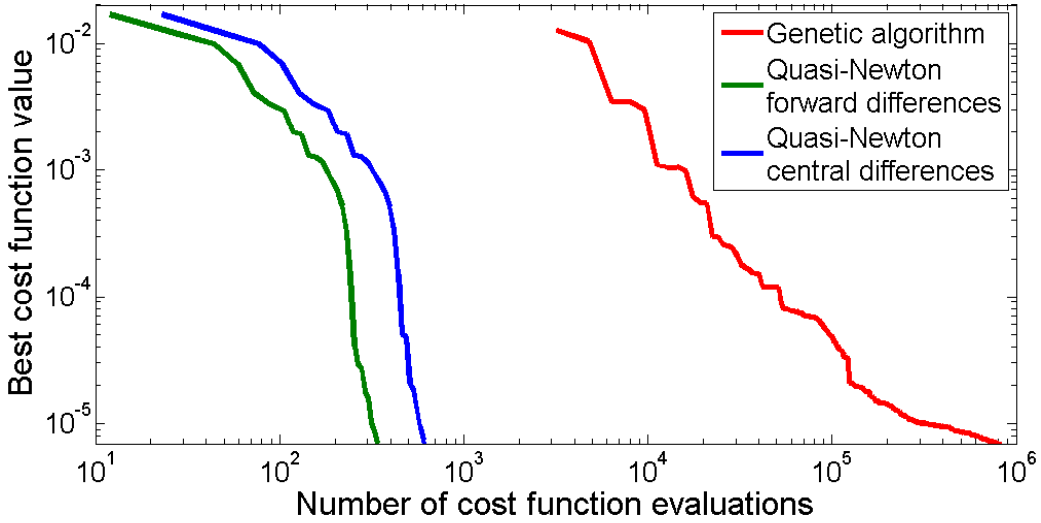

	PROM	FE model
Quasi-Newton with forward diff.	8.9 min	74.26 d
Quasi-Newton with central diff.	15.83 min	132.04 d
Quasi-Newton with analytic grad.	4.5 min	-
Genetic algorithm	14.4 d	373.84 a
Parallelized genetic algorithm (8 threads)	1.8 d	59.23 a

Example: Bandpass Filter Configurations

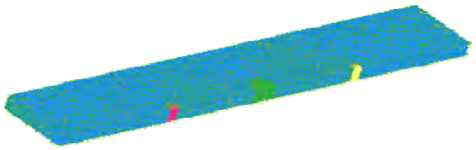

	l_{12}	d_1	d_2
Min	150	9	23
Max	210	30	74
Init.	180	16	40

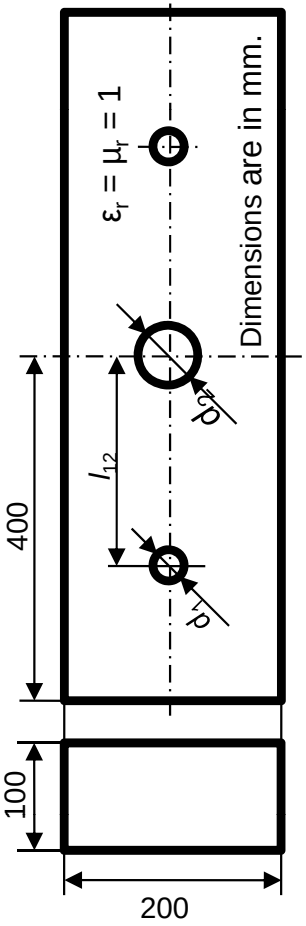

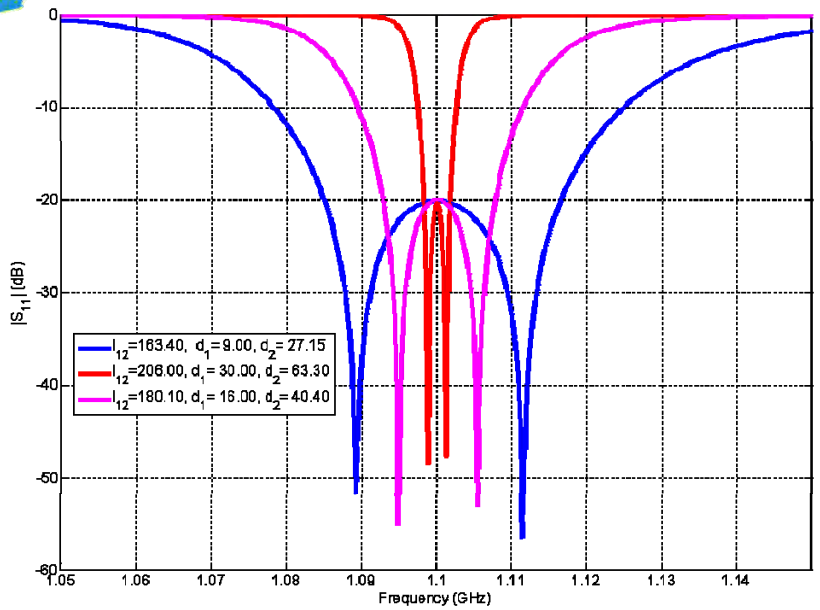

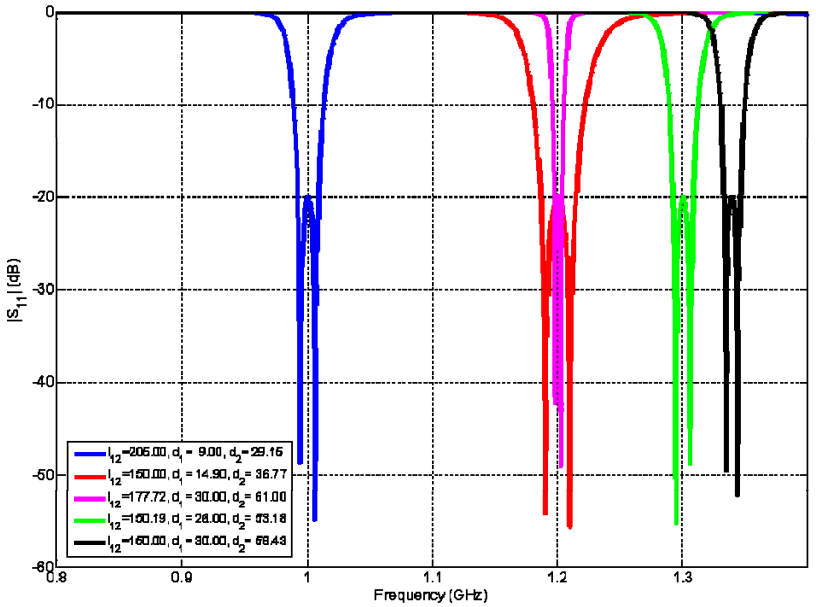

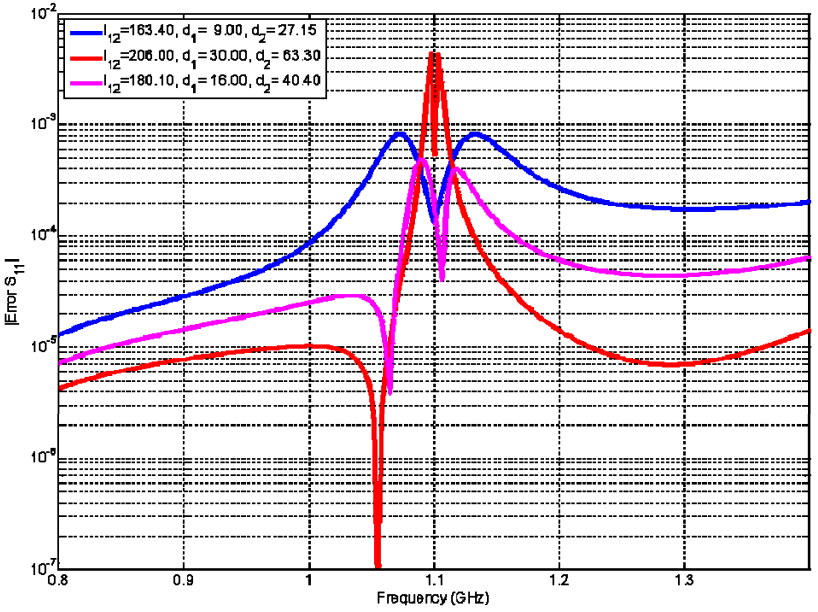

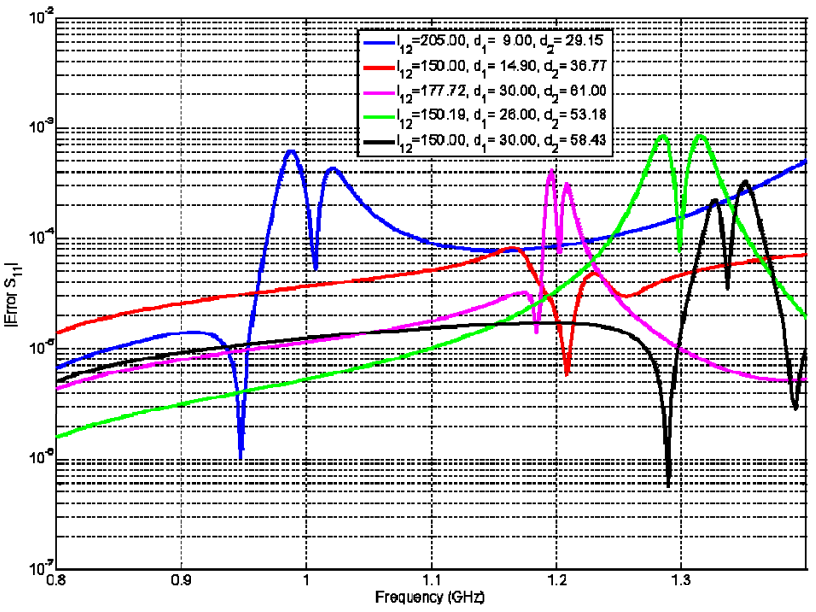

Error plots: 201 frequency points.

Outlook

- Challenges:
  - Electrically large structures.
  - Large numbers of parameters.
  - Geometrical parameters: multiple meshes.
  - Preservation of system properties (general setting).
  - Nonlinearities.

Thank you for your attention!

References I

[Albanese1988] R. Albanese, and G. Rubinacci, “An integral formulation for 3-D eddy current computation using elements”, Proc. Inst. Elect. Eng., vol. 135, pp. 457–462, 1988.

[Bai2000] Z. Bai, J. Demmel, J. Dongarra, A. Ruhe, and H. van der Vorst, “Templates for the solution of algebraic eigenvalue problems: A practical guide”, Society for Industrial and Applied Mathematics, Philadelphia, 2000.

[Barrault2004] M. Barrault, Y. Maday, N. C. Patera, and A. T. Patera, “An ’empirical interpolation’ method: application to efficient reduced-basis discretization of partial differential equations”, C. R. Math. Acad. Sci. Paris, vol. 339, pp. 667–672, 2004.

[Binev2011] P. Binev, A. Cohen, W. Dahmen, R. DeVore, G. Petrova, and P. Wojtaszczyk, ”Convergence rates for greedy algorithms in reduced basis methods”, SIAM J. Math. Anal., vol. 43, pp. 1457-1472, 2011.

[Bornemann1990] J. Bornemann, and R. Vahldieck, “Charaterization of a class of waveguide discontinuities using a modefied mode TE^{x}_{mn} approach”, IEEE Trans. Microw. Theory Techn., vol. 38, pp.1816 – 1822, 1990.

[Buffa2012] A. Buffa, Y. Maday, A.T. Patera, C. Prud’Homme, and G. Turinic, “A priori convergence of the greedy algorithm for the parametrized reduced basis”, ESAIM Math. Model. Numer. Anal., vol. 46, pp. 595-603, 2012.

References II

[Burgard2014] S. Burgard, O. Farle, and R. Dyczij-Edlinger , “An adaptive sub-domain approach to parametric reduced order modeling”, submitted to the Sixteenth Biennial IEEE Conference on Electromagnetic Field Computation, Annecy, France, 2014.

[Chen2010] Y. Chen, J. S. Hesthaven, Y. Maday, and J. Rodriguez, “Certified reduced basis methods and output bounds for the harmonic Maxwell's equations”, SIAM J. Sci. Comput., vol. 32, pp. 970–996, 2010.

[Chio2000] T.-H. Chio, and D. H. Schaubert, “Parameter study and design of wide-band widescan dual-polarized tapered slot antenna arrays”, IEEE Trans. Antennas Propag., vol. 48 , pp. 879–886, 2000.

[Eftang2010] J. Eftang, M. Grepl, and A. Patera, “A posteriori error bounds for the empirical interpolation method”, C. R. Math. Acad. Sci. Paris, vol. 348, pp. 575–579, 2010.

[Fares2011] M. Fares, J. S. Hesthaven, Y. Maday, and B. Stamm, “The reduced basis method for the electric field integral equation”, J. Comput. Phys., vol. 230, pp. 5532–5555, 2011.

[Hesthaven2012] J. S. Hesthaven, B. Stamm, and S. Zhang, “ Certified reduced basis method for the electric field integral equation”, SIAM J. Sci. Comput., vol. 34, pp. 1777–1799, 2012.

References III

[Huynh2007] D. B. P. Huynh, G. Rozza, S. Sen, and A. T. Patera, “A successive constraint linear optimization method for lower bounds of parametric coercivity and inf-sup stability constants”, C. R. Math. Acad. Sci. Paris, Ser. I 345, pp. 473–478, 2007.

[Maday2009] Y. Maday, N. C. Nguyen, A. T. Patera, and G. S. H. Pau., “A general multipurpose interpolation procedure: the magic points”, Commun. Pure Appl. Anal., vol. 8, pp. 383-404, 2009.

[Pomplun2010] J. Pomplun, and F. Schmidt, “Accelerated a posteriori error estimation for the reduced basis method with application to 3D electromagnetic scattering problems”, SIAM J. Sci. Comput., vol. 32, pp. 498 – 520, 2010.

[Rubia2009] V. de la Rubia, U. Razafison, and Y. Maday, “Reliable fast frequency sweep for the microwave devices via the reduced-basis method”, IEEE Trans. Microw. Theory Techn., vol. 57, pp. 2923–2937, 2009.

[Schultschik2009] A. Schultschik, O. Farle, and R. Dyczij-Edlinger, “An adaptive multi- point fast frequency sweep for large-scale finite element models”, IEEE Trans. Magn, vol. 45, pp. 1108–1111, 2009.

[Shin1999] J. Shin, and D. H. Schaubert, “A parameter study of stripline-fed vivaldi notch-antenna arrays”, IEEE Trans. Antennas Propag., vol. 47, pp. 879–886, 1999.

References IV

[Slone2003] R. D. Slone, R. Lee, and J.-F. Lee, “Broadband model order reduction of polynomial matrix equation using single-point well-conditioned asymptotic waveform evaluation: Derivation and theory”, Int. J. Numer. Meth. Engng, vol. 58, pp. 2325–2342, 2003.

[Sommer2013] A. Sommer, O. Farle, and R. Dyczij-Edlinger, “Efficient finite-element computation of far-fields of phased arrays by order reduction”, COMPEL, vol. 32, pp. 1721–1734, 2013.

[Sommer2013b] A. Sommer, O. Floch, O. Farle, R. Baltes, and R. Dyczij-Edlinger, “An efficient parametric near-field-to-far-field transformation technique”, Proceedings of the 2013 International Conference on Electromagnetics in Advanced Applications, Turin, Italy, pp. 332-335, 2013.

[Strube1985] J. Strube, and F. Arndt, “Rigorous hybrid-mode analysis of the transition from rectangular waveguide to shielded dielectric image guide”, IEEE Trans. Microw. Theory Techn., vol. 33, pp. 391–401, 2003.